DIPLOMARBEIT

Evaluation and Modeling of Power Control Information in a 3G Cellular Mobile Network

eingereicht an der Technischen Universität Wien,
Fakultät für Elektrotechnik und Informationstechnik
zum Zweck der Erlangung des
akademischen Grades eines Diplom-Ingenieurs

ausgeführt am
Institut für Nachrichten- und Hochfrequnztechnik

betreut von
Univ. Prof. Dr. techn. Markus Rupp
Dr. techn. Philipp Svoboda

von

Markus Laner

Matr.Nr. 0325687
Lammweg 28/B, 39050 Girlan, Italy

Wien, August 2009 _____

Betreuer:

Univ. Prof. Dr. techn. Markus Rupp
Institut für Nachrichten- und Hochfrequenztechnik, TU-Wien

Dr. techn. Philipp Svoboda
Institut für Nachrichten- und Hochfrequenztechnik, TU-Wien

Abstract

In modern 3^{rd} Generation (3G) networks such as Universal Mobile Telecommunication System (UMTS) Wide-band Code Division Multiple Access (WCDMA) is used for communication radio links. Power control is a very important issue in WCDMA, it reduces interference and power consumption of the transmission and therefore it needs to be addressed in relation with throughput maximization. Due to this fact UMTS deploys a strict power control, composed by the Inner Loop Power Control (ILPC) and the Outer Loop Power Control (OLPC). Whereas the ILPC was hardly tried to optimize in the last couple of years, the OLPC did not receive a comparable amount of attention. It seems not to undergo any evolution and there finds only few literature about optimization issues. The OLPC is a controller which adjusts the received Signal to Interference Ratio (SIR) to a predefined Block Error Ratio (BLER) by means of feedback to the transmitter. In resent research the OLPC algorithm was identified to introduce regular error patterns into radio connections, what is a sign for possible room of improvement.

This thesis aims to identify impairments of the OLPC algorithm and to find room for improvement by means of extensive measurements in a live UMTS network. The measurements were performed in the UMTS Terrestrial Radio Access Network (UTRAN), by the aid of a powerful tracing tool.

Measurement results have shown the nature of the uplink OLPC algorithm in detail. The behavior was characterized with the aid of statistical models. Furthermore additional parameters have been investigated, whereas especially one revealed a strong correlation to the BLER, i.e. the uncoded Bit Error Ratio (BER).

In consequence a new OLPC algorithm is proposed in this work, which exploits the additional information of the uncoded BER. In order to evaluate the possible gain simulations have been performed, which compare the old and new algorithm. The outcome is that the new algorithm is able to improve the power control mechanism. Under different conditions, i.e. constant and dynamic SIR demands, the gain was estimated between 0.2 dB and 1 dB difference in mean SIR, what can directly be interpreted as power savings of the same magnitude. The new algorithm is totally standard compliant and easy to implement in existing networks.

Kurzfassung

In modernen 3^{rd} Generation (3G) Netzwerken wie zum Beispiel Universal Mobile Telecommunication System (UMTS) wird Wide-band Code Division Multiple Access (WCDMA) als Zugriffsmethode für die Luftschnittstelle verwendet. Dabei spielt Leistungskontrolle eine sehr wichtige Rolle, Interferenzen und Leistungsverbrauch können auf ein Minimum beschränkt und somit auch der Datendurchsatz maximiert werden. Aus diesem Grund wird in UMTS eine strikte Leistungsregelung verwendet, welche aus einem inneren und einem äußeren Regelkreis besteht. Die jeweiligen Bezeichnungen sind Inner Loop Power Control (ILPC) und Outer Loop Power Control (OLPC). Während sich die ILPC im Laufe der letzten Jahre stetig weiterentwickelte, gab es keinen entsprechenden Fortschritt der OLPC zu verzeichnen. Entsprechende Literatur ist rar. Die OLPC ist ein Regelungsalgorithmus, der versucht die Blockfehlerrate konstant zu halten, indem das empfangene Signal zu Störungs-Verhältnis entsprechend angepasst wird. Das geschieht mit Hilfe einer Rückkopplung zum Sender. In letzter Zeit wurde festgestellt, dass der OLPC Algorithmus regelmäßige Fehlermuster bei der Übertragung verursacht. Dies ist ein Zeichen für suboptimale Auslegung und Verbesserungspotenzial.

In dieser Diplomarbeit sollen die Schwachstellen des OLPC Algorithmus festgestellt und Verbesserungsmöglichkeiten erarbeitet werden. Dies soll mit Hilfe von ausgiebigen Messungen in einem in Betrieb stehenden UMTS Netzwerk erreicht werden, wofür leistungsfähige Software zur Verfügung steht.

Die erhaltenen Messergebnisse zeigen das Verhalten des OLPC Algorithmus im Detail, welches anschließend mithilfe von statistischen Methoden modelliert wurde. Zusätzlich ist nach weiteren Parametern gesucht worden, mit denen der Regelungsmechanismus verbessert werden könnte. Dabei stellte sich die unkodierte Bitfehlerrate, genannt Bit Error Ratio (BER), als ein Wert heraus, der mit der Blockfehlerrate stark korreliert ist.

In weiterer Folge wird ein neuer Algorithmus vorgeschlagen, der sich die in der unkodierten Bitfehlerrate enthaltene Information zu Nutze macht um ein verbessertes Verhalten zu garantieren. Um die Leistungsfähigkeit dieser Methode beurteilen zu können wurden Simulationen durchgefhrt. Die resultierende Erkenntnis ist, dass der hier vorgeschlagene Algorithmus durchaus Potenzial zur Leistungssteigerung hat. Unter verschiedenen Umständen, wie zum Beispiel konstanten und dynamischen Leistungsanforderungen, wurden zwischen 0.2 und 1 dB an eingesparter mittlerer Leistung geschätzt. Außerdem ist der hier vorgeschlagene Algorithmus standardkonform und relativ einfach zu implementieren.

Danksagung

Ich möchte mich an dieser Stelle bei all jenen bedanken, die mich während meiner Diplomarbeit unterstützt haben. Ohne sie wäre diese Arbeit nicht zustande gekommen.

Allen voran möchte ich Herrn Prof. Dr. Markus Rupp danken, dass er mir das Arbeiten im professionellen Umfeld des Instituts für Nachrichten- und Hochfrequenztechnik der TU-Wien ermöglicht hat. Durch seine Hilfe konnte auch die ertragreiche Kooperation mit Partnern aus der Industrie verwirklicht werden.

Zu großem Dank bin ich auch meinem Betreuer Herrn Dr. Philipp Svoboda verpflichtet. Er ist mir bei diesem Projekt tatkräftig zur Seite gestanden, hat mir in vielen Diskussionen stets den richtigen Weg gewiesen und mich die Essenz des wissenschaftlichen Arbeitens gelehrt.

Des weiteren möchte ich den industriellen Partnern "mobilkom austria" und "ftw – Forschungszentrum Telekommunikation Wien" einen Dank aussprechen. Erst durch die Bereitstellung umfangreicher Rahmenbedingungen von ihrer Seite waren meine Forschungen möglich.

Ein herzliches Dankeschön an meine Eltern Maria und Rudolf, sowie an meinen Bruder Peter, dass sie mir während meines gesamten Studiums liebevoll zur Seite gestanden sind und immer an mich geglaubt haben.

Allen meinen Freunden und Studienkollegen möchte ich außerdem dafür danken, dass sie die schöne Studienzeit mit mir verbracht haben und ich immer auf ihre Hilfe zählen konnte.

Zum Abschluss möchte ich noch meiner Freundin Doro danken, sie hat mich stets unterstützt und gibt mir Kraft und Ausdauer auf meinem Weg.

Wien, August 2009 Markus Laner

Contents

Chapter 1

Introduction

In the last years the new 3^{rd} Generation (3G) communication system, Universal Mobile Telecommunication System (UMTS), became more and more popular in the world of mobile communication. In comparison to 2^{nd} Generation (2G) systems UMTS offers a lot of technical innovations and improvements. One of the biggest differences is the access method used in the new communication network. It is called Wide-band Code Division Multiple Access (WCDMA). In contrast to other access technologies, i.e. Time Division Multiple Access (TDMA) and Frequency Division Multiple Access (FDMA), all users share the same time and frequency resources and are distinguished by their spreading code only, that is a kind of signature different for every user.

The spreading codes are almost orthogonal to each other but if many users are active in a cell the created interference becomes more and more relevant. For this reason WCDMA deploys a tight power control, which prevents interference by reducing transmission power. The power control is organized in a double control loop, i.e. the Inner Loop Power Control (ILPC) and the Outer Loop Power Control (OLPC). Whereas the ILPC guarantees a certain Signal to Interference Ratio (SIR), the OLPC ensures for a specified Block Error Ratio (BLER).

Resent research on link level error characteristics revealed that regular error patterns are present in UMTS communication links, see [35]. It was claimed that the reason is the OLPC algorithm. In consequence the question arose if the algorithm could be improved to prevent regularities, save transmission power and reduce interference. Surprisingly only few literature dealing with this topic was published.

The goal of this thesis is divided into two parts. First is the evaluation of the OLPC mechanism in a live UMTS network. This should be done by means of extensive measurements. Aim of this part is to understand the dynamics of the actual OLPC method and the ILPC loop as control path, to be able to describe them mathematically. Furthermore research on possible space for improvement of the OLPC should be done. In UMTS the interfaces between network components are defined very accurately in the standard whereas the implementation of components is not specified. This also applies for the OLPC algorithm. Therefore any outcome of this work has no general significance but does only apply for the network and respective network components (Radio Network Controllers (RNCs)) involved in the measurements.

The second part is the modeling of the measured data. A general system model is targeted in order to be able to perform simulations and in consequence compare actually working OLPC schemes with new improved ones. This part includes the construction of new OLPC algorithms from scratch. It should be investigated if the deployment of new OLPC methods yields any savings in transmission power and in which order of magnitude they would be.

The remainder of this thesis is structured the following way:

Chapter 2 deals with the basics of UMTS. The important concepts are explained and further specified in order to be equipped with background knowledge for the following chapters.

Chapter 3 explains the measurement setup in the live UMTS network. It is analyzed what kind of data can be extracted and how useful this data is for analysis of the OLPC. Room for improvement of the control algorithm is shown. At the end measurement results are presented and respective interpretations are given.

Chapter 4 reveals how the overall power control loop can be modeled. Simplifications presumed in the concept are explained. A new OLPC algorithm is presented and simulation results are shown. Finally the simulations are compared to the actual used OLPC algorithm and concluding remarks are given.

Chapter 5 gives a summary of this work and reveals starting points of future research.

Chapter 2

Universal Mobile Telecommunications System

In the late 90s the 3^{rd} Generation (3G) of mobile communication systems was designed and standardized. This was done by an international advisory board called 3^{rd} Generation Partnership Project (3GPP). The outcome is called Universal Mobile Telecommunication System (UMTS), a radio access technology based on Wide-band Code Division Multiple Access (WCDMA). Different concepts have been standardized, e.g. access over satellite or terrestrial network, where the latter is the most important. Because of different legislations in different countries the standard comes in two flavors, i.e. Frequency Division Duplex (FDD) and Time Division Duplex (TDD). This nomenclature refers to uplink and downlink which work on two different frequency bands in FDD mode and are temporally multiplexed in TDD mode. This difference sounds inconspicuous but has a lot of consequences for the communication system. This work covers only the FDD mode, which was chosen because of its deployment in Europe.

In contrast to the former generations of mobile access technologies UMTS was designed not for voice traffic only but for data traffic as well. Additionally provided services are e.g. Internet surfing and video telephony. This leads to the fact that this network has to support packet-switched data traffic as well as circuit-switched traffic. Nevertheless the architecture of the core network of UMTS was keept as close as possible to the network architecture of the former generation, i.e. Global System for Mobile Communications (GSM) and General Packet Radio Service (GPRS).

Since the first releases of UMTS, Release 99, the standard was in steady further development. Over the years the standard was extended by several releases, which introduced a lot of new features. An important one is High Speed Downlink Packet Access (HSDPA), an extension to make UMTS more suited for web browsing and other data traffic.

Extensive literature about this topic can be found. Works containing good and exhaustive descriptions of UMTS are [33] and [37], whereon this chapter is also based.

2.1 Services and Applications

The UMTS communication system is designed to support various types of service at the same time. All these services have different demands to the communication system in terms of maximum delay, error rates, etc. A voice call for example has very tight restrictions on maximum delay and jitter whereas the integrity of the data plays a secondary role. An other example would be a file download over IP. In this case the integrity of the data is very important, on the other hand the jitter or delay of the packets are not.

Generally applications and services can be divided into groups with certain demands on Quality of Service (QoS). In UMTS this grouping leads to four different traffic classes [1]:

- *Conversational class*: This service class is dedicated to all kinds of human to human communication, e.g. voice, video telephony. The remarkable features of this class are to preserve time relation and variation between information entities of the stream and very tight restrictions on delay.
- *Streaming class*: Multimedia services and streaming applications should deploy this service class. The characteristics are as in the conversational class to preserve time relations of information entities of the stream. The difference to the former class is that the data rate is expected to have much higher variations.
- *Interactive class*: Applications for this service class are web browsing and network games. This class is tailored to handle request response patterns and to preserve data integrity. The requirements for delay are less severe than for the former two classes.
- *Background class*: This service class is made for downloading data, e.g. emails, etc. The destination is not expecting the data within a certain time, so the stream can be handled very flexible. The only restriction is to preserve data integrity.

In order to accommodate the demands of all these different classes and allow multiple instances of applications at the same time, a rather complex connection scheme has been introduced. It is called UMTS Bearer Service. Different protocol layers at different entities of the network offer respective bearers. The characteristics of those should be suited for the data type and the underlying network structure. In consequence negotiation an renegotiation procedures for bearer characteristics are defined. The bearers should be chosen according to the expected QoS and be able to handle it flexible. To cope with the QoS demands on the radio interface and provide enough flexibility is challenging. The resources are sparse and must be used in a efficient manner. In the following section the UMTS radio link is observed a little closer and the specific concepts are introduced.

2.2 Wireless Communication Interface

Wireless communication systems use the air interface to transmit data, the resources available are certain frequency bands. Cellular systems like UMTS divide the operational area into local regions to be able to reuse the resources. These regions are called cells. Every single cell in a cellular radio network can be understood as a multi-user communication system. All the users in the respective cell have to share the same resources to transmit and/or receive information. Therefore the resources have to be divided into several non-overlapping portions, normally called channels, to prevent users from interfering each other. In contrast to other data communication systems wireless communication systems have to do this segmentation in a very effective way because of sparsity of the resources.

There are several different techniques allowing multiple users to access a shared medium. Some important ones are Time Division Multiple Access (TDMA), time periods are divided into slots which are assigned to different users, e.g. Ethernet, or Frequency Division Multiple Access (FDMA), the assigned frequency band is split into sub-bands which are assigned to users, e.g. GSM, DECT, TV, radio broadcast (Figure 2.1(a)). The division into orthogonal parts works well with these methods but problems arise in case of unbalanced traffic. The channels are normally not variable which means the throughput cannot be adjusted instantanously to the single users needs. Consequently every user gets resources assigned which could be unused or even insufficient in case of bursty traffic , e.g. Internet surfing, voice traffic with pauses. In such cases FDMA and TDMA tend to be inefficient.

To overcome this problem it is possible to allow different users to use the same resources or channels by using spread spectrum signals. This can be conceived as different signatures assigned to different users (Figure 2.1(b)). By the use of this signature the user spreads its data over a wide

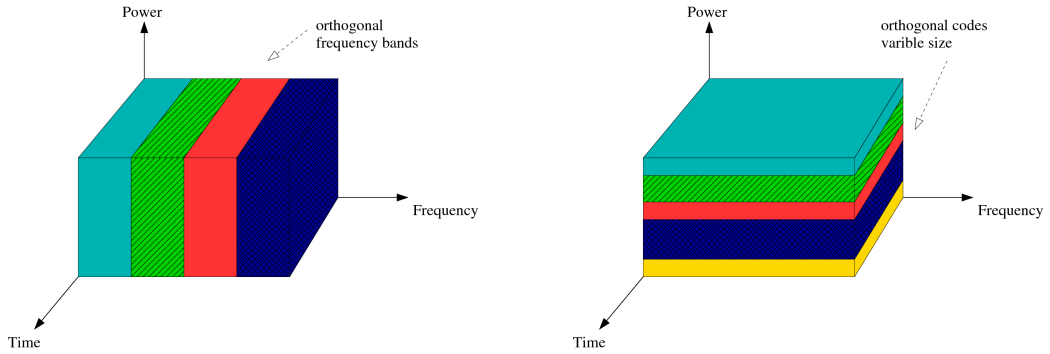

(a) FDMA resource allocation (b) CDMA resource allocation

Figure 2.1: Resource allocation in communication systems.

frequency range, data from different users is overlapping. The receiver can distinguish between the different signals because of the signatures of the users which are orthogonal. The signals can be separated again by cross correlating the received signal with each of the possible signatures. This multiple access method is called Code Division Multiple Access (CDMA) or Spread Spectrum Technique and is deployed in UMTS.

2.2.1 Spread Spectrum Technique

The theory to spread spectrum communication systems is existing since the 1950. Although engineers have been aware of the practical use of such systems it was not feasible to bring them to work. The resons were practical issues. Because of the properties of spread spectrum modulation (low power spectral density over a broad spectrum) there was big interest in this technique from the military. The main reason is that spread spectrum signals look like noise for receivers without kowledge of the spreading code. This fact was a big push for that technology. In the middle of the 80's the first spread spectrum systems started to work (e.g. GPS) and the legal regulations were defined. The first cellular communication system deploying spread spectrum modulation was called IS-95 pioneered by Qualcomm. It became operative in 1995. For more detailed information on spread spectrum techniques see [31].

Modulation and Demodulation

There are several different possibilities of spreading a data signal by means of a certain code sequence. Some fundamentally different examples are time hopping, frequency hopping or Direct Sequence Spread Spectrum (DSSS). The last possibility is the most common used for commercial cellular radio networks because of the relative ease of implementation in comparison to the others. DSSS is also used in UMTS.

In DSSS the signal spreading is achieved by modulating the data-modulated output signal a second time by a spreading sequence. The spreading sequence consists of a defined number so called chips. The chip-sequence has to closely approximate a random signal with uniform distributed symbols. Such sequences are for example digital Pseudo-Noise (PN) sequences over a finite alphabet.

The spreading operation is performed by multiplying every data bit by the spreading sequence, whereas the duration of this sequence is the same as the duration of one information bit. Again note that several chips are contained in the sequence. The length of the spreading sequence or equivalent, the number of chips per data bit is called "spreading factor" and denoted L_s. In consequence the resulting signal after spreading has higher temporal variation and therefore a

broader spectrum, this is the reason for the nomenclature of this procedure. The Bandwidth of the signals behaves approximately according to

$$W_{ss} \approx W_{data}\, L_s \tag{2.1}$$

where W_{ss} denotes the bandwidth of the spread signal, W_{data} the bandwith of the data modulated signal and L_s the spreading factor, respectively.

In WCDMA system capacities have to be maximized, therefore the spreading procedure is done in two steps. The signal to transmit from or to a certain user is first spread by the channelization code. This code consists of an Orthogonal Variable Spreading Factor (OVSF) code, constructed by means of the Hadamard matrix.. The code length is adjusted depending on the desired throughput, the lower the bit rates, the longer the assigned spreading code. An important property of such codes is that different codes, if in phase, are perfectly orthogonal, i.e. they satisfy the relation

$$\langle \mathbf{c_1}, \mathbf{c_2} \rangle = \sum_{i=-\infty}^{\infty} c_{1,i}\, c_{2,i} = 0 \tag{2.2}$$

where "$\mathbf{c_1}$" and "$\mathbf{c_2}$" are two different codes, respectively and "$c_{1,i}$" and "$c_{2,i}$" denote single elements of it. This fact guarantees the codes are separable at the receiver So a maximum number of active users is guarantied.

The next step in the spreading procedure is a cell-specific scrambling of all spread user sequences. This step is done to handle Inter-Cell Interference (ICI). The scrambling sequences are significantly longer than the spreading sequences but do not enhance the spectral width of the signal any more. Nevertheless spectral properties of the stream are changed, the result is a stream with a flat spectrum with no significant peaks. This properties guarantee the weakest interference if the stream is received by a base station not intended as data sink. The combination of these two signal processing procedures ensures the system wide maximization of throughput.

In order to visualize the spreading procedure it should be explained with the aid of a simple example (see Figure 2.2). In the first abscissae the magnitude of the original user-data stream is depicted over time. Right below the spreading sequence can be found. The spreading is done by simply multiplying each data symbol (1^{st} signal) with the spreading sequence (2^{nd} signal). The oucome is a spread signal, depicted next (3^{rd}signal).

The despreading procedure is exactly the same as the spreading procedure, the received spread signal (3^{rd} signal) is multiplied with the same spreading sequence again (4^{th} signal). The outcome should again look like the data sequence (1^{st} signal). In order to maximize the decision criterion and average out noise, an integration over the whole symbol period is done, which, together with the former step, results in a correlation of received signal and spreading sequence (5^{th} signal). As observable this function has its maximum at the sample instance, right at the end of each data symbol.

If this correlation is done with a code which is orthogonal to the spreading sequence (6^{th} signal), the resulting output signal is always zero at the sampling instances (7^{th} signal). This means that the receiver, if expecting a signal spread with this certain spreading code, does not even recognize a superimposed orthogonal signal (e.g. 3^{rd} signal).

It is important to note that the correlation detection at the receiver is able to raise the signal strength by the spreading factor (Figure 2.2, amplitude of the 5^{th} signal). This effect, called "processing gain", is common to all spread spectrum transmission schemes. For DSSS systems the processing gain "G_p" is equal to the spreading factor "L_s"

$$G_p = \frac{SNR_{out}}{SNR_{in}} = L_s \tag{2.3}$$

Therefore CDMA systems are robust against all kinds of interference, e.g. Inter-Cell Interference (ICI), narrow-band interference, noise. To get an idea of the benefits of the processing gain, some examples are given:

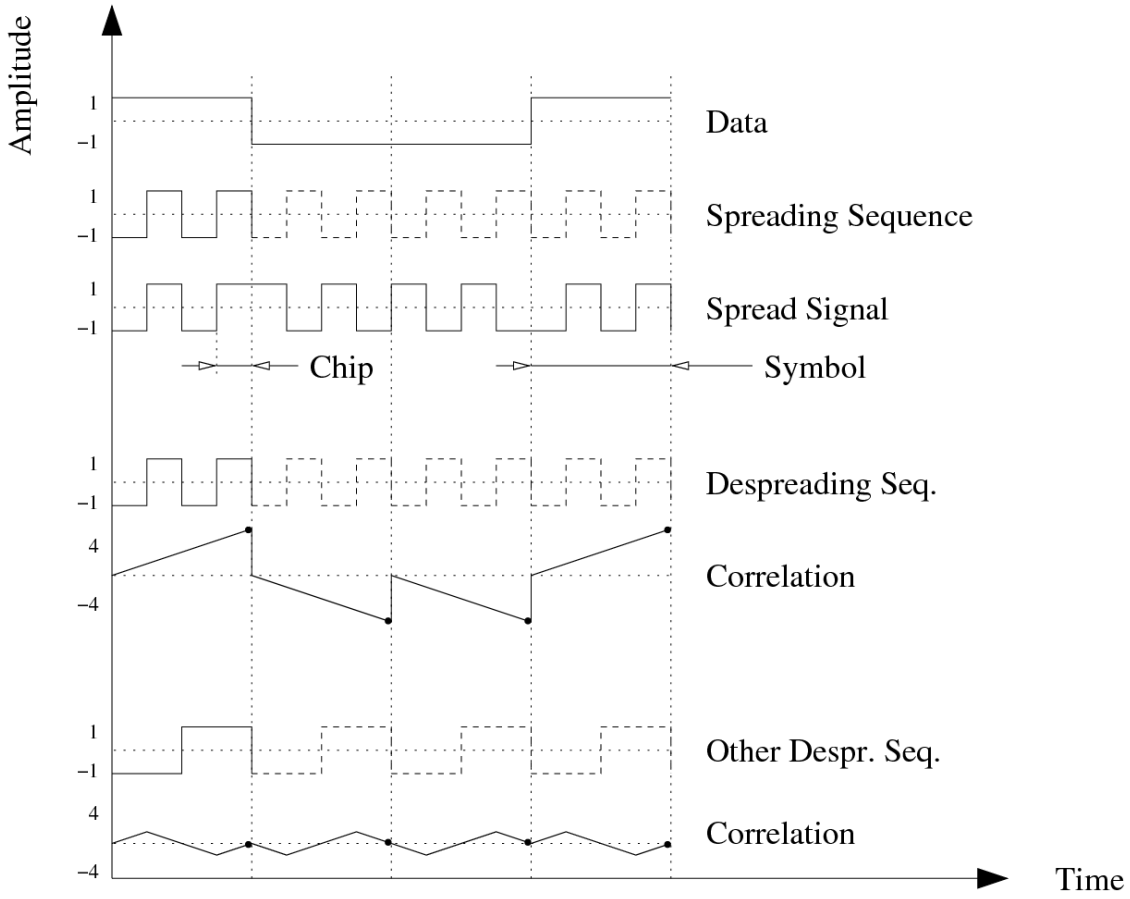

Figure 2.2: Example: Signal spreading by means of OVSF.

Spreading method	Direct Sequence Spread Spectrum (DSSS)
Total bandwidth	5 MHz
Chip rate	3.84 M chips/s
Chip duration	260 ns
Spreading sequence length	variable: 4 to 256
Spreading codes	Hadamard codes
Symbol duration	variable: $\sim 1\mu s$ to $\sim 66\mu s$
Modulation	4QAM (64QAM in HSDPA)
Data rates	variable: 1920 k bit/s to 15 k bit/s
Scrambling sequence length	38400 chips period
Scrambling codes	Gold codes

Table 2.1: UMTS specific radio parameters.

- *Robustness against narrow-band interference*: Assuming a spread spectrum system and a narrow-band interferer within the utilized bandwidth. At the receiver the transmit signal is superimposed by the interfering signal. The receiver itself has to despread the received signal in order to decode it. On the other hand the despreading can be understood as spreading of the interfering signal since spreading and despreading are the same procedure. This means that the power of the narrow-band interferer is spread over a wide band whereas the power of the desired signal is concentrated. The robustness against such interferes is increased strongly.

- *Robustness against white noise*: Assuming a spread spectrum system and white noise within the utilized bandwidth. White noise contains no special patterns, so after the despreading it can still be assumed as white noise. After summation over the symbol period the noise energy per symbol duration is enhance by the spreading factor. On the other hand the desired signals amplitude is enhanced by the spreading factor as well. Hence the symbol energy increased by the square of the spreading factor. The overall processing gain is therefore equal to the spreading factor, see Equation 2.3. This means spread spectrum signals can be weaker than thermal noise and still be recovered correctly. This property makes the communication system attractive for secure transmission of sensitive context. Without any knowledge of the spreading sequence it is nearly impossible to decode the signal.

- *Robustness against frequency selective fading*: If the propagation scenario in which the radio link is established allows for multi-path propagation and the different paths have equal strength, it is very likely that the resulting transfer function of the channel has narrow but deep fading dips at certain frequencies because of destructive interference of different propagation paths. By using spread spectrum techniques the influence of such fading dips is reduced because the signal is spread over a large frequency range. Note that this mechanism is by far not optimum, e.g. OFDM systems can compensate frequency selective fading.

To close this section a short overview of the WCDMA-parameters deployed in UMTS is given in Table 2.1.

Multi-path Channels

A possible characterization of a transmission channel is its time-variant impulse response, $h(\tau, t)$. In a mobile radio environment the channel normally consists of several time-delayed components, resulting from different reflections in the propagation environment. The reason are natural obstacles such as buildings, hills, walls, etc. Such a situation is called a multi-path environment. The time-variance is caused by the movement of the objects in the mobile scenario, i.e. User

Equipment (UE) and reflecting objects. In consequence a signal transmitted in a multi-path environment will be received as many replica of the original signal, all with different delays and amplitudes.

The DSSS modulation scheme enables the use of sophisticated receivers, such as the RAKE receiver. This kind of receiver can make use of the energy received from different propagation paths as long as the delay between them is longer than one chip duration and shorter than a symbol duration. The RAKE receiver recognizes at which time instances the strongest replicas of the desired signal arrive at the UE. At these instances a respective correlator, called finger, starts to decode the sequence. After one symbol duration the reception should be accomplished and the output signal from the different fingers are combined using Maximum Ratio Combining (MRC). Thus the signals coming from different paths are combined as

$$y = \sum_{i=1}^{N} h_i^* y_i \tag{2.4}$$

wherer "y_i" denotes the i^{th} received signal and "h_i" the respective channel coefficient, which has to be known at the receiver. The Chauchy-Schwarz inequality yields this is optimum for signal to noise ratio maximization. It leads to an enhancement of the signal to noise ratio "γ", assuming white Gaussian noise, i.e.

$$\gamma = \sum_{i=1}^{N} \gamma_i \tag{2.5}$$

So the RAKE receiver does not only compensate for the multi-path environment, it makes use of it. The shorter a chip duration, the higher the temporal resolution of the rake receiver. The trade off is the increasing chip rate which results in an increased transmission bandwidth.

Soft and Softer Handover

In every mobile cellular network the possibility of changing cells during an active connection creates a problem which absolutely has to be addressed. The fact that CDMA communication systems reuse the same frequency band in every cell, often referred to as frequency-reuse one, gives an advantage in comparison to other systems. TDMA and FDMA radio access networks have to terminate an existing connection from a cell to a certain UE before a new connection to the next cell can be established. In CDMA networks contemporary connections to more than one cell are possible. This situation is called "Soft Handover (SHO)".

During SHO the UE is in the overlapping cell coverage region of adjacent cells. Two or more radio links are established, one to each cell. This requires different scrambling codes for every radio link to allow the UE to distinguish between them. The two signals are received at the mobile station by the RAKE receiver, which has to place a finger on each of them. This procedure is very similar to multipath-reception except that the different fingers have to descramble the sequences with different codes. So SHO is a form of diversity, increasing the signal to noise ration assuming constant transmission power. In the uplink the situation is similar, several Base Stations (NodeBs) are receiving the transmitted signal. A difference arises in the combination of the signal, which can not be combined according to MRC because of latency constraints. Instead the best signal from the set is chosen, the other ones are discarded (Selection Combining). This can be formulated as

$$y = y_i, \qquad \arg\min_i(BER_i) \tag{2.6}$$

In the case of UMTS the Bit Error Ratio (BER) is the indicator to minimize for choosing a signal, but in general also other indicators like Signal to Interference Ratio (SIR) could be used.

If the UE finds itself in a scenario where it is connected to different sectors of the same NodeB contemporary, MRC can again be deployed, see Equation 2.4. This scenario is referred to as "Softer Handover".

Soft and softer handover come with the drawbacks of enhanced resource use. More than one NodeB have to allocate the same resources for one single mobile, i.e. RAKE-fingers and spreading sequences. The need of more than one radio link is called "soft handover overhead". However by doing the handover this way it is ensured that no mobile comes to close to the center of cells which have no control over it. The connection to multiple sites also allows the mobile to spend less power by transmitting the signal which saves battery energy and reduces interference. This is called "soft handover gain". Note that in urban scenarios with high density of NodeBs a UE could be permanently in SHO.

Advantages and Drawbacks

In the following a summary of UMTS air interface parameters and procedures is given and the advantages and drawbacks in comparison to non-CDMA systems are revealed.

Deployment of WCDMA in UMTS brings many advantages. The first one to mention is the processing gain of the communication system. The tradeoff is the enhanced bandwidth used for communication. The more bandwidth available, the better WCDMA works, but bandwidth is a sparse and expensive resource. The processing gain guarantees for a certain robustness against noise and interference, already mentioned in Chapter 2.2.1, page 6.

Because of the separation of users by means of their spreading sequence and not of frequency bands frequency-reuse one is possible (see Chapter 2.2.1, page 9). Communication systems before UMTS had a frequency-reuse of at least three. This means only a third of the available bandwidth is assigned to a cell. So UMTS could raise the system wide throughput for a factor of three, hence it is very economic for a service provider. The tradeoff by making use of frequency-reuse one is the strong interference from neighboring cells, if they are fully loaded. In this case the throughput is decreasing.

In cases where ICI is very strong, i.e. connections to users at cell borders, the resources dedicated to this UE are allocated also in neighboring cells and multiple radio connections are established to one UE. Such SHO scenarios (Chapter 2.2.1, page 9) bring a performance boost, the UE is able to save transmit power and the ICI is reduced. Again we encounter a tradeoff, i.e. more network resources than necessary are dedicated to one user equipment.

Because of sharing the resources among each other it is very likely that different users also interfere each other. In fact UMTS implies a tight power control mechanism for UEs as well as NodeBs to mitigate any kind of interference. Creating less interference means enhancing the throughput of other users and therefore every transmitter should take care of not transmitting with higher power than absolutely required (for its desired throughput and QoS).

By deploying WCDMA in the radio link UMTS systems put high demands on hardware. Many restrictions on various parameters make network entities very complex. Some examples are:

- Maximum delay restrictions force to apply a decentralized network architecture.
- Due to high decoding complexity the receivers have to be able to do massive parallel processing (e.g. RAKE fingers).
- The HF amplifiers of the transmitters must be very linear because of the high dynamic range of WCDMA signals. Otherwise the distortions would make the transmission scheme inefficient.

These facts make the hardware costly and raise the power consumption.

2.2.2 User Data Transmission

As already described in Chapter 2.1, page 3, UMTS has to be able to cope with multiple services and applications resulting in a variable bit rate and QoS. Hence the system is designed for long term duration and respective concepts to provide the necessary flexibility for further evolution are

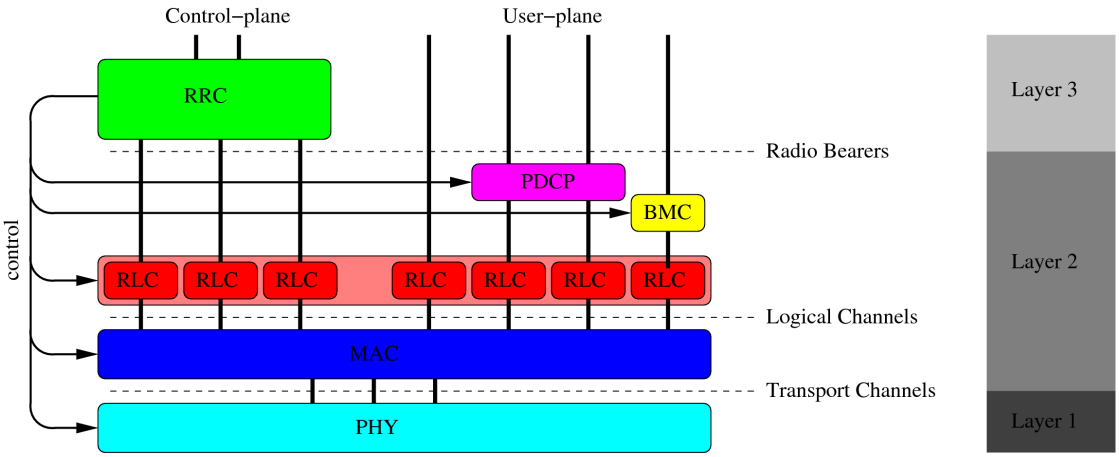

Figure 2.3: Radio interface protocol architecture.

implemented. The realization of these drafts mostly affects the lowest layers in the communication protocol stack. The design and functionality of the Medium Access Control (MAC) layer and the Physical (PHY) layer are summarized in the following (Chapter 2.2.2, page 11 and Chapter 2.2.2, page 12 respectively).

In 3GPP the UMTS architecture is grouped according to high-level functionality in Access Stratum (AS) and Non-Access Stratum (NAS) (see [11]). The NAS is the group of protocols which allow for higher-layer communications. These protocols are service or application specific, e.g. call control for circuit switched voice and data, Short Message Service (SMS) or session management. The AS is the group of protocols that provide the connection of UE to the core network of the mobile operator for NAS protocols. All the procedures concerning the radio link like handover, variable data rate CDMA transmission or random access, are handled in the AS. It is desired to provide a common and unified interface between AS and NAS, which is realized with so called "Service Access Points (SAPs)". Furthermore communication through SAPs must be data-transparent for NAS protocols. In the following AS procedures are considered in more detail.

Channelization

The data received by the AS through the SAPs is handled by data channels (Figure 2.3) There may exist multiple parallel channels contemporary. These data channels may be unidirectional or bidirectional and can be used for data transmission or controlling of the AS. Depending on the respective network layer, different higher-layer channels are processed and handed to lower-layer channels. Control instances, e.g. Radio Resource Control (RRC), Radio Link Control (RLC), in the AS define the processing of the channels in the respective layers according to specifications made by the NAS and actual data rates.

Medium Access Control Layer Data Handling

The MAC layer corresponds to layer 2 of the Open System Interconnection (OSI) model. Detailed informations about MAC can be found in [13]. Its task is the mapping of logical Channels onto appropriate Transport Channels (TrCHs). Logical channels are bidirectional channels coming from the upper layer (RLC). Separate channels are transporting information from different sources. Transport channels on the other hand differ in the way information is transmitted at the air interface (e.g. shared connection or dedicated link, QoS, data rate). They are unidirectional. So MAC supports multiplexing/demultiplexing upper layer Packet Data Units (PDUs) into/from transport channels. Some other features of the MAC are ciphering, traffic volume measurement

and splitting of the TrCH data into Transport Blocks (TBs) of suitable length. Last but not least the MAC layer provides an efficient use of the TrCH by selecting an appropriate Transport Format (TF) based on the instantaneous source rate.

In order to get an insight into data processing of the PHY layer, it is useful to be aware of the format which is used to send data from MAC to PHY layer. Its general structure is described in the following. Before explaining the composition of the TrCHs some terms valid for all types of TrCH are introduced (for more detail see [12]):

- *Transmission Time Interval (TTI)* denotes the length of the basic time interval used for information exchange. It is fixed for a certain TrCH and can take on 10 ms, 20 ms, 40 ms or 80 ms.
- *Transport Block (TB)* is the basic information unit delivered from MAC to PHY. Its length is variable and set by the MAC.
- *Transport Block Set (TBS)* is the set of TBs that is exchanged in the same TTI on the same TrCH. The number of TBs in the TBS is variable. All the TBs in one TBS have to have the same length.
- *Transport Format (TF)* terms a collection of parameters possibly assigned to a TBS. It refers to a certain TrCH and contains for example the TB-size, the number of TBs in the TBS, the coding type, QoS indicators. Some parameters of the TF are static whereas others are dynamic (may vary from TTI to TTI). A TF is provided by the RRC.
- *Transport Format Set (TFS)* is the group of all applicable TFs for one specific TrCH. In every TTI one TF from the TFS is chosen by MAC and applied to the respective data. The static parameters of the TFs are the same in the whole TFS.
- *Transport Format Indicator (TFI)* identifies a certain TF in a TFS. It corresponds to a label attached to a TBS and is used for inter-layer communication, i.e. to communicate PHY which TF MAC has chosen for the respective TBS.
- *Transport Format Combination (TFC)* is a term used when more than one TrCH are active. It denotes the combination of the different TFs coming from different TrCHs in the same TTI. Theoretically the number of TFCs is equal to the product of the numbers of TFs in the TFSs of every TrCH. In reality not every arbitrary combination is possible but it has to be authorized by RRC.
- *Transport Format Combination Set (TFCS)* is a collection of all authorized TFCs.
- *Transport Format Indicator (TFCI)* identifies an authorized TFC in the TFCS. It is a label attached to the data transmitted on the air interface to communicate the receiver the transmission format of the actual frame.

To give an overview of the functionality of the TrCH-mapping an example is depicted in Figure 2.4.

Physical Layer Data Handling

In the following the physical layer data processing is tread in more detail because it is essential for the practical part of this work (Chapter 3), especially data transmitted in the uplink (from UE to the NodeB). The focus will be on Dedicated Channel (DCH) data because most of the transfered uplink data belongs to this type (except packet data in UMTS releases after Release 5). For the sake of completeness Table 2.2 gives a listing of all transport channels.

The physical layer implies the whole WCDMA transmission scheme as well as Forward Error Correction (FEC) multiplexing of various data streams and High Frequency (HF)-transmission. A

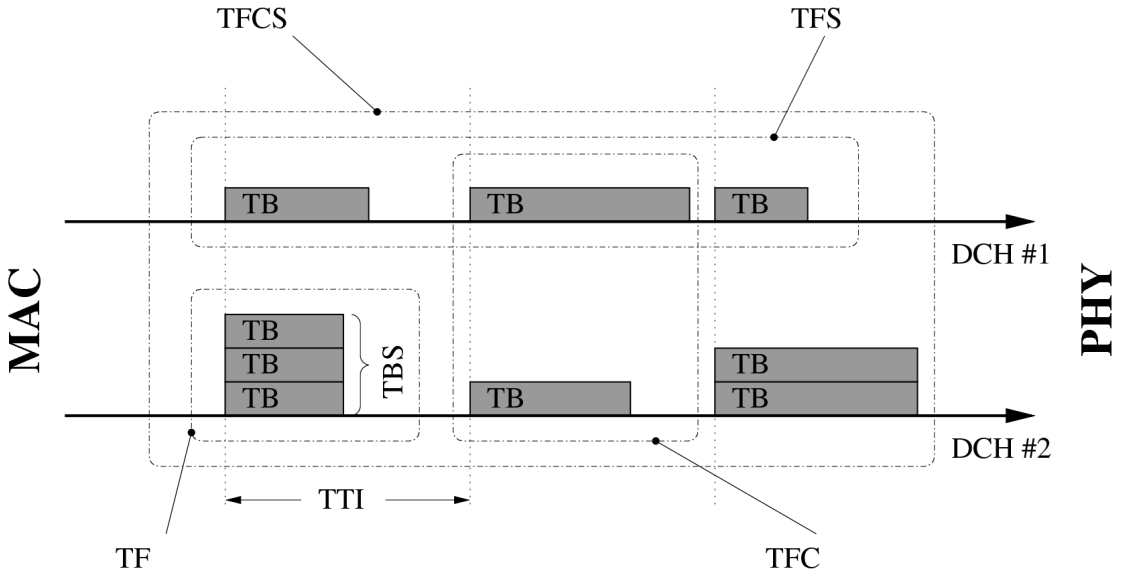

Figure 2.4: Example: Data flow over TrCHs.

Transport Channel	*Physical Channel*
Dedicated Channel (DCH)	Dedicated Physical Data Channel Dedicated Physical Control Channel
Enhanced Dedicated Channel (E-DCH)	Enhanced DPDCH Enhanced DPCCH
Random Access Channel (RACH)	Physical Random Access Channel
Broadcast Channel (BCH)	Primary Common Control Physical Channel
Forward Access Channel (FACH) Paging Channel (PCH)	Secondary Common Control Physical Channel
High Speed Downlink Shared Channel (HS-DSCH)	High Speed Physical Downlink Shared Channel HS-DSCH-related Shared Control Channel
no corresponding TrCH	Common Pilot Channel Synchronization Channel Acquisition Indicator Channel Paging Indicator Channel

Table 2.2: Mapping of transport channels onto physical channels.

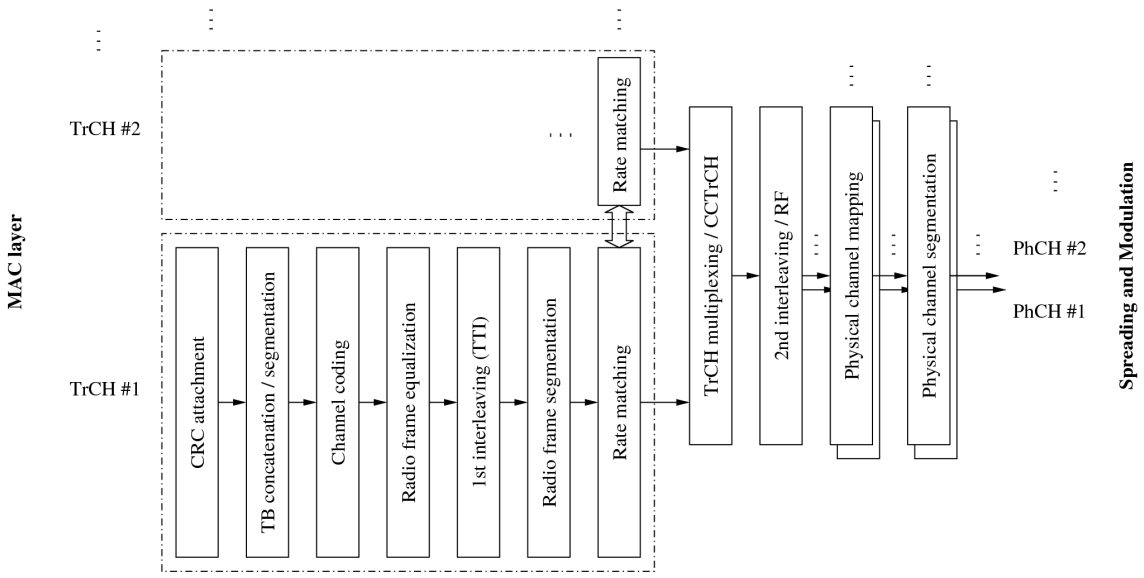

Figure 2.5: Example: Physical layer data processing chain.

general description is given in [6] and detailed information about the different parts of the PHY can be obtained in [7], [8], [9] and [10].

Figure 2.5 depicts the data encoding chain of the physical layer in the uplink direction. The downlink chain looks quite similar although some additional processing units are present and some parameters are different. The decoding chains of uplink and downlink can be imagined as the exact inverse of the encoding chains. For sake of simplicity only the uplink encoding chain will be explained in more detail:

- *CRC attachment*: After reception of the TBs by means of the TrCHs a Cyclic Redundancy Check (CRC) checksum is attached to every TB. The length of the sum is controlled by the RRC protocol via TFs and can vary from 0 to 24 bits.
- *Code block concatenation/segmentation*: The TBs are concatenated and segmented into blocks of equal size to fit the encoder length, i.e. 504 bits for convolutional coding, 5114 bits for turbo coding.
- *Coding*: In the following the blocks undergo the channel coding procedure. This procedure is also controlled by the RRC protocol via TFs. There are two possible types of channel encoding, either convolutional coding or turbo coding. Also the coding rate can be chosen, i.e. one (no coding), half or third.
- *Radio frame equalization*: After coding the radio frame equalization takes place. It performs a padding of the input blocks to ensure that the block length is suited for the following procedures.
- 1^{st} *interleaving*: The data blocks are interleaved, which is performed over the whole TTI. This corresponds to a simple permutation of the incoming bits.
- *Radio frame segmentation*: Now the data blocks are segmented depending on the respective TTI. Blocks with long TTIs are broken down to shorter blocks with a length adapted to a TTI of 10 ms. This is done because different TrCHs may have different TTIs but must be multiplexed to the same common channel. This transmission instance of 10 ms is called Radio Frame (RF).

- *Rate matching* is a complex procedure that prepares the data blocks from the single TrCHs to be multiplexed. First an appropriate spreading factor has to be chosen which is suited for transmission of the actual incoming amount of data. According to this spreading factor a so called "gain factor" is calculated in order to maintain a certain level of QoS. This is done according to

$$\beta_j \;=\; \beta_{ref} \sqrt{\frac{L_{ref}}{L_j}} \sqrt{\frac{K_j}{K_{ref}}} \tag{2.7}$$

  where "j" id the index for the TFC, "ref" denotes one TFC for which parameters have been communicated from the Serving RNC (SRNC), "L" is the number of Dedicated Physical Data Channels (DPDCHs), and "K" a factor calculated as follows

$$K_j \;=\; \sum_i RM_i \; N_i \tag{2.8}$$

  Thereby "i" denotes the different TrCHs in the j^{th} TFC, "RM" is the rate matching attribute and "N" is the number of bits output by the radio frame segmentation block for the i^{th} TrCH, which in turn is dependent on the spreading factor. The gain factor is the value which indicates the amplitude ratio of control signal and data signal. Now the single data blocks from the different TrCHs are processed to guarantee certain QoS ratio between different streams. Every TrCH has a Rate Matching (RM) attribute, also controlled by RRC via TFs, which is a measure for importance of the respective data. So in this step important channels are protected better than unimportant ones. This is achieved by puncturing or repeating single bits of the data blocks.

- *TrCH multiplexing*: Data blocks from different TrCHs are combined into one common channel, called Common Coded Transport Channel (CCTrCH). There is only one single CCTrCH for a transmission.

- *Physical Channel Segmentation* divides the CCTrCH into several physical channels if the total number of bits exceeds the maximum number of bits on one physical channel. In this case multi-code transmission is deployed (if UE and NodeB are capable to do so).

- 2^{nd} *interleaving*: The data blocks are interleaved a second time, now on a radio frame basis (10 ms). Note that this interleaving also exchanges bits from different TrCH.

- *Physical channel mapping*: In this step the information on the physical channels is mapped on radio frames with respective symbols to be transmitted. The out coming signal of this last processing block is called DPDCH.

Some fundamental examples of how data is processed are shown in [3]

To conclude this section the dedicated physical channel structure is introduced. Again, as an example, only the structure of the Dedicated Channels (DCHs) is explained. Figure 2.6 shows the uplink and downlink channel structure respectively. The modulation scheme is 4-Point Quadrature Amplitude Modulation (4QAM). The superior unit is the so called radio frame which is corresponding to a data block at the CCTrCH. For the duration of a radio frame all radio parameters are constant. Its duration is 10ms, corresponding to 15 slots or 38400 chips. One slot contains 2560 chips and its duration is 667 μs, which matches a power-control period. The structure of a slot is depicted detailed.

There are two different types of dedicated channel transmitted on the radio link, i.e. the DPDCH and the Dedicated Physical Control Channel (DPCCH). The DPDCH contains all the user data as well as control information from higher layers. Its bit rate is variable according to the spreading factor in use, e.g. if the spreading factor is 256, one slot contains 10 bits (15 kbits/s). The DPCCH on the other hand contains all the layer 1 control information which is needed to

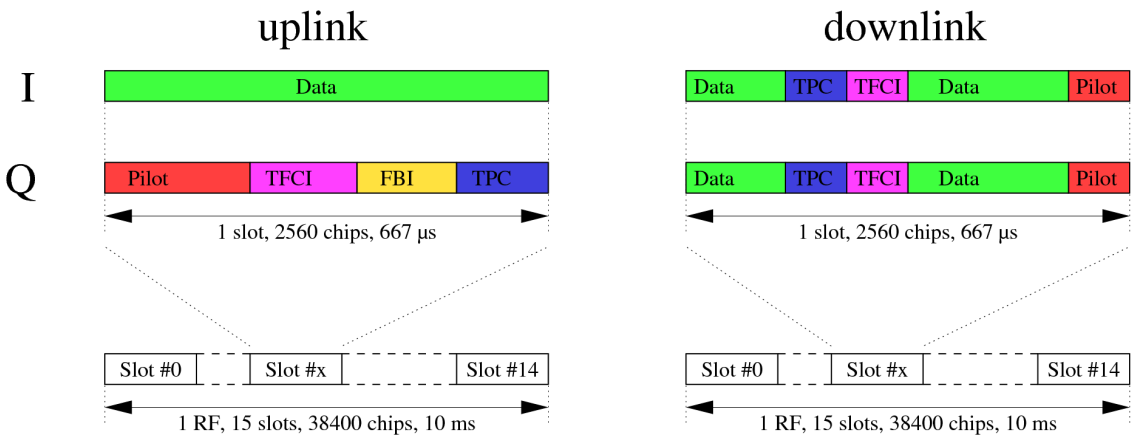

Figure 2.6: Structure of dedicated channels in uplink and downlink.

decode the frame correctly. It comprises predefined pilot symbols, power control information and optionally the TFCI and Feed-Back Information (FBI) for multi-antenna techniques. In contrast to the DPDCH its bit rate is constant, i.e. 15 kbits/s.

As depicted in Figure 2.6 the mapping of the data to 4QAM symbols is different in uplink and downlink. In the uplink DPDCH and DPCCH are modulated on the In-phase (I) and Quadrature (Q) component respectively. Because of the different power levels used for data and control transmission this results in a stretched 4QAM constellation. In the downlink DPDCH and DPCCH are time-multiplexed whereas every two bits form a 4QAM symbol. Only in the downlink transmission gaps are possible because no further data is to be transmitted, in the uplink the rate matching algorithm prevents this situation. On the contrary, in the uplink transmission gaps are possible if the UE works in compressed mode. This mode enables the UE to scan other frequency bands for the possibility to hand over, e.g. to another provider or another Radio Access Technology (RAT).

2.2.3 Physical Layer Procedures

The UMTS physical layer has to handle many procedures essential to guarantee the proper functionality of the different connections. Examples are power control and soft handover as well as other functions partially already described in Chapter 2.2.1. In addition procedures concerning the networking are handled by the PHY layer. Some of them are random access procedures, paging, handover measurements and operations with transmit diversity. These procedures have been shaped by the WCDMA specific properties. Further information can be found in [10]. In the following processes of high relevance for the practical part of this work (Chapter 3 and 4) are explained.

Power Control

As descried in Chapter 2.2.1 a power control mechanism is essential for all kinds of CDMA communication systems. It ensures for low interference at the receivers in the whole network. The reason is the so called “near-far-problem”. It is explained best by a simple example, see Figure 2.7. Lets assume two mobile stations in a cell. UE1 is very close to the base station whereas UE2 is located at the cell border. It may be that UE2 suffers a Free Space Path Loss (FSPL) which is more than the processing gain above the path loss of UE1. Since the signals of both mobiles are transmitted at the same time and frequency they are only separated by their spreading codes. If there were no mechanism to control the transmission power of the mobiles it could easily be that

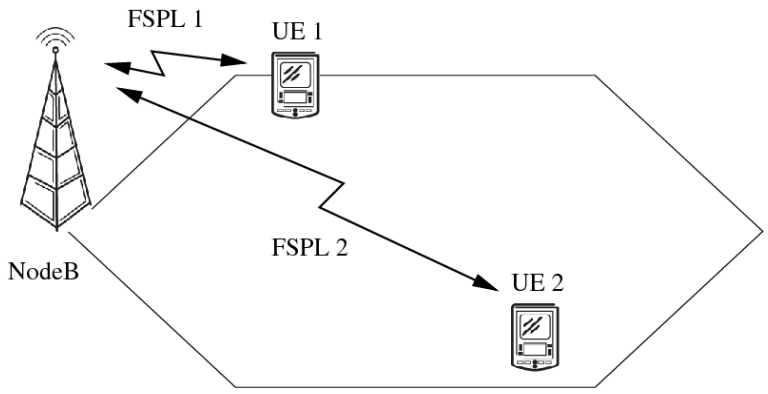

Figure 2.7: Near-far problem in UMTS.

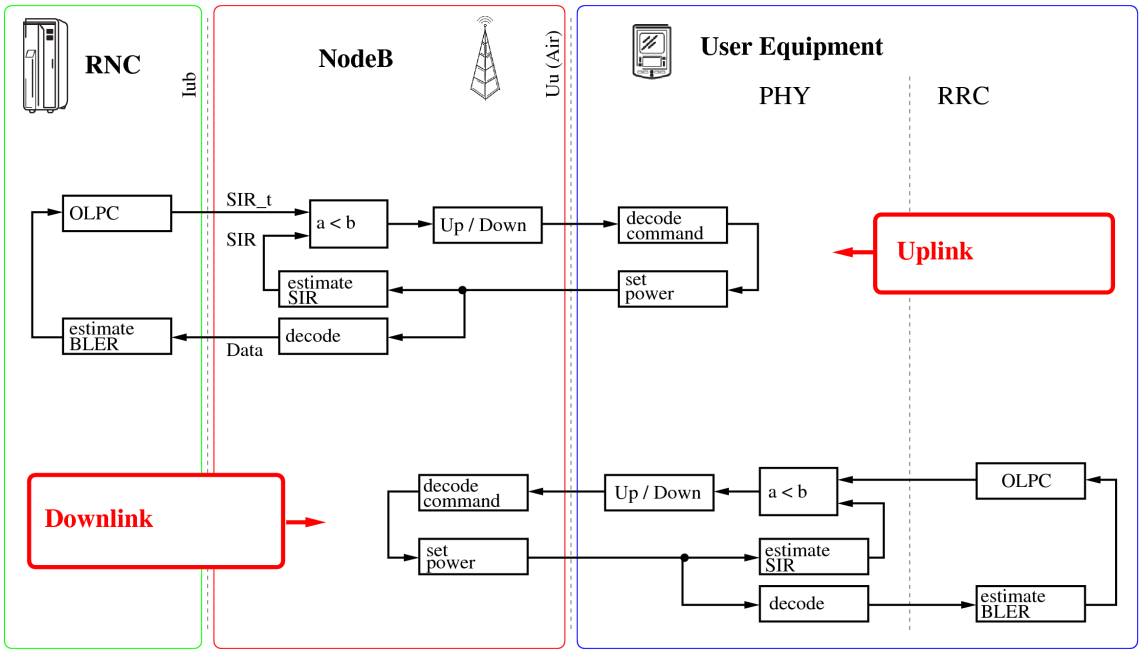

Figure 2.8: UMTS power control loop.

UE1 is over-shouting UE2. In this case one mobile would block a large part of the cell preventing all the other users from transmitting data. The best strategy in terms of improving throughput is to equalize the received power of all UEs at all times. For informations about the impact of power control on capacity see [43], [30]. More details about the UMTS specific power control can be found in [26].

Experience shows that the attempt to use a so called open-loop power control to overcome this situation would be far to inaccurate. Open-loop power control is a mechanism which tries to estimate the transmission path loss by means of the strength of the received signal. The main reason it does not work is that the fast fading in uplink and downlink is uncorrelated because of the large frequency separation of the respective bands in WCDMA FDD mode. Open-loop power control is used however in UMTS but only to provide a loose initial value for the power settings at the transmitters.

The solution deployed in UMTS is a so called closed-loop power control. This type of power

control is implemented in both transmitter and receiver. The receiver measures the power of the incoming signal and compares it to a target value which is based on QoS restrictions. According to the outcome of the comparison a feedback is given to the transmitter via reverse link. This closed-loop power control is based on a double control loop depicted in Figure 2.8. It can be seen that the loop extends over three network elements, the UE, the NodeB and the Radio Network Controller (RNC). The power control is used in uplink and downlink. The double control loop is divided into Inner Loop Power Control (ILPC) and Outer Loop Power Control (OLPC), which are separately explained in the following paragraphs.

This work is focused on the power control of DCHs, see Table 2.2. Figure 2.8 shows also the power control mechanism of DCHs. Power control mechanism for other channels may be different and will not be concerned, e.g. power control in the connection establishment phase, power control in High Speed Packet Access (HSPA), etc.

Inner Loop Power Control The ILPC or fast closed-loop power control can be identified in Figure 2.8 as the loop between UE and NodeB. Every time the receiver gets a signal, it estimates the received SIR after despreading the data stream. It is calculated according to

$$SIR = \frac{RSCP}{ISCP} L_s \tag{2.9}$$

where Received Signal Code Power (RSCP) is the unbiased measurement of the received power on one code and Interference Signal Code Power (ISCP) is the interferecne on the received signal. L_s denotes the spreading factor. This estimate is compared to a target SIR value. If the actual value is below or above the target value, the receiver gives a feedback to the transmitter via reverse channel either to rise or lower the transmit power. The respective commands are transmitted at the DPCCH (see Chapter 2.2.2, page 12). The transmitter has to react to this command immediately and adjust the power level accordingly.

The execution of the ILPC procedure happens on slot (see Chapter 2.2.2) basis, i.e. 1500 times a second. The high frequency of the control mechanism guarantees that no significant change of path loss happens during one cycle. Indeed it is even fast enough to compensate path loss changes due to Rayleigh fading up to certain speeds of the UE. In consequence fast close-loop power control ensures for perfect balance of the different received signals.

The respective signal strength is constant over time and the channel can be considered as time-invariant. The up and down step size is per default 1 dB, a command for keeping the power constant does not exist. But there exist different control modes and in consequence the step size can be adjusted up to 2 dB and even a 0 dB step size can be emulated. In general step sizes below 1 dB are not suggestive because of difficulties of implementation. The problem is to ensure the accuracy over the large dynamic range.

The SIR target value mentioned above is given by the OLPC, which is explained in the next section. While the fading removal is highly desired at the receiver it comes with the drawback of increased average transmission power at the transmitter.

Outer Loop Power Control OLPCis a mechanism to control the SIR target value the ILPC should be locked on. It aims at providing the desired QoS in terms of Block Error Ratio (BLER). If the received signal is better than required, the SIR target can be lowered to meet the error specifications of the underlying service. Otherwise resources would be waste. If the received signal is worse than required the SIR target must be raised to guarantee proper work of the respective higher layer service. For the uplink connection this is done by a control mechanism placed in the RNC. It has to estimate the QoS by use of available parameters and give a feedback to the respective NodeB. The controller must be located in the RNC because it is the first instance in the network where the information streams from SHO are combined. For the downlink the controller as well as the respective receiver are located in the user equipment. An OLPC is needed in both

uplink and downlink because of the presence of an ILPC in both branches. For the sake of stability the OLPC has lower dynamics as the ILPC. The SIR target may be changed every 10 to 100 ms.

The question arises why the SIR target needs to be controlled and not just fixed for a certain QoS. The reason is that depending on the mobile speed (Doppler spread) and multi-path propagation conditions the achievable QoS changes in comparison to the SIR, e.g. if the Doppler spread is very high, the connection is not as power efficient as without Doppler spread. In general it turns out that the higher the variation of the received power, the higher the SIR target needs to be to fulfill the same QoS restrictions. This variations can come up to several dBs what justifies the deployment of an OLPC.

There are several parameters available at the controller that provide a more of less accurate estimation of the actual QoS. One of the most simple and reliable indicators is the CRC code attached to every packet (see Chapter 2.2.2). By evaluating the CRC one can investigate whether the transmitted frame contains a block error or not. The problem is that there is just one CRC every TTI (10 to 80 ms). This leads to a low dynamic of the whole algorithm, especially for connections with high QoS where an error occurs e.g. every ten seconds. On the other hand the QoS parameter can also be estimated by the use of soft frame reliability information, i.e. uncoded BER of soft output of turbo or convolutional decoder, providing much higher dynamics (see Chapter 3).

The stability of this control loop not only depends on the UE and NodeB but also on all the other UEs in the cell. Note that the SIR target is controlled, which also includes the interferers. For this reason the dynamic range of the OLPC is limited. This providence also prevents the transmitter to drift into regions below minimum transmit power or above maximum transmit power.

If multiple services are requested by the UE, multiple streams with different QoS requirements are set up. Since there is only one DPCCH only one ILPC exists per UE and only one OLPC is needed. In consequence the OLPC must be locked on the best QoS. The rate matching mechanism gurantees in consequence that the different QoSs are in the same ratio to each other as the respective rate matching attributes (see Chapter 2.2.2).

2.3 Access Network Architecture

This chapter gives a general overview of the UMTS network architecture and its single components. The system is build to coexist with second generation networks, like GSM. Therefore many components from old networks are reused. One objective of the UMTS network design and specification is to guarantee an open standard. This means that arbitrary manufacturers are allowed to produce hardware suitable for UMTS networks. In order to satisfy this criterion the system has to be defined in such detailed way that even equipment from different manufacturers plays together. 3GPP pursued the approach to specify the interfaces between different network components and the tasks of them. The way of implementing is totally open to the manufacturer, what makes the system responsive for new technologies and further evolution. Specific information can be found in the standard, i.e. [4], [15], [16] and [17]. Good summaries of this topic are also provided by [27] and [34].

The UMTS network can be divided into three main parts, i.e. the User Equipment (UE), the UMTS Terrestrial Radio Access Network (UTRAN) and the Core Network (CN). In Figure 2.9 an example of such a network is shown. This sketch contains only components located on the data path, there may be others to aid for user location, billing, etc. It can be observed that the network is connected to two different types of external networks, i.e. Public Switched Telephone Network (PSTN), including other Public Land Mobile Network (PLMN), and the Internet.

The network is highly modular, the number of same components in a network is not specified. This is valid for every network entity. An UMTS network can be desired as complete and functional if at least one component of every type is present (note that certain features of the network are

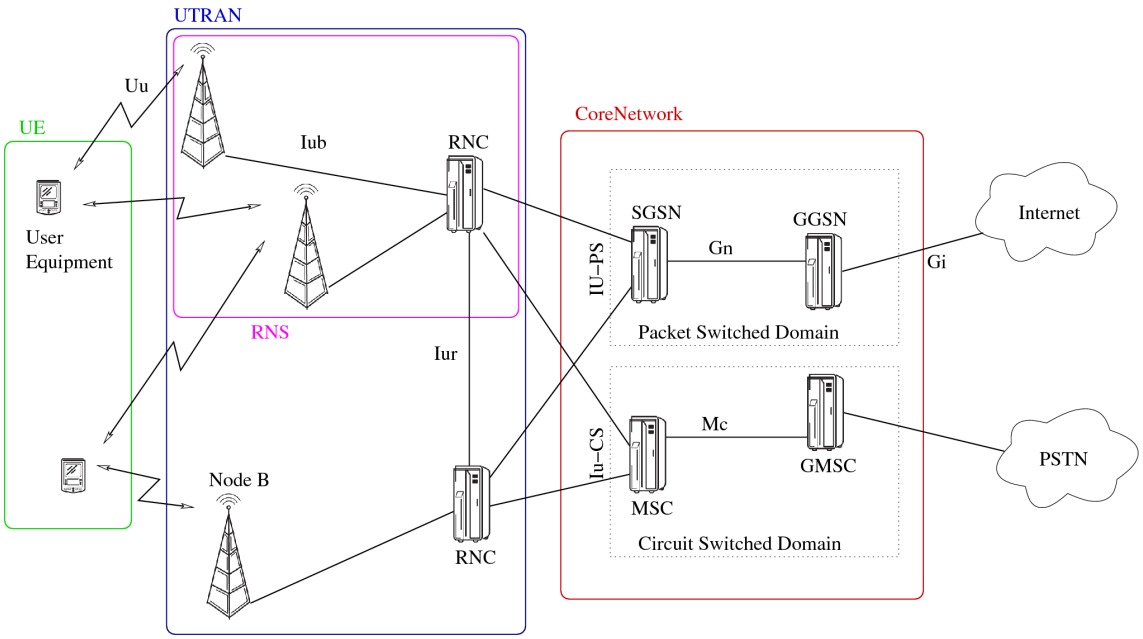

Figure 2.9: UMTS network entities and connections.

optional and so are also the respective components).

2.3.1 Core Network

In essence UMTS uses the GSM core network. But to support higher data rates upgrading of the involved entities is necessary. As shown in Figure 2.9 the UMTS CN is logically divided into two parts, the Packet Switched (PS) domain and the Circuit Switched (CS) domain. Network entities common to both domains are e.g. location registers (used to locate mobiles in the network), authentication center and equipment identity register (used to verify the user identity) and Short Message Service (SMS) related entities.

The CS domain contains the Mobile-service Switching Center (MSC) and the Gateway MSC (GMSC). All circuit switched connections are passed through entities of the CS domain. The terminology “circuit switched” means that a connection is established and maintained between two different circuits. Examples would be connections to transmit voice or fax-data.

The PS domain on the other hand contains the Serving GPRS Support Node (SGSN) and the Gateway GPRS Support Node (GGSN). As already understandable from the naming of the entities they are adopted from the GPRS network. They are exclusively used for processing packet-data, e.g. Internet traffic. Packed switched data has in contrary to circuit switched data no established connection from source to sink. The packets are forwarded by network elements according to their destination addresses.

For the underlying network and connectivity structure of the core network exist two approaches, i.e. Asynchronous Transfer Mode (ATM) based networking and Internet Protocol (IP) based networking. ATM is suited for the UMTS core network because it already comes with a connection-oriented mode and QoS support. IP is perfectly suited for Internet traffic for obvious reasons and it is an efficient solution for simultaneous services. The connection oriented services relying on QoS have to run on other protocols upon IP, e.g. Transmission Control Protocol (TCP), Voice over IP (VoIP).

2.3.2 UTRAN Architecture

The UMTS Terrestrial Radio Access Network (UTRAN) contains all the parts of the network to allow the UE access the providers CN. It is the bridge between Uu and Iu interface. Its main task is to provide so called Radio Access Bearers (RABs) between UEs and CN. This is part of the bearer concept introduced in Chapter 2.1. The RAB can be understood as a persistent path between UE and CN, which means UTRAN has to handle all short-term mobility issues. Furthermore the UTRAN has to guarantee a certain QoS for the RABs, assigned by the CN.

UTRAN can be divided into one or more Radio Network Sub-systems (RNSs), as depicted in Figure 2.9. A RNS consists of one RNC and at least one NodeB. Different RNS are interconnected via Iur-interface between the RNCs, whereas the connection between RNC and NodeB is called Iub-interface.

The main characteristics of UTRAN are:

- Support of all WCDMA specific functionality, e.g. transmission, reception, SHO, etc.
- Performance of Radio Resource Management (RRM) procedures, e.g. admission control, packet-scheduling, etc.
- Maximum commonalities between packet-switched and circuit-switched traffic.
- Maximum commonalities between UMTS and GSM.
- Possible use of ATM or IP oriented network.

Radio Network Controller

The RNC is the controlling and switching entity in the UTRAN. It is connected to the two CN entities, i.e. SGSN and MSC, via Iu-interface, to one or more NodeBs via Iub-interface and optionally to other RNCs via Iur-interface. As controlling instance of the UTRAN the RNC is the termination point for the RRC protocol, the central protocol of the networking layer (layer 3) in UMTS networks. Its tasks can be divided into logical roles which are explained briefly in the following:

- *Controlling RNC (CRNC).* A RNC has control over certain cells and NodeBs. It is responsible for load and congestion control, admission control and radio link establishment as well as code allocation and management in its cells. For this purpose RNC and NodeBs are connected by a persistent link, deploying a special protocol called NodeB Application Part (NBAP), see Chapter 2.4.
- *Serving RNC (SRNC).* Concerning RABs the RNC performs a mapping of them onto Radio Bearers (RBs), which can be handled by NodeBs. A RB is a dedicated connection between UE and RNC that carries user-data related information. In case the RNC is the termination point of the RB, it is called SRNC for a certain UE connection. In this case the Frame Protocol (FP) is deployed for data communication between them, see Chapter 2.4. Another task is to perform RRM for the specific UE. This includes procedures as OLPC for uplink and SHO decisions. Every UE has one and only one SRNC.
- *Drift RNC (DRNC).* In a soft-handover scenario the UE may be connected to more than one RNS. In this case a second RNC other than the SRNC is involved in the data path. This RNC is than called DRNC. It is the CRNC of the cells connected to the UE but not allowed to control the RBs related to the UE. It has to forward the respective data to the SRNC corresponding to the UE via Iur-interface. The DRNC may only perform macro-diversity combining of the UEs data streams, except common or shared data channels are used.

Note that one RNC may have a multitude of concurrent active connections and has to act according to one of those three different logical roles for any of it.

Base Station

The base station or NodeB incorporates the PHY layer (layer 1) of the protocol stack at the provider side, see Chapter 2.2. It is connected to the UE via Uu-interface (air-interface) and to the RNC via Iub-interface. As already mentioned there are controlling connections on the Iub-interface, deploying the NBAP protocol as well as connections for data transmission, using the FP protocol. A NodeB is composed of several cells, most common are three cells because every sector of a site forms an autonomous cell. For this reason softer-handover, as described in Chapter 2.2.1, can be performed for two such cells. Conversely, for cells without common NodeB the temporal delay and signalling overhead would be far too high and in consequence soft handover must be deployed. Also ILPC, see Chapter 2.2.3, is terminated in the NodeB and handled independent from the SRNC.

2.3.3 User Equipment

The terminal with what a user is getting access to the UMTS network is called User Equipment (UE). Because of the difference in the operational life span of UE and the network, the UE can be considered as most flexible of all UMTS entities. The standardization of functionality of a UE only implies the UMTS architecture, for the application and service side there are no restrictions given. This is the key competitive factor for manufacturers in mobile communication business.

The terminal is often seen as a single device, but actually it consists of the Mobile Equipment (ME) and the Universal Subscriber Identity Module (USIM). The ME is the device which bears all the technical functionality to connect to a UMTS network, whereas the USIM is a module with the user identity related information. This concept is considered to be an impulse for competition in the business. Users can exchange the ME without any administrative issues, just by changing the USIM.

Because UMTS is considered to be deployed over decades and even evolve, there are and will always be UEs with different capabilities. Arbitrary UEs have to communicate with arbitrary networks and have to somehow negotiate the basic properties of the connection. In this issue UMTS has adopted GSM-like policies, i.e. the network is broadcasting a lot of information about its capabilities whereas the UE knows its own and informs the network about them after a basic radio link has been established.

2.4 Interface Protocols

In UMTS a multitude of different protocols is deployed. This come with the fact that UMTS is a communication network which may use many different types of connections, e.g. wireless link between NodeB and UE, microwave radio relay between RNC and NodeB, etc. To ensure the protocol stack is flexible enough to handle this variety a strong modularity has been introduced. In the evolution of UMTS certain modules will change whereas others may keep their actual structure. A detailed summary of this topic is given in [32]. Examples for many signaling-procedures can be found in [2].

2.4.1 UTRAN Protocol Architecture

The UMTS protocol stacks at different connection interfaces are designed by use of the same model. Figure 2.10 gives an idea about that model and the modularity discussed before. The structure is based on maximum autonomy of the single instances. Although several interconnections in the CN as well as in the UTRAN are made according to this model, in the following only the latter will be considered, see [15].

A distinction between two horizontal layers is made, i.e. the “transport network layer” and the “radio network layer”. The structure of the transport network layer is strongly dependent

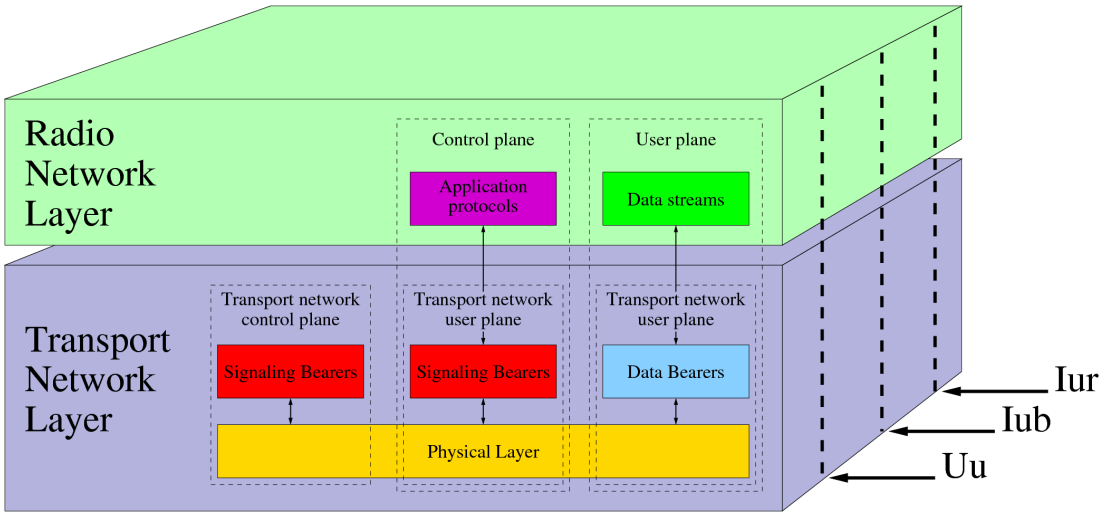

Figure 2.10: General UMTS protocol model.

on the connection type used for a specific network element, e.g. if ATM is used to interconnect the entities, this part of the protocol stack may look completely different than if IP is used. The radio network layer on the other hand contains all facilities concerning the UTRAN, for which the transport layer is transparent.

Furthermore three different planes are depicted. The first plane is called “transport plane”. It contains the traffic types generated by the low-level transport protocols of the UTRAN, e.g. data generated by ATM for establishment of a persistent connection or pilot signals at the air-interface. The next plane is the “control plane”. It comprises protocols for communicating UTRAN control information. This control protocols would be e.g. NBAP or RRC. The control plane makes use of the transport network user plane, this means nothing else that higher layer control-data is regarded as user data in lower layers. The third plane is called “user plane”. This plane represents the collection of all protocols exclusively dedicated to user data transmission, such as Adaptive Multi-Rate (AMR) or IP.

There are five different interconnections between the different network entities in UTRAN, i.e. Iu-CS, Iu-PS, Iur, Iub and Uu interface. But in the following only the protocol stack at the Iub-interface shall be discussed in more detail, because this information is relevant for the practical part of this work, see Chapter 3. Figure 2.11 shows this stack.

The logical model of a NodeB, see [20], explains how it communicates over Iub. Thus, the NodeB consists of a “common control port” for general controlling issues and several traffic termination points, each of them consisting of a “dedicated control port” and a certain number of data ports. One may think there is an association between cells and traffic termination points but in fact there is not, one cell may be served by several traffic termination points and vice versa.

The transport network control plane contains a protocol stack with the Access Link Control Application Part (ALCAP) protocol at the top. This protocol is equivalent with the International Telecommunication Union (ITU) recommendation Q.2630.2. It is responsible e.g. for setting up the network as well as multiplexing and demultiplexing data streams for certain traffic termination points. Specifications or references to ITU specifications can be found in [18], [21] and [23].

2.4.2 NodeB Application Part (NBAP)

The NBAP protocol is found in the control plane of the radio network layer of the protocol stack. It is used to control the base station via the control channels. Because of the two different types

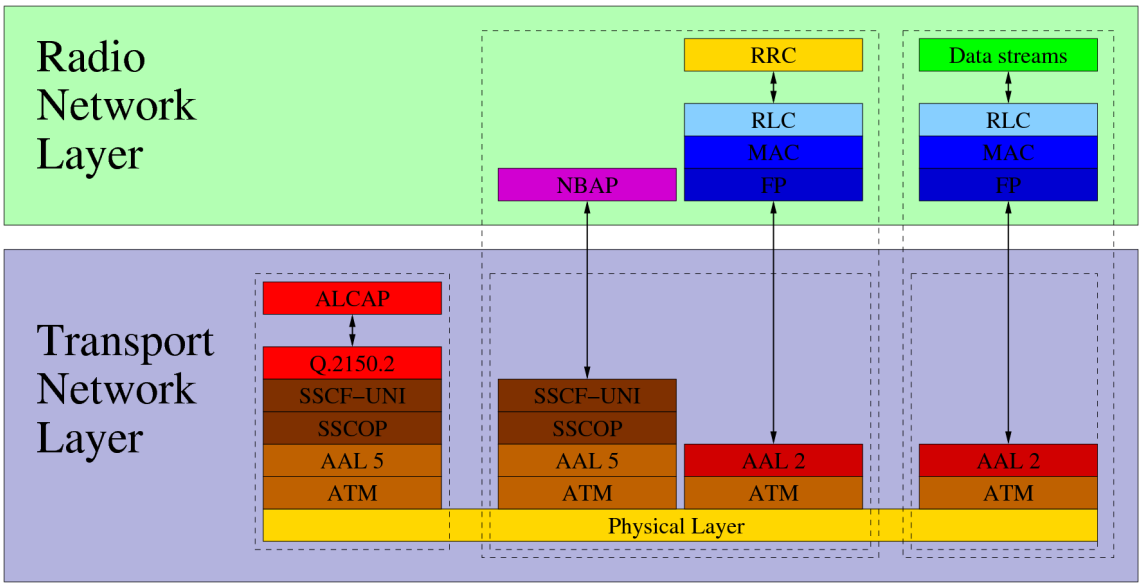

Figure 2.11: Protocol stack at the Iub connection.

of control channels it can be distinguished between “common NBAP” and “dedicated NBAP”. Common NBAP procedures apply for any kind of messages except user context related ones, e.g.

- Cell configuration and setup,
- Communication of general radio parameters,
- NodeB specific measurements,
- Fault management.

Dedicated NBAP includes procedures which are related to certain UEs. It is used for communication on dedicated control ports, which in turn are used for controlling the data-ports of the respective traffic termination point at the NodeB. Functions of dedicated NBAP are, e.g.

- Radio link setup procedure,
- Handling of radio links of individual UEs,
- Radio link specific measurements,
- Radio link specific fault management.

The specification of the NBAP protocol can be found in [22].

2.4.3 Frame Protocol (FP)

The Frame Protocol (FP) is used to transport MAC PDUs over the Iub-interface. Therefore it can be seen as a physical realization of the TrCHs described in Chapter 2.2.2. The PHY layer data stream is decoded, demultiplexed and reassembled to single independent TrCHs in the NodeB and transmitted over the Iub-interface by use of the FP protocol afterwards.

On the other hand the FP protocol is used for specific control issues as well. It is capable of handling OLPC information, timing adjustment, synchronization messages and congestion indication messages. More details can be found in the specifications, see [19].

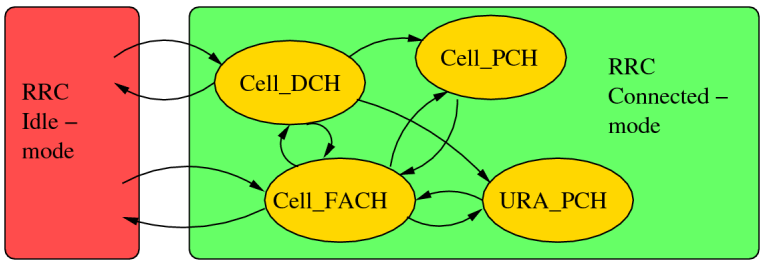

Figure 2.12: RRC modes and respective states for a single UE.

2.4.4 Radio Resource Control (RRC)

The RRC protocol is the key protocol in the whole UTRAN protocol suite. This protocol handles setting up, maintaining and releasing connections between all different protocols in UTRAN and UE. This is done trough peer-to-peer signalling-connections between the UTRAN and UE RRC entities. Other tasks are, e.g., paging, QoS maintenance and measurement procedures, system information broadcasting, etc. The specification can be found in [14].

The RRC mechanism can be divided into different service states as depicted in Figure 2.12. Every UE is in one of two possible modes, i.e. “idle-mode” and “connected-mode”. The UE comes into RRC idle-mode after it is switched on and still has to select a suitable PLMN. This state is known as “camping on a cell”. The connected-mode is divided into four different states:

- *Cell_DCH*: The UE is connected to UTRAN and a DCH is established. Data transmission and control signaling take place.
- *Cell_FACH*: The UE is connected but no DCH is established, RACH and FACH are used instead. Transmission of signaling messages and small amounts of data is possible.
- *Cell_PCH*: In this state the UE is known to the SRNC but no data can be transmitted. The UE has to undergo the paging procedure to re-establish a data connection.
- *URA_PCH*: This state is very similar to the “Cell_PCH” state.

Detailed examples about RRC procedures such as connection setup or handover can be found in Appendix B and [32].

Chapter 3

Measurements in a Live UMTS Network

The advantage of measurements in live networks in comparison to simulations or demonstrations is the vicinity to the real application and the manifold of different scenarios. Disadvantages are impractical reproducibility of measurement results and the relatively high effort to bring tracing and measurement systems to work. In the following section the measurement setup is described in order to give the reader an idea of how data was collected and show the limits of the respective procedures.

3.1 Measurement Setup

Traffic Monitoring and Analysis (TMA) is often applied in live networks of any kind. It refers to measurements in the network to attain insight into the dynamic network behavior. This knowledge may be valuable for troubleshooting and network optimization but it can also be used for research purposes such as system evaluation by means of modeling and simulation.

The classical approach of TMA is aggregation and joint analysis of data measured by components of the network. It allows large-scale measurements. However, this attempt bears problems such as variety of the gathered data and difficulty of joint evaluation. Other problems are reliability issues of data recorded during network malfunction and possible modification of the measurement setup because of modifications of the network setup.

In addition a common used TMA approach is small-scale measurements as troubleshooting action if problems have been discovered. This is done by means of a protocol analyzer. The advantage is the decoupling form monitored network and measurement tool.

For this work another opportunity of TMA was given, namely the measurement of network traffic via passive wiretaps installed at specific links in a 3G network. This approach combines the advantages of those mentioned before. The measurement system is independent of any network equipment but still large-scale measurements are possible. The traffic can be analyzed at very high granularity, e.g. packet level, and results come in uniform structure.

The TMA tool deployed for this purpose is called “METAWIN”, developed at the research institution Forschungszentrum Telekommunikation Wien (FTW) and currently maintained by Kapsch CarrierCom. It is designed to capture data traffic in UMTS and GPRS networks, with the possibility to access different interfaces, e.g. Gn, Gi, Gb, Gs, IuPS and Iub, and link this data at the user level. The goal of this measurement setup is to allow scientific analysis of:

- large scale statistical data sets,
- data flow at application level,

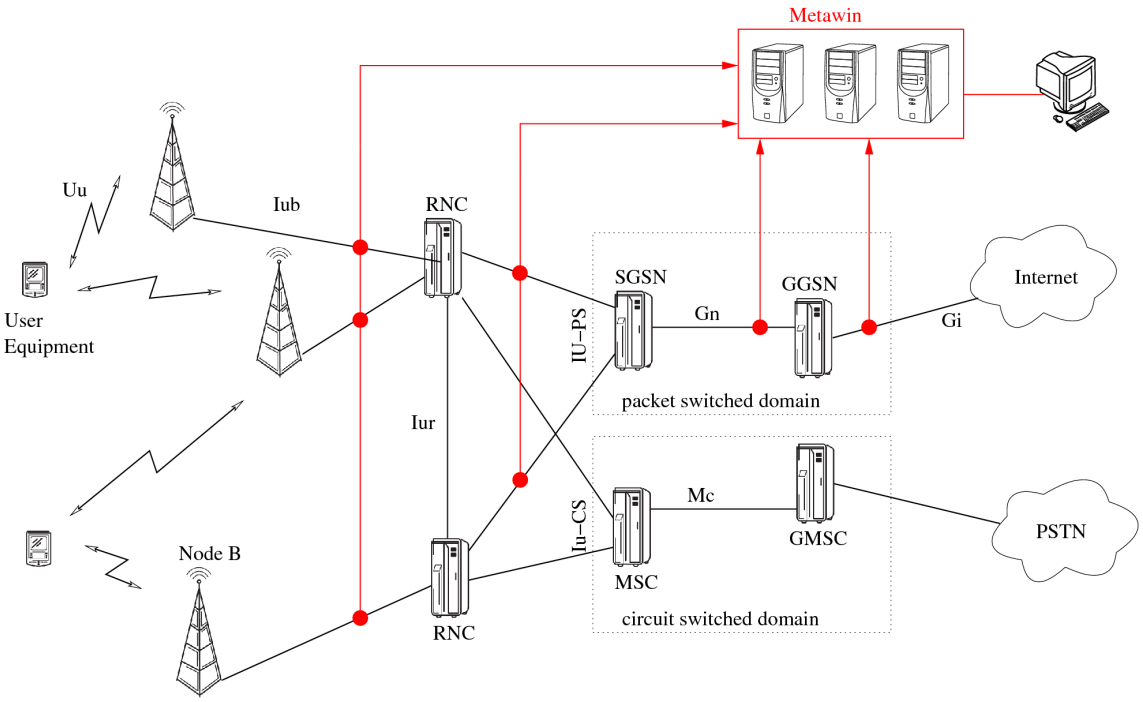

Figure 3.1: Physical setup of the METAWIN monitoring system.

- correlation of recorded data at different protocol layers.

Although the concept is to provide a tool to capture packet switched traffic at higher protocol layers, the Iub-extension enables tracing of any kind of transmitted data. In order to meet privacy restrictions all user specific data, such as identifiers and payload, is anonymized or even dropped. More information about the measurement setup can be found in [39], on which this section is based.

3.1.1 Physical Setup

The physical setup of the METAWIN project is depicted in Figure 3.1. It consists of special Data Acquisition Modules (DAGs) which are installed at the network links that should be traced. It is possible to trace ATM based as well as IP based links. The acquired data is forwarded to a high-end PC cluster were the respective processing is done.

3.1.2 Software

The software developed for the project is running on a Linux platform. An overview is depicted in Figure 3.2. It consists of a central module called “MOTRA” whereof several instances may be executed simultaneously. This module is responsible for parsing the whole protocol stack and may contain plugins for specific tasks, e.g. anonymization. In the scenario shown, the data coming from the acquisition device is parsed by a first instance of MOTRA. The respective output is saved on a ring buffer in a specific format. Two other instances are reading from this buffer. One is processing the sniffed packets (often referred to as traces) by means of plugins, producing an output of statistical data sets for immediate analysis (e.g. histogram of IP packet length). The second is anonymizing the packets and sends them on a mass storage device for later evaluation.

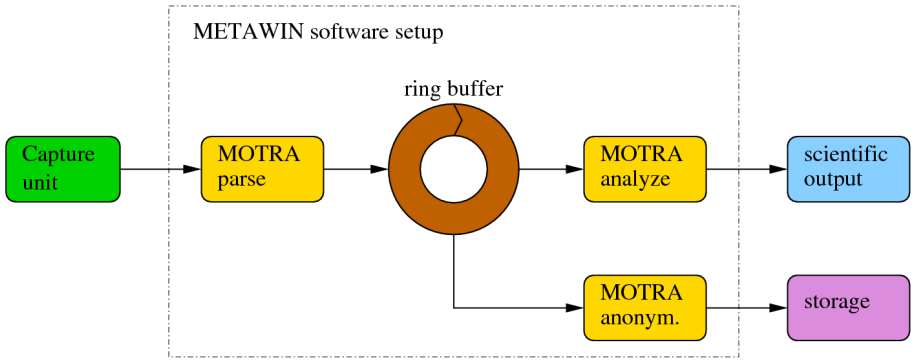

Figure 3.2: Software setup of the METAWIN monitoring system.

3.2 Extraction of Physical Layer Data

In this section it is briefly summarized what kind of data is accessible, how data was extracted and how the output data looks like. In order to evaluate the resulting data, measurements have been performed at two points in the UMTS communication system, i.e. at the Iub-interface and at the UE, whereas the main results of this work have been obtained form the Iub-interface. Therefore it is discussed in more detail.

3.2.1 Accessible OLPC Data

In a first step it is important to understand what kind of data can be observed and measured and if it could be related in any way to the OLPC, i.e. depend on it or influence it. Further the reliability, frequency and accuracy of certain observed values must be considered in order to understand its potential usefulness. In this context it must be mentioned that the uplink and downlink OLPC are completely independent form each other (see Figure 2.8) and may also be observable via different parameters. Further note that only DCHs are power controlled by the specific OLPC algorithm under investigation and therefore only DCHs are considered in the following.

Another detail becomes clear from Figure 2.8, i.e. the OLPC procedure only reaches to the SRNC and not deeper into the core network. If any tracing should be done it may be possible only on UTRAN interfaces if no data loss is tolerated. In other words it is desired to trace an interface as close as possible to the Uu-interface, so the best choice is the Iub-interface.

In Figure 2.11 all different protocols present at the Iub-interface are depicted. Since power control is a network layer procedure, no higher protocols than RRC are involved. The protocols that were focused because they potentially contain relevant data are:

- *RRC*: It contains most information about the radio connections, e.g. QoS, new radio link setup, etc.
- *FP*: The uplink OLPC target SIR values are transmitted on this interface as well as frame error indicators.
- *NBAP*: General measurements are transmitted on this protocol. Some of them maybe of interest for OLPC issues, e.g. total transmitted power, total received power, etc.

In the following the feasibility of investigations via tracing on the Iub-interface is studied, where the distinction between different types of OLPC is made.

Uplink OLPC

The most interesting parameter observed at the Iub-interface, when investigating on OLPC, is the target SIR value of the uplink OLPC. It is transmitted via FP-DCH protocol in a special control frame. The range is from -8.2 dB to 17.3 dB and it is transmitted in intervals of approximately 100 ms. The specification can be found in [19]. This information is extremely valuable for analysis and modeling the actual OLPC behavior. By tracing and evaluating the DCH setup phase on the RRC and NBAP protocols the belonging of the control frames to certain UEs can be determined. But without tracing the setup phase of the radio connection, temporary connection identifier can not be associated with a user equipment and the information contained in the respective packets is therefore lost.

The OLPC is based on QoS requirements, as already stated in Chapter 2.2.3. The most important parameter which can be used as QoS indicator on low communication layers is the CRC checksum. It is added to the single TBs in the PHY layer (see Chapter 2.2.2). This means it is already removed from the data transmitted over the Iub-interface, because all PHY layer issues are handled in the NodeB. Nevertheless the SRNC has to know about correctness of the received data for the sake of soft combining and therefore an indicator for erroneous data is attached to FP-DCH frames. This indicator is called CRC-indicator (CRCi) in the standard, see [19]. The CRCi value is one single bit and it is zero if the CRC check performed in the NodeB revealed no block error, otherwise it is one. It comes with every TB so at least ones for every TTI (10 to 80 ms) and for every TrCH, if any data is transmitted.

Another accessible parameter is the uncoded Bit Error Ratio (BER). This value is attached to every TBS transmitted via FP-DCH. So it is basically received as frequent as the CRCi parameter. This parameter is provided for two purposes. First it is used in the SRNC in the case of selection combining to estimate which packet is better and should be forwarded if all packets are received erroneous. This may be useless in case of packet transfer but in case of speech transfer erroneous data is tolerated. Second it is scheduled by 3GPP to provide the BER to the OLPC to enhance its operation by means of a second parameter. The transmitted value is called “Quality Estimate (QE) value” in the standard (see [19] and [5]). It is a logarithmical mapping of the uncoded BER, see Equation 3.3 and has to fulfil the accuracy specification of 10% of the actual value.

The RRC protocol provides a manifold of different messages which are of interest concerning the OLPC. All properties of a radio connections are communicated via RRC. Depending on the radio parameters different transmission power and different resulting service quality is expected and has to be controlled. The radio parameters can only be accessed at the beginning of the communication, during the connection setup phase, and in case reconfigurations take place. They have to be recorded and linked to specific DCHs.

Concerning multi-user and multi-cell environment other RRC messages were expected to reveal an influence on the OLPC, i.e. connection setup, modification and release messages addressed to other users. After initial measurements it turned out that this is not the case. The explanation is that the ILPC is locked on the interference created from other users and it is able to compensate well for it. So if there are changes on other users ILPC target SIRs, they need their time to reach the respective value. In the meantime the ILPC of the considered user already observes changes of the interference and compensates for it.

The outcome of the initial feasibility study is to further focus on the SIR target values, the CRC indicator information, the uncoded BER (QE parameter) and parameters transmitted via RRC related to QoS issues. By the aid of these parameters it may be possible to specify the characteristics of the control path of the OLPC, build a model for it and also improve functionality by means of new algorithms. The actual used power control algorithm is expected to only use the CRCi parameter to estimate the QoS level, which in turn makes improvements by deployment of the QE parameter possible. Further investigations on this assumption can be found in Chapter 3.3.

Downlink OLPC

Concerning downlink power control there is not as much information transmitted on the Iub-interface as in the uplink case. This becomes clear from Figure 2.8. The downlink power control loop involves only the NodeB but not the SRNC. The NodeB has just to set the right transmit power level dictated by the UE and does not report on it. Nevertheless it would be interesting to identify power control algorithms of single UEs in order to evaluate the respective quality.

To gain this power control information with the measurement setup described above (Chapter 3.1) the idea was to evaluate information transmitted via NBAP protocol. Common as well as dedicated procedures have been taken into account, whereas the focus was on measurement procedures. There are several parameters that could reveal interesting information (see [22]).

By investigating common measurement procedures the following parameters attracted attention:

- Received total wide band power
- Transmitted carrier power
- Received total wide band power without HSPA
- Transmitted carrier power for cell portion
- etc.

The problem resulting by trying to trace this kind of messages was that single cells may be identified but not assigned to physical cells. The reason is that these measurements are reported via common control port of the NodeB and they are always activated. This means the measurement type gets an identifier assigned at the network setup phase and it is used forever. If this phase is not traced by the measurement tool it is hardly possible to identify physical cells by means of their measurement IDs only.

On the other hand reports are transmitted in time intervals of seconds or even tens of seconds, which makes their use for dynamic measurements questionable. Especially if it is considered that the OLPC loop should be executed 10 to 100 times a second.

Parameter of interest concerning the dedicated measurement procedures where:

- SIR
- SIR error
- Transmitted code power
- Received Signal Code Power (RSCP)

It turned out that these kind of measurements are reported on a very irregular base. Their primary use is the evaluation of soft-handover scenarios, so the measurements are performed after certain events occurred, whereas periodic measurements where not observed.

Due to the difficulties explained in this section, it was decided to not further work on the downlink OLPC in this work. Additionally it has to be mentioned that tracing on the Iub-interface may not be suited to investigate downlink power control issues at all.

HSPA Power Control

In UMTS Release 6 specifications for High Speed Uplink Packet Access (HSUPA) where made. The HSUPA extension allows for improved packet transfer in UMTS, to make it better suited for Internet traffic. The extension should guarantee higher throughputs, reduced latency and improved system capacity. The main new features are broad shared packet channels, Hybrid Automatic Repeat Request (HARQ) and the possibility of scheduling. Different new types of

transport channels were specified to meet the demands of HSUPA, whereas also a new type of data channel was defined, the Enhanced Dedicated Channel (E-DCH). More information about UMTS evolution can be found in [28], which this section is based on.

Internet traffic is most often desired to be transmitted without errors. There are protocols based upon IP which guarantee this QoS demand, e.g. TCP. This is done by requesting retransmission of erroneous received packets. But this principle is not suited for UMTS because the SRNC would have to buffer every packet for acknowledge issues. This is a very memory-demanding task considering the high number of cells per RNC. Therefore HSPA introduced the so called HARQ. It is a procedure between UE and NodeB. The receiver acknowledges for every TB and if it was not received correctly, it can be retransmitted immediately. The advantages are the reduced latency and the fact that higher layers (e.g. RLC, IP, TCP, etc.) profit from a effectively errorless connection.

The power control for E-DCHs works similar as the power control for DCHs. There is an ILPC locked on the SIR target provided by the OLPC which tries to keep a certain QoS level. If there is a DCH configured in addition to the E-DCH the power control algorithm is the same as usual, but if no DCH is set up, the burstyness of E-DCH due to scheduling and the flawlessness of the E-DCH due to HARQ lead to problems totally different as those known from the conventional OLPC. There must be used different algorithms and input values (e.g. number of re-transmissions) for estimation of the SIR target.

Because of this issues it is resigned to treat HSUPA power control in this work. It would be another topic with few similarities to DCH power control. But in general measurements of E-DCH power control parameters would be feasible on the Iub-interface and an interesting branch to proceed research on this topic.

3.2.2 Data Extraction at the Iub-Interface

As already said the main focus of the METAWIN project lies on higher layer data extraction and not no measurements of low layer control information. Therefore the tracing framework, described in detail in Chapter 3.1, had to be extended to allow for adequate tracing of power control data. This was done by means of post-processing modules. The most important one allows for extraction of physical layer transmission parameters from RRC messages and their association to data transmitted via FP protocol. This is necessary to obtain a QoS measurement value. In the following a description of this module is provided.

Before the overall functionality of the module is described, the input and output parameters and the respective format are specified. The input streams contain the FP and RRC data streams, already preprocessed by MOTRA (parsed, anonymized, etc.). The information comes in certain data structures, similar to the respective protocol frames (RRC, see [14], and FP, see [19]). In addition the structures are already associated to the respective UEs (i.e. labeled by a random but unique identifier) and contain associated information (such as time of arrival).

It has to be mentioned that the radio capabilities and parameters of various UMTS releases are different. Because of the HSUPA extension in UMTS Release 6 (including the possibility to configure an E-DCH, see Chapter 3.2.1) and heavy changes of the frame layout, the module only supports RRC frames up to Release 5. This means that most of the packet traffic is a priori discarded, i.e. HSPA traffic. An exception is traffic transmitted by older data cards (produced before 2005) and by mobiles constituted for transfers with only small amounts of data.

The expected output of the tracing module should be based on transmitted TBSs, i.e. one TBS is resulting in one output frame. The extracted values per output frame are described in Table 3.1. A set of these values should be adequate to determine the QoS conditions during transmission on the Uu-interface. The output is send to a mass storage device and saved in terms of a table.

The exact functionality of the module is depicted in Figure 3.3, more information about it can be found in Appendix C. The most demanding routine is the RRC preprocessing, it contains the re-construction of the PHY layer parameters, this means the whole physical layer processing chain

Value	*Comment*
Timestamp	Exact arrival time
Cells	Identifier of all cells (of one NodeB) involved in softer handover (in case of soft handover several equal TBSs are received)
U-RNTI	UTRAN Radio Network Temporary Identifier (U-RNTI)
TTI length	Length of the respective TTI
CRC length	Number of bits per CRC checksum
TrCH	ID of the TrCH on which the TBS was received
RLC length	Number of bits in the payload (RLC frame) per RF
TFI	Transport Format Indicator (TFI)
CRCi	CRC-indicator (CRCi)
QE	Quality Estimate (QE)
SIR target	Last received value of OLPC SIR target
Coding rate	Coding rate of channel coder
Coding type	Coding type of channel coder (turbo or convolutional coding)
Spreading factor	Spreading factor of the respective PHY channel
Gain factor	Power ratio of DPDCH and DPCCH
PHY channels	Number of PHY channel allocated to the UE
ILPC algorithm	Algorithm used for ILPC and its step size
Quality target	BLER target value recorded on the downlink DPDCH

Table 3.1: Output values of the processing module per TBS.

(see Figure 2.5) has to be emulated. The database to the left side stores one entity for every UE, it contains values like different TFCSs, timeout values, U-RNTI, etc. The other database stores one entity for every received TBS (if one TBS is received by several NodeBs, there are several entities). Such an entity contains values like ID of the received cell, time of arrival, etc.

3.2.3 Data Extraction at the UE

In order to check the significance, correctness and quality of the data measured at the Iub-interface, measurements have also been performed on the UE side, see Figure 3.4. At the same time the data was recorded at the Iub-interface so that two comparable data traces have been obtained. The test equipment was a UMTS data card working with UMTS Release 5 specifications. Indoor as well as outdoor scenarios and soft-handover cases have been tested. The transfered data type was bulk download from Internet, but the uplink traffic was satisfactory high to gain reasonable results with constant data transmission.

The software suite used was "TEMS^{TM} Investigation" by Ascom, see [25]. This software solution is designed for network analysis and optimization via measurements at the UE. The specialty is that the measurement equipment may be a commercially available mobile connected to a normal PC, which first allows for measurements as close as possible to real communication scenarios and second requires no expensive and complicated equipment. The software enables detailed analysis of the transmission conditions at Uu-interface and offers many possibilities for data logging, extraction and processing.

The connections traced at the UE by means of TEMS reveald no differences to the respecitve traces extracted by the METAWIN system. No data loss or modification took place at both measurement branches. In consequence the METAWIN system ans the additional modules are assumed to work properly.

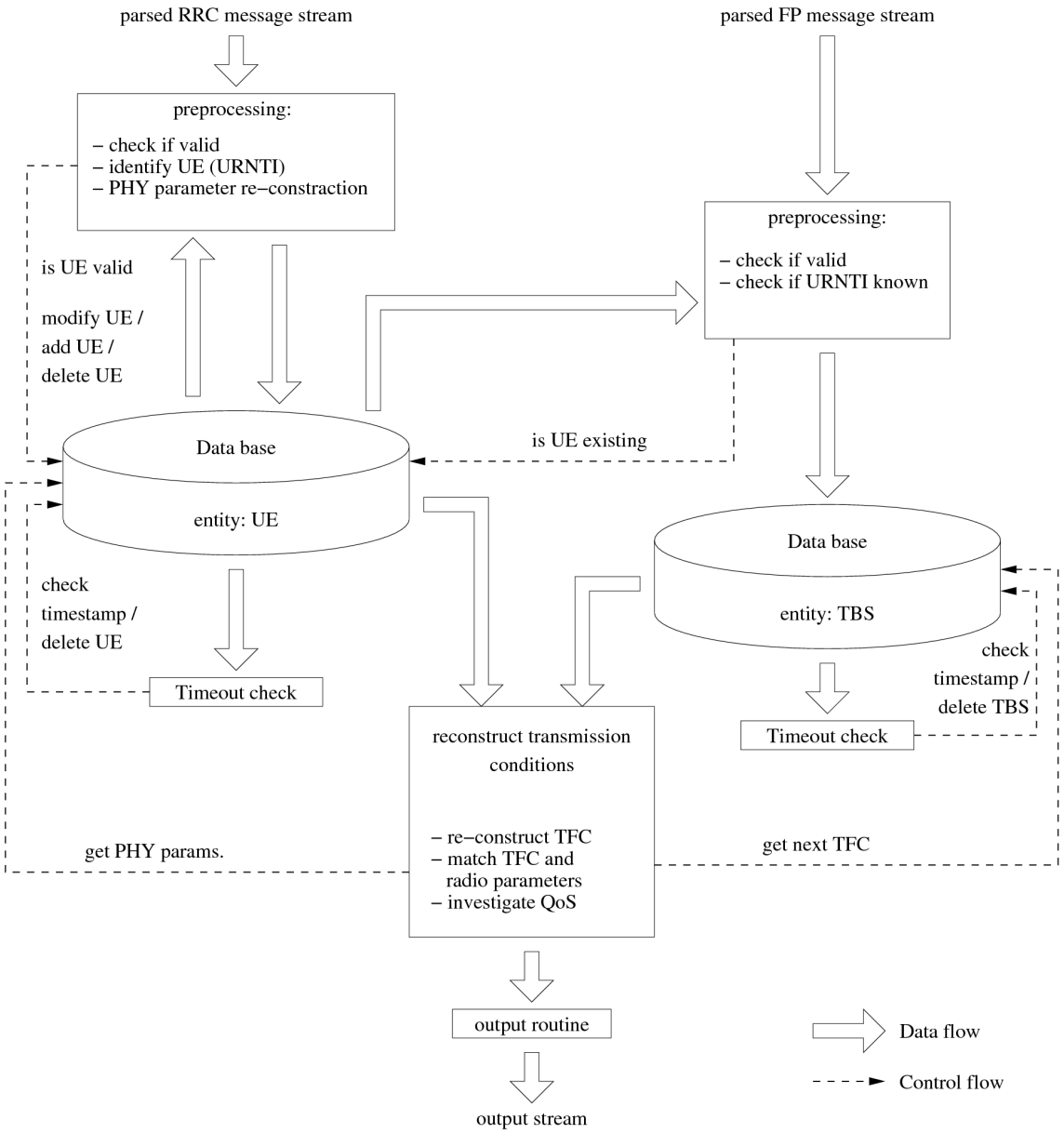

Figure 3.3: Extension module for physical layer data extraction.

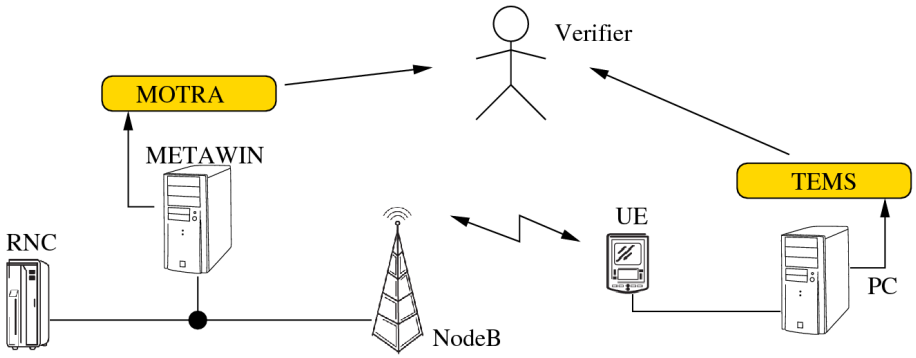

Figure 3.4: Data verification by means of measurement at the UE.

3.3 Measurement Results

In this section the results within the scope of this thesis are revealed. First an analysis of single connections is done, in order to verify how the actual OLPC works and what its main flaws are. Second investigations on certain connection parameters are performed, which is done in a distributed way in order to average out specific conditions of single cells and users. The results are generally valid only if a network setup, deploying certain algorithms for OLPC and QE estimation, is taken into account. They allow for modeling the power control mechanism.

3.3.1 Analysis of Single Connections

The analysis of single connections as a first step is important in order to understand the different behavior of various UEs and cells in the network. For example several UEs may require different target SIR offsets, not only because of different multipath propagation and Doppler spectral conditions but also because of possibly different implementation of decoding algorithms.

Temporal Behavior of Target SIR Values

The very first issue to analyze is the temporal behavior of the OLPC by means of constituted target SIR values transmitted to the NodeB via FP protocol. A measurement example is shown in Figure 3.5(a).

The figure gives information about the deployed OLPC algorithm. It is a step algorithm, performing a big step up if a CRC error is registered and a small step down if no error occurs. This can be seen comparing Figure 3.5(a) and 3.5(b). The different step sizes are performed because of the problematic that the controller can not afford to cause several consecutive errors. This means the OLPC has to guarantee a SIR target level above the level which actual would be needed. Anyway this step algorithm is quite sophisticated in terms of capability to maintain a certain BLER and provides ease of implementation. The exact procedure of the step algorithm is summarized in the formula

$$SIR_{target,k} = \begin{cases} SIR_{target,k-1} + \Delta K & \text{if block error} \\ SIR_{target,k-1} - \Delta & \text{if no block error} \end{cases} \tag{3.1}$$

Thereby "k" is the time index, "Δ" is an arbitrary step size and "K" is a factor calculated as

$$K = \frac{1}{BLER} - 1 \tag{3.2}$$

A detailed explanation can be found in [41].

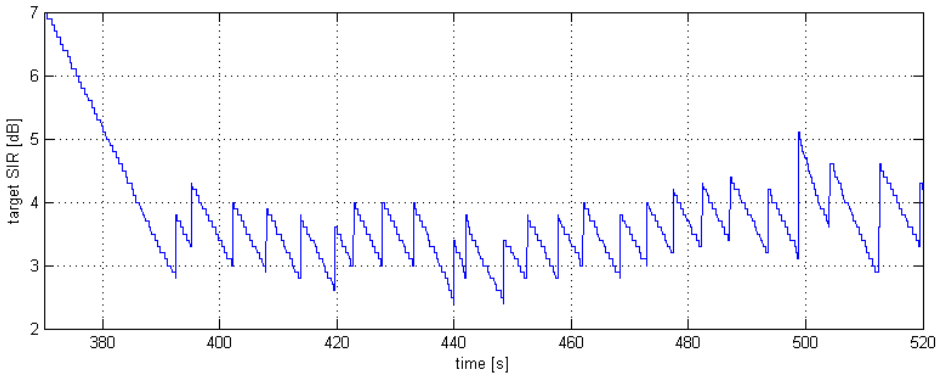

(a) SIR target over time

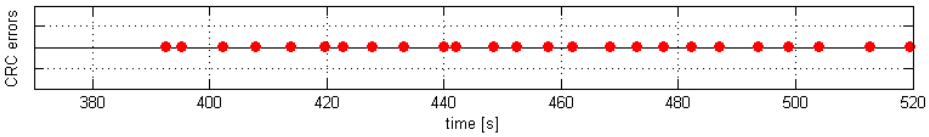

(b) CRCi values over time

Figure 3.5: SIR targets and CRC indicators over time for a single connection.

The algorithm can be explained by an intuitive example: If the BLER of 1% is targeted, the down-step size has to be approximately 1% of the up-step size. Now if a block error occurs a up-step of lets say 1 dB is performed. If the SIR demands for a fixed QoS are rather constant, no more errors are expected at this new SIR level. Consequently the OLPC algorithm starts to step down the power with 0.01 dB per TTI. After 100 received TBSs the SIR is again at the level where the last error happened and the probability of the next error event is quite high. A visualization of the process is depicted in Figure 3.6.

One fact becomes clear from the example above, namely a constant error pattern is introduced to the communication link by the OLPC. This is clearly not optimum as for example stated in [35].

The only input parameter this algorithm needs is the CRCi transmitted for every TBS. The problem resulting from this fact is the relatively low amount of information that can be extracted from the CRCi in general for reasonable time periods. For example if a BLER of 1% is targeted it would require a number of at least 100 transmitted TBSs and respective CRCis to estimate the actual BLER, if it is close to its target. This would require from 1 to 8 seconds by taking the duration of a TTI into account. This explains why algorithms deploying only the CRCi parameter are not able to have high dynamics. In the case of the step algorithm mentioned above this problem is solved by the difference in the step sizes, so, generally spoken, the algorithm tends to demand target SIR values which are above the level actually needed. This effect is not carrying weight in channels with constant SIR demands where the algorithm has enough time to converge, on the other hand in very dynamic cases a lot of unnecessary power may be transmitted.

Another weakness of the algorithm is the enlargement of the convergence time by an increasing the targeted BLER. The conclusion is that it may not be suited for applications where a very low error rate is desired, convergence may take too long. Note that the normal duration of one sawtooth in Figure 3.6 is several seconds, at a BLER of 1%. If the BLER would desired to be 0.1%, the duration would be several tens of seconds.

An advantage of the step algorithm is the short time it needs to react on errors. Right after

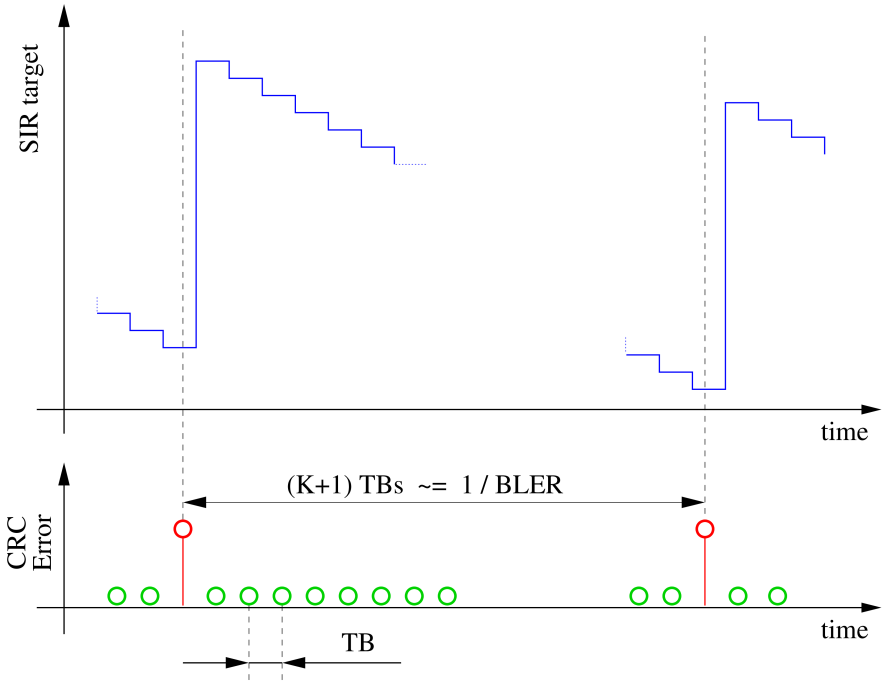

Figure 3.6: Principle of the OLPC algorithm by Sampath, et al.

the detection of an CRC error the SIR target is raised for a relativly high value, e.g. 1 dB. This makes the probability of a consecutive second error rather small, assuming the channel does not undergo strong changes.

At the beginning of the connections there is a long period, in which the control algorithm produces no errors. This extended initial convergence time results from the fact that the OLPC needs an initial target SIR value for which the connection can work properly and offers a reasonable low BLER. The initial value is estimated by means of the Open-loop power control deployed in the connection establishment phase, see Chapter 2.2.3. For obvious reasons it has to be estimated higher than the absolutely necessary target value. This long convergence period forces the UE to spend far more power than needed. Measurements showed that this period may be in the range of several tens of seconds.

Few attempts have been performed in order to correct for the shortcomings of the OLPC algorithm, see [36], [44] and [42].

QE parameter

As described in Section 3.2.1 also the QE parameter is extractable from the Iub-interface. This parameter corresponds to the uncoded BER, namely the number of bit errors over the total number of bits in a TBS before channel decoding.

The signaling bounds of the QE parameter are the following: the smallest possible value may be 0, corresponding to a BER of less than 0.8 % whereas the maximum value is 255, corresponding to a BER of 1. The mapping is done by means of the formula

$$10^{-2.071875 + 0.008125\,(QE-1)} < BER \leq 10^{-2.071875 + 0.008125\,QE} \tag{3.3}$$

conversely,

$$QE = \left\lceil \frac{\log_{10}(BER) \; + \; 2.071875}{0.008125} \right\rceil \tag{3.4}$$

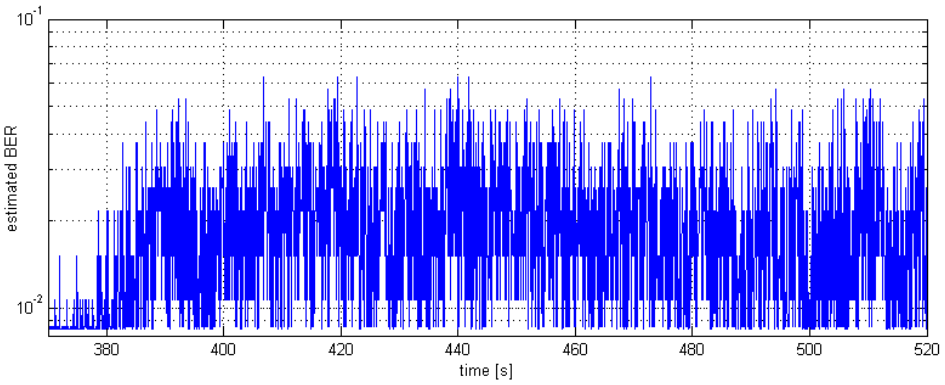

(a) QE target over time

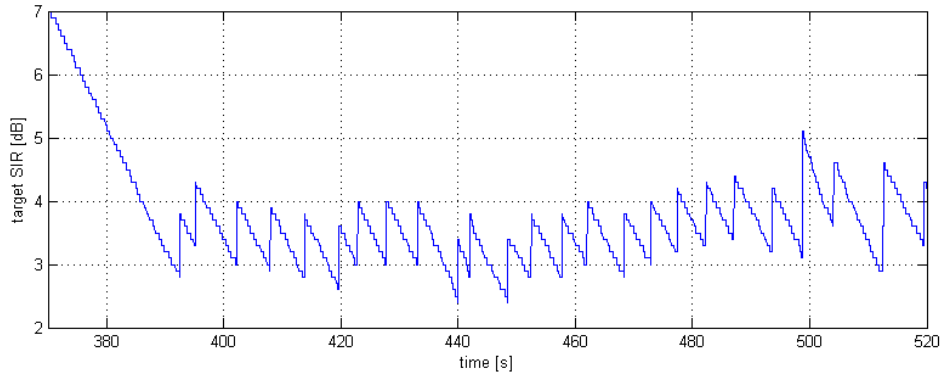

(b) SIR target over time

Figure 3.7: Temporal behavior of the QE parameter and the target SIR values.

The brackets stand for the higher integer number and QE values below zero are forbidden.

In Figure 3.7 the behavior of this parameter over time can be seen. A first glimpse reveals that the parameter behaves as expected, i.e. if the SIR target is high, the QE value is low which corresponds to low BER and the more the OLPC lowers the SIR target, the higher the QE becomes. In addition a strong overlayed noise component can be observed, which causes the need of preprocessing these values. In the following the behavior of this parameter is treated in more detail.

For the statistical analysis of the QE parameter (see Figure 3.8) its mean value was estimated by calculation of the mean over time. Because of the steady variation of the SIR target value by the OLPC the calculation of the mean QE is always stopped by the reception of a new SIR target value (approximately after ten values). Furthermore the QE parameter is a logarithmic measure of the BER, so taking the mean of the QE value means taking the logarithmic mean of the BER.

Figure 3.8(a) shows the deviation of the QE parameter around its estimated mean. It can be seen that the distribution is concentrated around its mean, with a standard deviation of approximately 20 which corresponds a to a value of 40 % in terms of BER. For the later modeling of the QE parameter this is assumed as Gaussian noise overlayed the actual value, what can be verified by means of visual inspection of Figure 3.8(a). The smooth line is a Gaussian function fitted to the measured values represented by the jagged one. Moreover this makes perfect sense because the QE value is estimated by means of short signal sequences which are affected by Gaussian noise. In

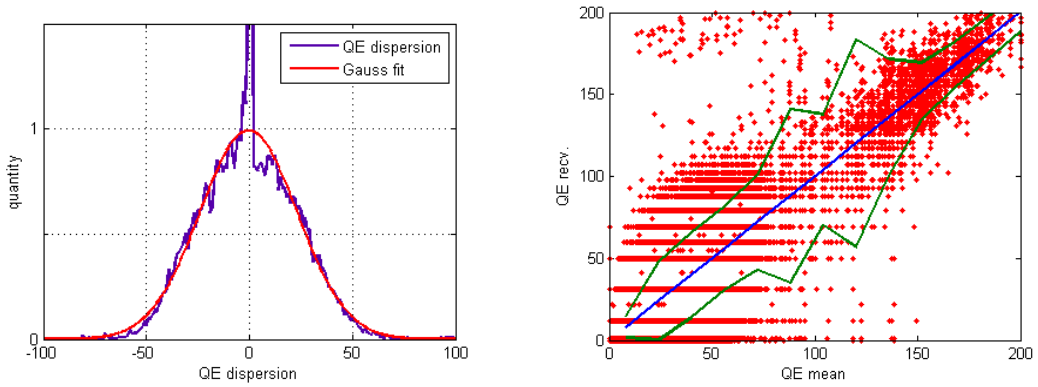

(a) Distribution of the deviation of the QE parameter from its mean.

(b) Scatter plot of the QE parameter over its mean.

Figure 3.8: Statistical analysis of the QE parameter.

Figure 3.8(a) measurement values around the deviation zero have been omitted. A large number of blocks was registered at this value, represented by a spike in the figure. This is due to the fact that for very good channel conditions always QE values of zero are registered. In consequence the mean is also zero and the deviation as well. So this artefact is an indicator that the quality of the communication link was often much higher than required.

In Figure 3.8(b) the spreading of the QE value for different means can be seen. The straight line in the middle represents the mean value, whereas the lines below and above the mean represent the interval of the standard deviation around the mean for every QE value. The red dots represent single registered QE values received with one TBS. It can be seen that the standard deviation is rather constant, except at mean QE values below 20 and between values of 80 and 120. The first exception can be interpreted as saturation effect as explained in the former paragraph. The variations in the middle of the range are because few amounts of data is transmitted in this region. The crowded clusters in the left lower corner and in the right upper corner result from data transmitted correctly and from data received in the soft handover case from a bad cell, respectively. The small cloud in the left upper corner comes from traffic with scarce data transmission where the channel has time to change over a period of averaging. It is a measurement artefact.

Relations between Parameters

In the following the relation between SIR target value and QE parameter will be analyzed in more detail. The relation between QE parameter (corresponding to a well defined BER) and BLER is at least as interesting but it may be more useful to analyze it by means of a multitude of connections instead of a single one. Therefore this topic is treated in Section 3.3.2.

The SIR target over QE behavior on the other hand cannot be treated in a distributed way because it may undergo heavy changes depending on the connection conditions provided by the UE. A very fast UE may behave totally different than a static one and the same applies for indoor and outdoor. Especially different SIR target offsets are expected.

In Figure 3.9 the SIR target values over mean QE values can be observed. Every circle is representing the average QE value at this certain SIR target value for a single UE and NodeB, performed over the whole duration of the connection. Circles in different colors are values obtained from different NodeBs.

In order to consolidate the former assumption of different SIR offsets, in Figure 3.9 curves of different connections are plotted. It can be seen that the arrangement of the measurement points

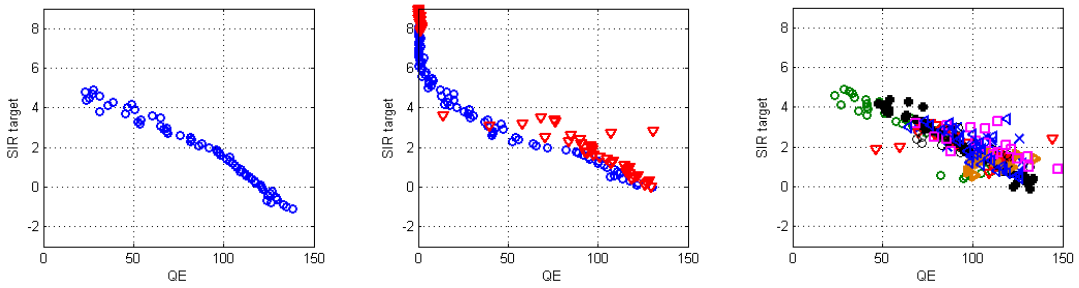

(a) Connection "A". (b) Connection "B". (c) Connection "C".

Figure 3.9: Example: SIR target over QE behavior for different connections.

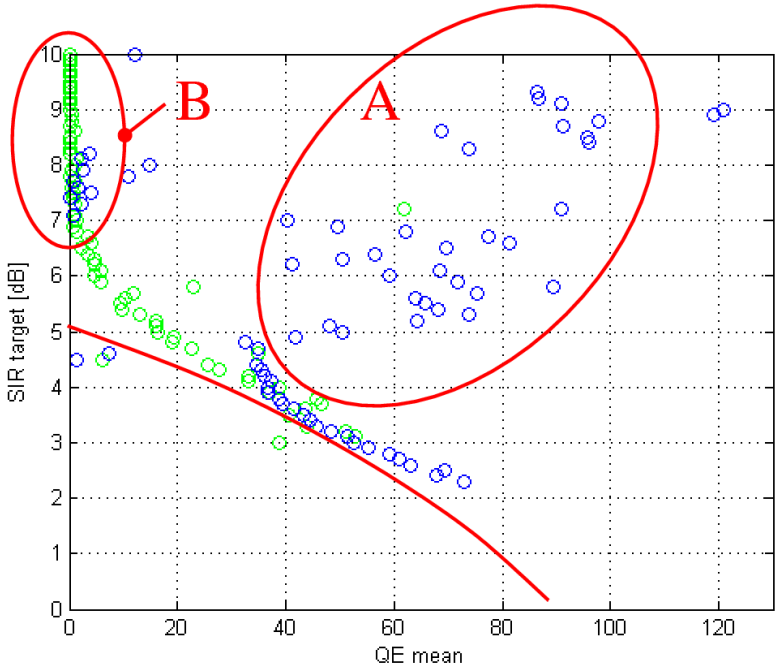

Figure 3.10: Relation between SIR target values and QE parameter.

is more or less the same in every realization, whereas the offset in terms of SIR target is varying. Furthermore there are plots which have a strong concentration of points at the lower end of the cluster of measurement points, whereas others are arranged more loose. This comes from constant channel conditions, in terms of SIR demands for a fixed BLER, in the first case and varying channel conditions in the second, respectively. Note that constant channel conditions are, e.g., constant velocity of the UE or no transitions between indoor and outdoor scenarios. If the SIR demands are not constant the SIR target offset may change and this in turn makes the line fuzzy.

To show the interpretation of a single plot, Figure 3.10 is provided with additional highlighting. Some important points are explained in the following.

- It is visible that most of the measurement values lie on a line. This line is interpreted as SIR target over QE curve. It reveals that this UE must have been in a constant scenario, in order to guarantee the same propagation conditions over a long time range. Effectively this was

the case because this specific curve was recorded from data transmitted by the measurement equipment described in Section 3.2.3.
The solid line shows a typical course of a SIR over BER curve, it is slightly bent downwards. The measured values on the other hand do not show very strong convexity. This is first because of saturation effects at low values of mean QE and because of the narrow region of received QE values. If transmission of data at lower target SIR values would have taken place the bending would be visible.

- The cluster of measurement values denoted by "A" is typical for a soft handover scenario. RFs from the UE are received at NodeBs with good and bad channel conditions and forwarded to the SRNC. The second NodeB tries to decode the frames, what results in rather bad quality. The SRNC on the other hand is of course aware of the better connection and locks its OLPC on the respective indicators. This means that every measurement value in region "A" has its counterpart measured in the base station with better conditions, which lies further to the left. So especially for high SIR targets it is likely that such a scenario happens and therefore region "A" lies at the upper part of the figure. The reason why the better QE indicators form a nice line and the worse do not is the ILPC. The ILPC commands from only the best NodeB are respected but all the other commands are discarded.

- Finally there is another cluster of measurement values denoted with "B". This cluster comes from saturation effects of the QE value and forms a vertical line. Transmission in this region should be avoided because of the waste of power resources. Even below the region tagged with "B" saturation effects are recognizable, they prevent the curve to become more flat, as it would be expected.

The overall result of the measurements of the condidered relation is that the SIR offset is heavily varying for different connections and in case of high mobility also within a connection. This offset may also depend on the ILPC algorithm, see [10], therefore only connections deploying "Algorithm 1" with a step size of 1dB have been taken into account. On the other hand if the measurement points are arranged in a line, there is only a slight bending of this line. In consequence linear regression can be applied, which reveals a slope of approximately 0.04 dB target SIR per 1 QE. This slope is considered the same for all different connections.

3.3.2 System-wide Analysis

In contradiction to the former section, a system-wide analysis is provided here. It may be advantageous because much more data can be measured. Nevertheless it must be verified if such joint measurements are allowed namely if the same conditions are given for every connection. Most of the results presented in this section base on two measurement series on a whole RNC of one hour respectively.

Distribution of the SIR target values

The distribution of the SIR target parameter is of interest because it reveals how a normal channel behaves and shows on the other hand impairments of the actual power control algorithm. In Figure 3.11 the outcome of this investigation is shown. In this figure as well as in the following ones absolute values are replaced by an arbitrary scaling.

In order to guarantee the measurement of valid data only, restriction have been imposed on connection conditions, i.e. only connections on which bulk transfer is expected are measured. Connections with a spreading factor above 64 for example are assumed to be setup channels for HSPA connections (HSPA is not traced at all). Taking these channels into account would distort the results and reveal a too high population of channels working with high SIR targets, because in the setup phase it is expected to be high.

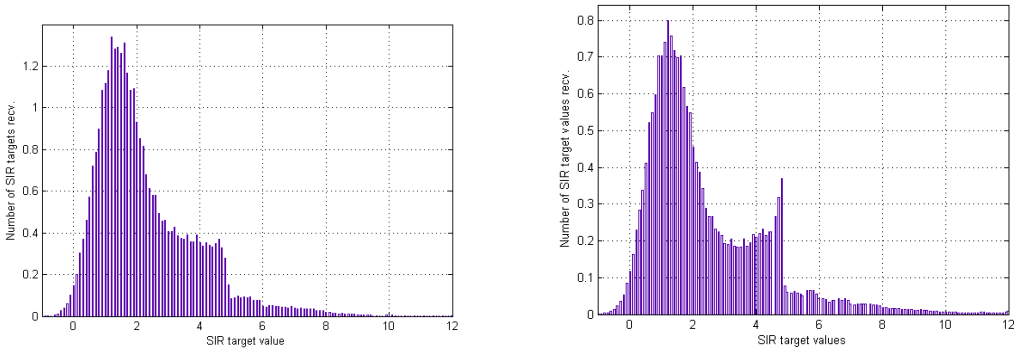

(a) Typical voice traffic conditions.

(b) Low traffic conditions.

Figure 3.11: SIR target distribution for different transmission conditions.

Nevertheless the distributions show sharp edges at SIR target values around 4 to 5 dB. This is a hint for impairments of the OLPC algorithm because there are no obvious reasons for a respective behavior of the channel itself. Exactly such a behavior is expected for the step algorithm explained in Chapter 3.3.1, because most of the connections start the data transmission with target SIR values much higher than required and they converge slowly to reagions with reasonable SIR values.

Distribution of Quality Estimate Parameter

Before measurements are shown, it is quickly explained how the QE parameter may be measured at the NodeB. In the standard the exact way of implementation is as usual left open, but it says that the value should be estimated on data transmitted on the DPDCH. If this is not possible also the DPCCH may be used. There are a few well known techniques which are suited for this task. First the so called "brute force technique" can be used, it estimates the BER by use of the pilot bits. It has the disadvantage that the granularity is very low (usually some tens of pilot bits are transmitted for some hundreds of data bits). The BER is calculated as

$$BER = \frac{\text{number of erroneous pilot bits per TTI}}{\text{number of pilot bits per TTI}} \tag{3.5}$$

Next the "decoding-recoding" method can be used. It decodes the data and recodes it, afterwards received and recoded data is compared. This method is quite accurate but requires much processing power and leads to a long delay. The BER is calculated as

$$BER = \frac{\text{number of erroneous data bits per TTI}}{\text{number of data bits per TTI}} \tag{3.6}$$

Other methods are for example based on the soft-outputs of the channel decoder and are mentioned in [24].

Figure 3.12 shows the measured distribution of the received QE parameters. The green curved to the left belongs to correctly received frames whereas the red curve indicates wrong decoding. Measurements show that there are only certain values of BER that are signaled to the RNC, even if the number of transmitted bits per TBS should allow for much higher granularity. This leads to the assumption that the "brute force technique" is used for estimation, see Equation 3.5. The cause for that may be the tight restrictions on processing delay in the NodeB which may not allow for more sophisticated estimation procedures. Please note that the pilot bits are transmitted in the DPCCH, which may have different radio parameters than the DPDCH.

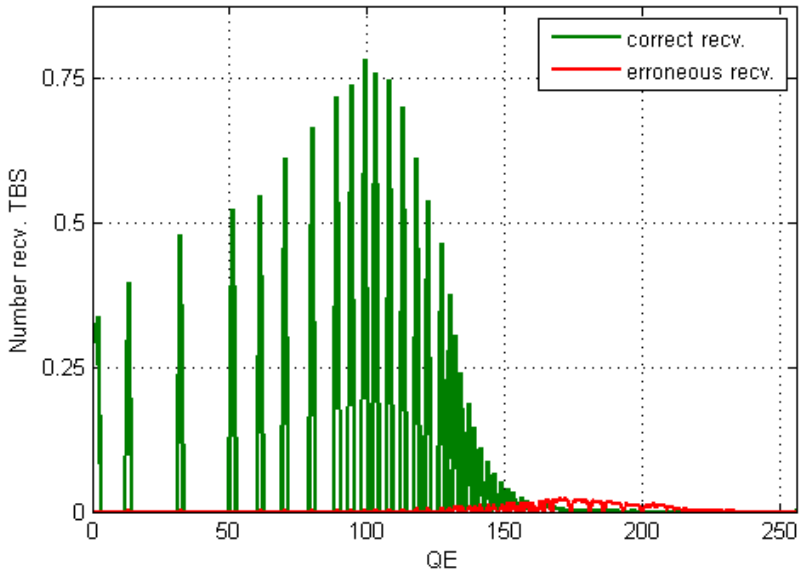

Figure 3.12: Distribution of the QE parameter, correct and erroneously decoded (voice traffic).

Also in this figure (like in Figure 3.11) it is observable that a large quantity of frames are transmitted at good channel conditions, producing low BERs around a QE of zero, even if the same restriction concerning bulk transfer have been applied. It again leads to the interpretation that the OLPC algorithm may suggest SIR targets which often exceed the minimum needs for a given QoS.

The curve for incorrect decoded frames has significant values for very high BERs. This is because of soft handover scenarios, where only one of several NodeBs receives a decodable frame.

Block Error Ratio and QE Parameter

On of the most interesting questions concerning the QE parameter and its possible usage for improvement of the OLPC algorithm is how it is related to the actual BLER. From Section 3.3.2 became clear that the estimation of the QE parameter may be done by means of the pilot bits on the DPCCH. Since this channel is always encoded with the same radio parameters, and the DPDCH may have varying settings, not only the channel coding may influence the relation between BER and BLER but also other radio parameters. In order to verify this assumption the different extractable measurement parameters introduced in Section 3.2.2 have been analyzed. By grouping the traced traffic according to the radio parameters into a manifold of clusters the following has been discovered:

- Obviously the relation between BLER and BER is strongly depending on the *coding rate*.
- Additionally the relation is dependent on the *spreading factor*, which confirms the assumption that the "brute force technique" is used (made in Section 3.3.2).
- Another parameter has been found on which the relation between BER and BLER is depending on, i.e. the *gain factor*, which is the relation between the transmit power of the DPDCH and the DPCCH. It is again an indicator that the "brute force technique" is in use.
- The implied relation is depending on the channel coding type and on the length of the respective coding blocks. Anyway this fact does not lead to very high variations and is

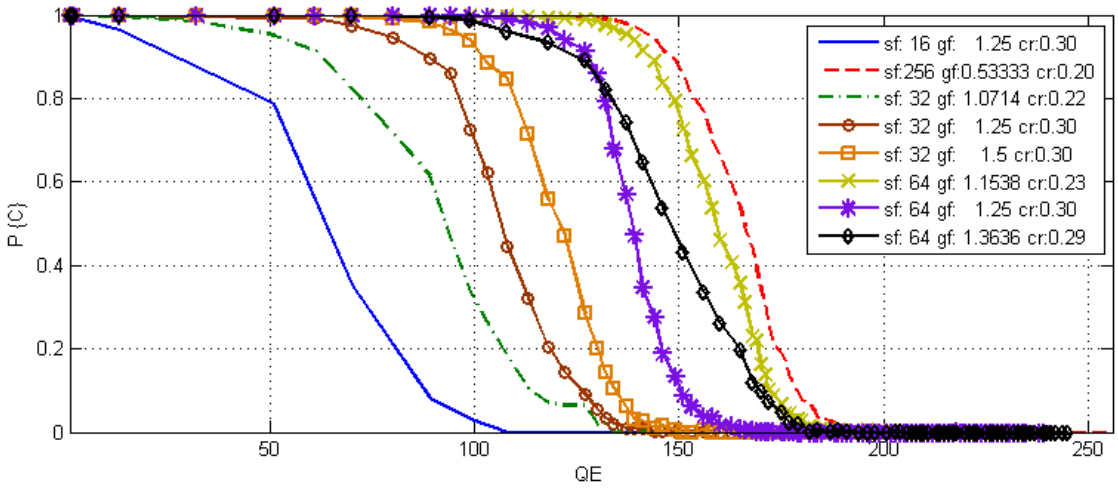

Figure 3.13: Relation between BLER (in terms of probability of correct frame reception) and BER (in terms of QE parameter), for different radio parameters.

therefore not treated with more detail. In the following it is considered as residual error.

Figure 3.13 shows the behavior of the probability of correct reception of a frame over the QE parameter. The different curves refer to different radio parameter sets, listed in the legend. Thereby "sf" denotes the spreading factor, "gf" the gain factor and "cr" the coding ratio. The shown curves have been selected out of a large number of possible combinations because they belong to the most common parameter sets, i.e. they result from the largest data sets.

What can be seen is that depending on the parameter set huge variations in the curves are possible, what manifests in shifted versions of the curves. Note that the desired operational point on the curves are found at the their left end, where the respective curve intersects the value of one minus the desired BLER. For the leftmost curves this may result in a QE value close to zero, what makes the improvement of the OLPC algorithm by means of the QE parameter questionable for these specific parameter sets. Further note that the leftmost curves look awkward because of the quantized nature of the transmitted QE parameter. This comes from the estimation algorithm working on the pilot bits.

Now considering that spreading factor, coding rate and gain factor may vary on a basis of a single RF, it would be useful to get rid of this discrepancy in order to be able to bring consecutive received QE values in relation to each other and to use them as indicator for the BLER. In fact by considering the differences of energy per coded bit, this is possible in an approximative way. The following relation reveals how energy per coded bit depends on those three parameters,

$$E_b \sim \frac{\beta^2 \, L_s}{R_c} \tag{3.7}$$

where β denotes the gain factor (amplitude of DPDCH over amplitude of DPCCH), L_s denotes the spreading factor and R_c stands for the coding ratio.

Using this indicator every received QE value can be weighted in terms of an offset, in order to obtain reasonable information about the quality of the respective RF. This weighting can be done the following way,

$$QE_{corr} \;=\; QE + \alpha \, \log_{10}\!\left(\frac{\beta^2 \, L_s}{R_c}\right) \tag{3.8}$$

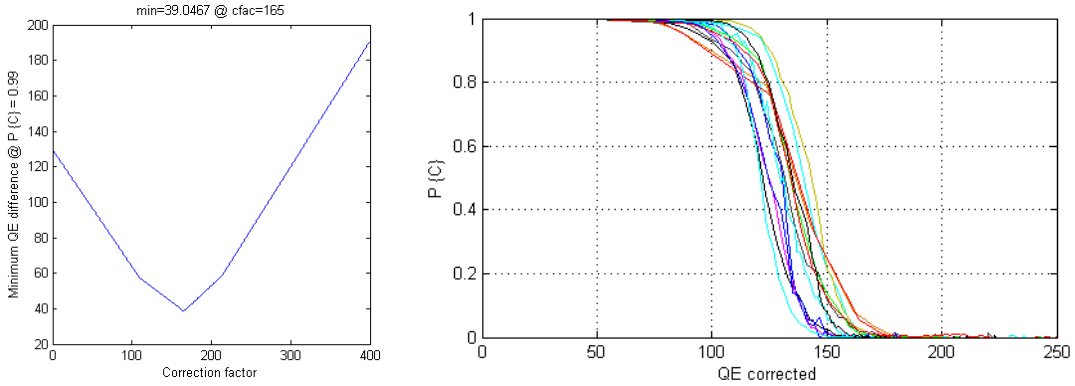

(a) Numerical minimization of α.

(b) Aggregation of BLER over BER curves.

Figure 3.14: SIR target distribution for different transmission conditions.

where α is the factor that minimized the discrepancy. Numerical minimization has been performed and is shown in Figure 3.14(a). The optimum factor α equals 165, what leads to a convergence of the curves with a residual difference of 40 in terms of QE (80% in terms of BER). The minimization has been performed at a value of P{C} equal to 0.99, what corresponds a BLER of 1%. The resulting corrected curves can be observed in Figure 3.14(b). Note that this step has to be repeated if the target BLER changes.

The residual error is expected to result from the different types of coding (see Chapter 2.2.2) and different lengths of the code blocks (long blocks may be encoded more efficient).

After this correction one single curve may be identified as representative for the general behavior of BLER over BER, even if some residual errors will be made.

Another more accurate way of getting rid of the discrepancy between the curves would be measurement aided processing of incoming QE values, e.g. one of the following:

- Shifting incoming values by a certain offsets, different for every radio parameter set. The offset could be calculated from measurement and should bring the respective BLER over BER curve info the best position to match the general representative curve.
- Storing all possible different BLER over BER curves by means of lookup tables would be a solution as well. This allows for immediate extraction of the current BLER but comes with the additional need of available memory.
- The simplification of the former approach is to fit all single curves to some kind of functions and only store the respective resulting parameters. This has the huge advantage that the curves are present in its originally form but there are only few values per curve to be saved. The conventional approach is to fit curves by polynomials. However, this may result in high order polynomials because of the shape of the measured curves. Therefore it is reasonable to apply other models. An example is presented in Chapter 4 where the curves are fitted with the aid of the so called Generalized Linear Model (GLM). This requires to save only two values instead of the whole curve but comes with enhanced computational demands.

Chapter 4

Modeling of the Outer Loop Power Control

In order to show a practical case of application of the measurement results obtained in Chapter 3 and to evaluate potential benefits in terms of power saving, simulations have been performed, which are presented in this chapter. These simulations do not claim to be done in a very sophisticated manner or to be highly related to real scenarios, they rather should give a first clue of what could be achieved by optimization of the power control algorithm.

To obtain reliable simulation results, a faithful designed simulator would be needed. This could be a system-level simulator which is able to emulate the lower protocol layers of UMTS in a multiuser environment. Because no such simulator was available and the creation of a respective tool is far beyond the scope of this thesis, the modeling of the ILPC loop as control path for the OLPC was done by means of statistical methods with the aid of the measurement results from the former chapter.

4.1 Closed Control Loop

Figure 4.1 again shows the control loop to be modeled. The division between controller and control path is made. First it is essential to model the control path in a adequate way, once this is done different control mechanisms can be implemented in the controller. This two topics are treated in the next sections separately.

One of the most sever simplifications of the model shown in the figure is that the multiuser aspect is neglected. As indicated there is only one single UE involved in the simulated process. In the real world the ILPC tries to compensate for interference from other users, within the same cell and from other cells, respectively. How accurate this procedure is depends on the implemented ILPC algorithm and on the measurement precision of the NodeB. By neglecting the multiuser issue, the model for the control path may be satisfactory for cells which are less loaded, in cases with high population or even congestion scenarios, this model should be abandoned.

Not considering multiple users also has another impact on the control loop, i.e. the change of the stability criterion. In general stability of the OLPC is strongly dependent on the number of active users in the cell, the respective throughput and QoS. For a certain conditions the OLPC can satisfy QoS conditions for every user, but if too many users are active, resources are getting scarce and in the worst case they are not sufficient any more. The resulting scenario would be that the OLPC tells every UE to transmit with more and more power what of course cannot be satisfied. So the key mechanism ensuring stability of the OLPC in a multi-user case is the admission control. More detailed investigation on this topic was already done in the early days of CDMA communications, see [40] and [45]. The conclusion for this work is to reject any stability

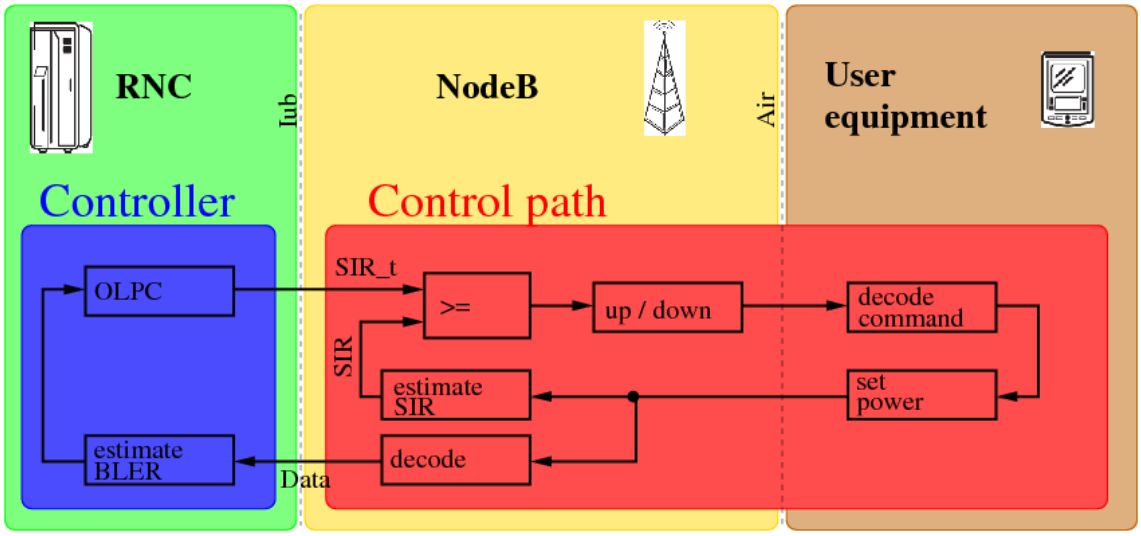

Figure 4.1: Control loop modeled for simulations.

study because very important issues like admission control can not be addressed.

4.1.1 Modeling the control path

As already said, the methods used for modeling the control path are statistical ones. This is done for the sake of simplicity. In the following the model is explained in detail. Figure 4.2 reveals the exact structure of the model. It is tried to imply as many measurement results as possible, but there are still unexplained components on which further investigation should be performed. In the following the single blocks are explained in more detail.

The model has one single input, i.e. the SIR target value. It is quantized as defined in the standard (see [19]) and its value is fetched for every TBS. The output on the other hand is composed of five different values, i.e. the three radio parameters known to influence the QE parameter (spreading factor, coding rate and gain factor), furthermore the QE parameter itself and of course the CRCi value. All these parameters can be assumed as known at the RNC for every single TBS. The execution of the model itself is done for every TBS, because it is assumed to be the longest period of guaranteed constant radio parameters. Actually this is not totally correct because there may be many simultaneous TrCHs with different TTI lengths and within the transmission of TBSs on a TrCH with long TTI a TrCH with short TTI may change. But for the case of multiple configured TrCH some restrictions have to be made which solve this issue as well (see below).

The first action of the model is to add a virtual SIR level to the SIR target. This step represents the channel conditions, i.e. Doppler spread and multipath environment, and is taken into account to enable simulation of dynamic changes of transmission quality.

$$SIR_k \simeq SIR_{target,k} - SIR_{virtual,k,k-1,\ldots,k-n} \tag{4.1}$$

shows how the actual assumed SIR, whereby the index “k” denotes the execution of the control loop. Within the scope of this thesis the exact behavior of this parameter has not been identified. This is due to the fact that sophisticated analysis of this parameter would require to manipulate the OLPC algorithm, what was not possible for the given measurement setup. Anyway, bounds for the variation of the parameter can be identified in Figure 3.11, i.e. it can be seen that most of the SIR target values finds within a region of 5 dB. Consequently, it is not reasonable to assume

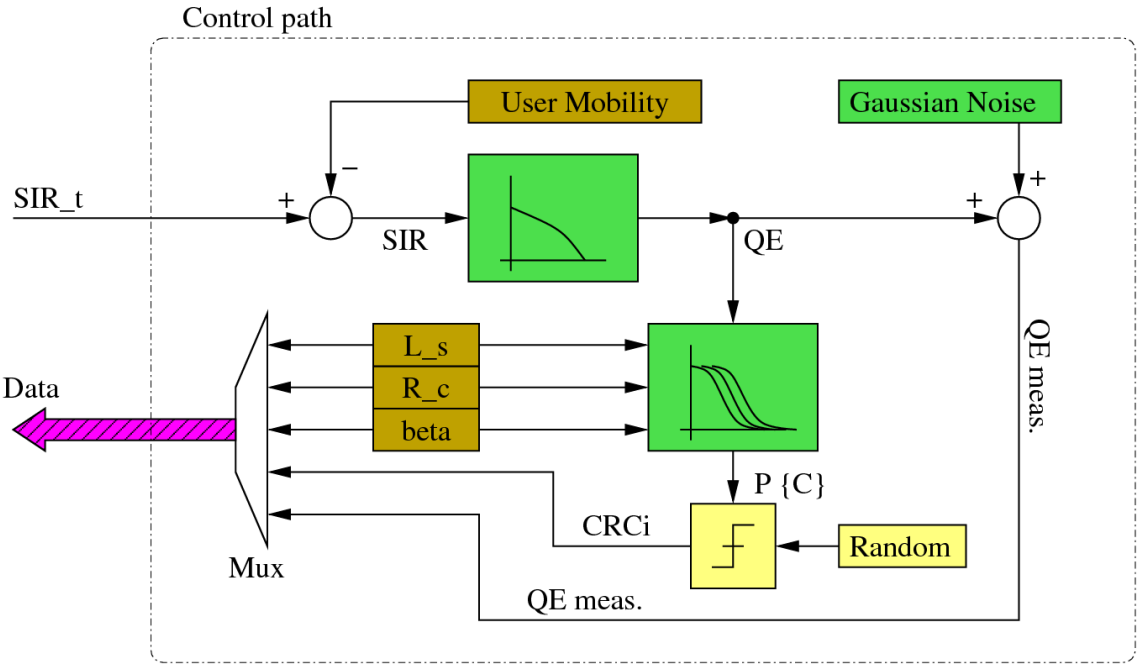

Figure 4.2: Model for the control path.

this target to vary for more than that value. Because of no further knowledge, the dynamics are modeled by a a slow random walk.

The next block is used to convert the SIR into a respective QE value. This is done by means of an expected SIR over BER behavior, further investigated in the former chapter. The respective measurement results can be observed in Figure 3.9 and 3.10, respectively. As already explained the measured curve has only a weak bending. The modeling by a second order polynomial failed because of the big uncertainty between different realizations and therefore a linear regression was preferred.

$$QE \simeq a\,SIR + b \tag{4.2}$$

where "a" and "b" are the parameters to be optimized by means of fitting to measured values. More information about curve fitting can be found in Appendix A. Afterwards an intermediate QE value is obtained which is used in two ways. First it is used to calculate the block error probability and second the QE value to be send to the RNC is calculated.

The block error probability is calculated from the intermediate QE parameter by means of the curves measured as relation between BLER and QE. The big influence of the three radio parameters as already determined in the former chapter was also taken into account. The block error probability over QE curves have been implemented by means of a Generalized Linear Model (GLM), the respective outcome is shown in Figure 4.3. The modeling function was chosen as

$$BLER \simeq \frac{1}{1 + e^{-a + b\,QE}} \tag{4.3}$$

The parameters "a" and "b" are the variables to fit to the measurement values. More information about GLM can be found in Appendix A and [38].

The out coming probability of a correct received block is fed into a threshold element which generates a binary random variable with exactly the same probability. This is done with the aid of a equal distributed variable.

The intermediate QE value on the other hand is processed to be send to the SRNC. This is done by simply adding Gaussian noise to the QE value. This method is reasonable by taking the

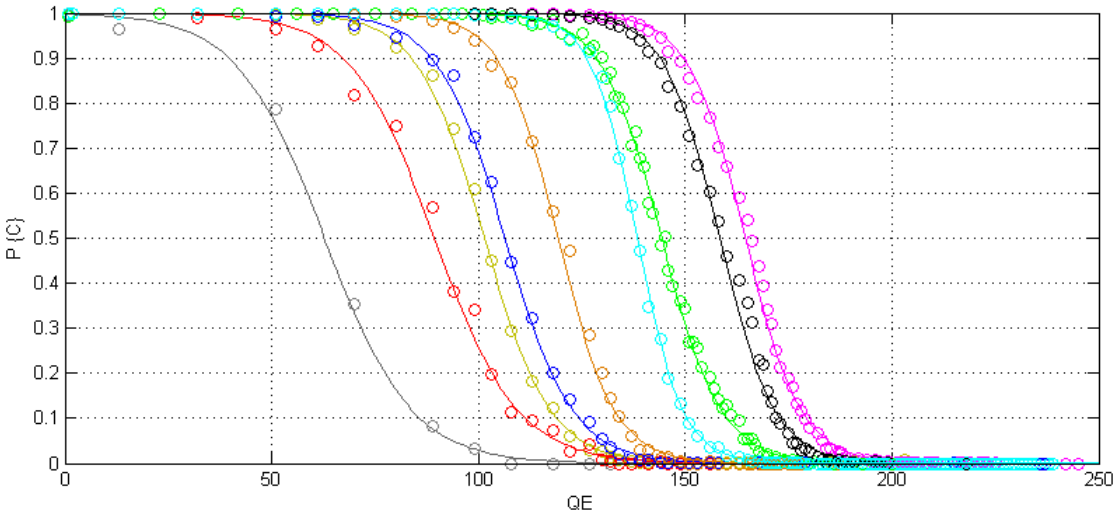

Figure 4.3: Fitting of measured data by means of the GLM.

measurements into account, see Figure 3.8(a). The distribution of the parameter to be send to the OLPC algorithm has in consequence the format

$$p(QE_{meas}) \simeq \frac{1}{\sigma\sqrt{2\pi}} e^{-\frac{(QE_{meas}-QE)^2}{2\sigma^2}} \tag{4.4}$$

where "σ" denotes the parameter to be fit to the measured values, see Appendix A. The only open issue is that the variance of this variable may vary with different QE values, see Figure 3.8(b). This fact is totally neglected by the model.

4.1.2 Simple Controller Deploying QE Information

In this section a simple new algorithm for OLPC is introduced. It is not optimized but used to simply get an idea of how big the gain of OLPC algorithms can be, if they take the QE information into account. To get comparable performance values for the OLPC algorithm currently in use, also the step algorithm (see Chapter 3.3.1) was implemented and simulated.

In Figure 4.4 this controller is shown. It consists of a double "integral" controller. The inner controller tries to keep the QE value at a certain level determined by the outer controller. It is tagged with "D2", "P2" and "I2" for the three control elements. The outer controller gets a QoS (BLER value) assigned from the respective service the connection is used for. It has to adjust the QE target value, which is the input value for "D2". Its elements are denoted "D1", "P1" and "I1". The two Finite Impulse Response (FIR) filters perform preprocessing of the measured QE and CRCi values respectively. This is basically taking the mean of the consecutive measured values.

Mathematically the system can be characterized by

$$QE_{target,k} = \left(- BLER_{target,k} + \sum_{i=1}^{n} \alpha_i \, BLER_{meas,k-i} \right) P_1 + QE_{target,k-1} \tag{4.5}$$

$$SIR_{target,k} = \left(- QE_{target,k} + \sum_{j=1}^{m} \beta_j \, BLER_{meas,k-j} \right) P_2 + SIR_{target,k-1} \tag{4.6}$$

where the index "k" again denotes the execution of the the control loop, "α" and "β" are the FIR coefficients and "P_1" and "P_2" refer to the proportional factors, respectively. "$QE_{target,k}$" in

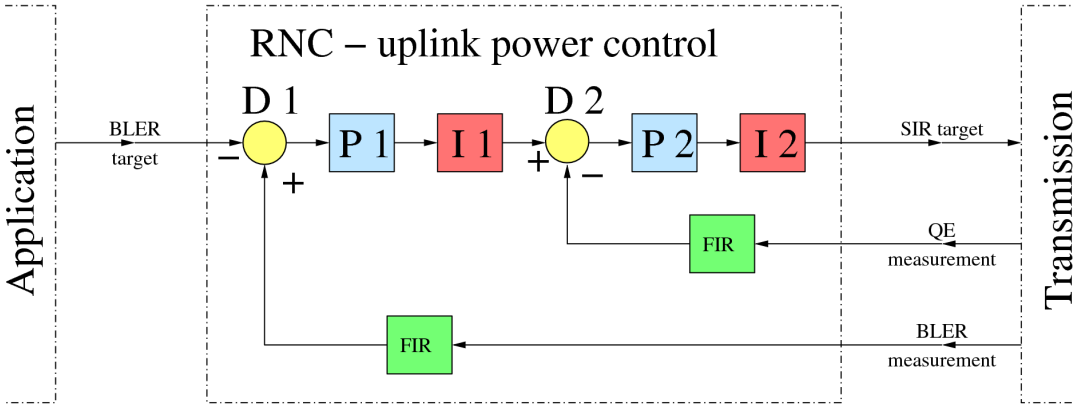

Figure 4.4: Proposed OLPC controller, deploying QE information.

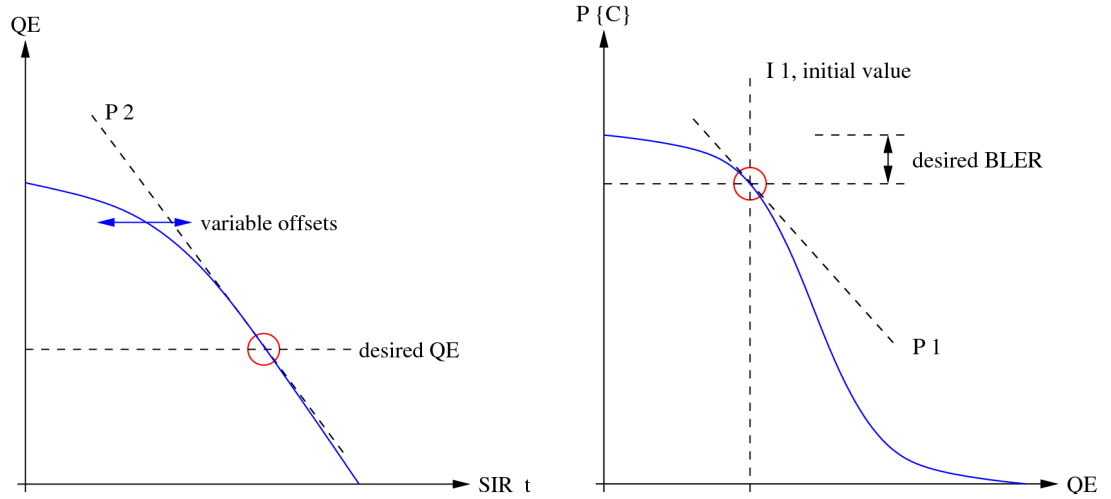

(a) Determination of the parameters for the SIR controller.

(b) Determination of the parameters for the QE controller.

Figure 4.5: Determination of different parameters of the controller.

Equation 4.5 and "$SIR_{target,k}$" in Equation 4.6 are the output values of the integral elements "I1" and "I2".

The main advantage of the system is, that the mean of the QE measurements is quite accurate after some tens of values. This means a good estimation of the underlying BLER can be made and the SIR target is adjusted accordingly. In consequence the estimation of the BLER by means of the CRCi values can take much more time, e.g. some hundreds or even thousands of TBSs. In contrary the step algorithm has to estimate the BLER immediately which is done in a binary way, i.e. the step algorithm figures out if it is too high or too low.

The integral controller consists of a proportional element, comparable to an amplifier, which implies a predefined multiplier. The integral element on the other hand can be preloaded with a certain value. In the following it is summarized how this parameters are determined.

The initial value of the integral element labeled "I2" is suggested to be the same as the initial value for the actual OLPC algorithm. This value is the power level detected by the open loop power control in the connection setup phase. It may be the most reasonable approach because of

the potentially high SIR offset resulting for different UEs, see Figure 4.5(a).

The proportional element should multiply with a factor of approximately the inverse slope of the tangent to the QE over SIR target curve in the desired operational point. Because of the respective slight bend of the curve the choice of the operational point is not considered important.

The initial value of the integral element denoted "I1" is considered rather critical. It is the target QE value on which the QE controller is locked at the first instance. Because of the slow convergence of the controller for the BLER this value should be in a reasonable region from the beginning. The value is chosen from the measured data depicted in Figure 3.13 for different sets of radio parameters respectively. The ways this can be done were already mentioned in Chapter 3.3.2. In this case the offset is calculated from the energy per uncoded bit whereas a safety margin is added because of the discrepancy between different parameter sets (see Figure 3.14 and Equation 3.7 respectively). An example is depicted in Figure 4.5(b).

Finally the proportional factor of the element tagged "P1" is set as the inverse of the slope of the tangent to the P{C} over QE curve in the desired operational point (see Figure 4.5(b)). In this case the curve is bend strongly, therefore the multiplier of the proportional element should vary according to the desired BLER.

One of the most important outcomes of Chapter 3 is that the QE parameter is strongly dependent on three radio parameters, i.e. the spreading factor, the coding rate and the gain factor, which can be different for every RF. In this control algorithm this fact is handled the way that only the TBSs from the TrCH with the lowest target QE value are taken into account for BLER calculations.

4.2 Numerical Results

Finally some simulation results are shown and concluding observations are stated in this chapter. Again note that the simulations can not be considered as very meaningful but should give a general overview on the OLPC algorithms.

4.2.1 Constant SIR demands

The first simulation was done with the assumption of a totally constant power demand, see Figure 4.6. The duration of the communication was set to 200 seconds. In the upper part of the figure the performance of the step algorithm can be observed, with the characteristic sawtooth course. In the lower part the performance of the algorithm explained in the former section is shown.

It can be observed that the dynamic range of both algorithms is more or less the same. The most distinctive difference arises at the beginning of the connection. Whereas the step algorithm needs some time to reach the SIR value corresponding to the targeted BLER, the algorithm deploying the QE parameter comes into the right region after a couple of transmitted TBSs. This is possible because of the adequate initial value of the integral element "I1", see Figure 4.4. Most of the saved energy in comparison to the step algorithm is assumed to come from this interval. Moreover also the impact of the safety margin added to this initial value can be observed, i.e. in the first tens of seconds a constant lowering of the SIR target is visible, this is because the outer controller (BLER controller) has first to compensate for this margin.

In the figure the dynamics of the two integral controllers can be observed, i.e. the inner controllers dynamic (QE controller) is most conspicuous at the very beginning of the connection, manifested in the sharp edge down to reasonable values after some tens of received values. Furthermore the dynamics of the outer controller (BLER controller) can be observed as slight oscillation around a certain SIR value for the whole duration of the connection.

It is noticeable that the fast fluctuations of the SIR target value determined by the controller proposed in this work are rather high. Effectively they can be compared to the fluctuations triggered due to the step algorithm. This is because of a tradeoff that has to be made during the

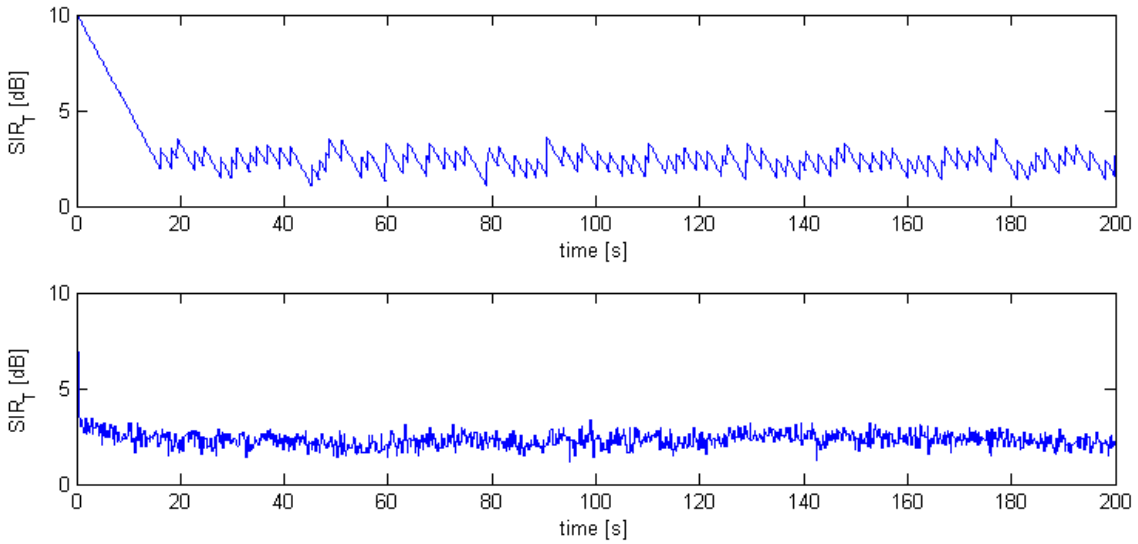

Figure 4.6: Simulation of connection with constant SIR demands.

design phase of the controller, i.e. if the FIR filter that processes the incoming QE values is long, the fluctuations will be less but the reaction time on dynamic changes of the power demands is enhanced, what could result in high error ratios. The actual problem of this issue is again the way the QE parameter is estimated in the NodeB. If this could be done more accurate the fluctuations could be decreased (compare Figure 3.8(a)).

4.2.2 Dynamic SIR demands

The second simulation, shown in Figure 4.7, emulates connections undergoing a slight (Figure 4.7(a)) and heavy (Figure 4.7(b) change of power demands. Again in the upper part of the figures the conventional OLPC algorithm is depicted and in the lower part the algorithm described in the former section was applied.

As already mentioned in Section 4.1.1, the dynamics of the SIR demands are modeled by a random walk. This is because the real dynamics could not be measured in the actual measurement setup. Also in literature there is no adequate model formulated which could have been applied for this kind of simulations. Since the dynamics in the power demands can be lead back to changes in macroscopic movement (e.g. humans or objects), there is no reason to expect changes with high frequency. In consequence they have been modeled as a slow random walk for this simulations. Thereby changes in the magnitude of more than 5 dB are not considered reasonable, regarding this, Figure 4.7(b) shows the limiting case.

The observation that can be made in the figures is that, as expected, the algorithm deploying QE information is able to follow the power demands of the connection quite close. This is manifested in the smooth changes similar to a random walk with low frequency. The step algorithm on the other hand can not follow the dynamics of the random walk, the outcome is a rather constant developing at SIR values which are most often higher than required. Additionally it can be observed that consecutive block errors are very likely by means of up-steps in a row.

At this place it has to be mentioned that a random walk is much more suited for the controller presented in this work than for the step algorithm. If the changes in the SIR demands would be more aggressive, e.g. single peaks or rectangular functions, the proposed algorithm would produce more errors at every edge than the step algorithm. In a limiting case (i.e. if the changes come to often) the algorithm is not able to balance the BLER any more. In this case modifications in

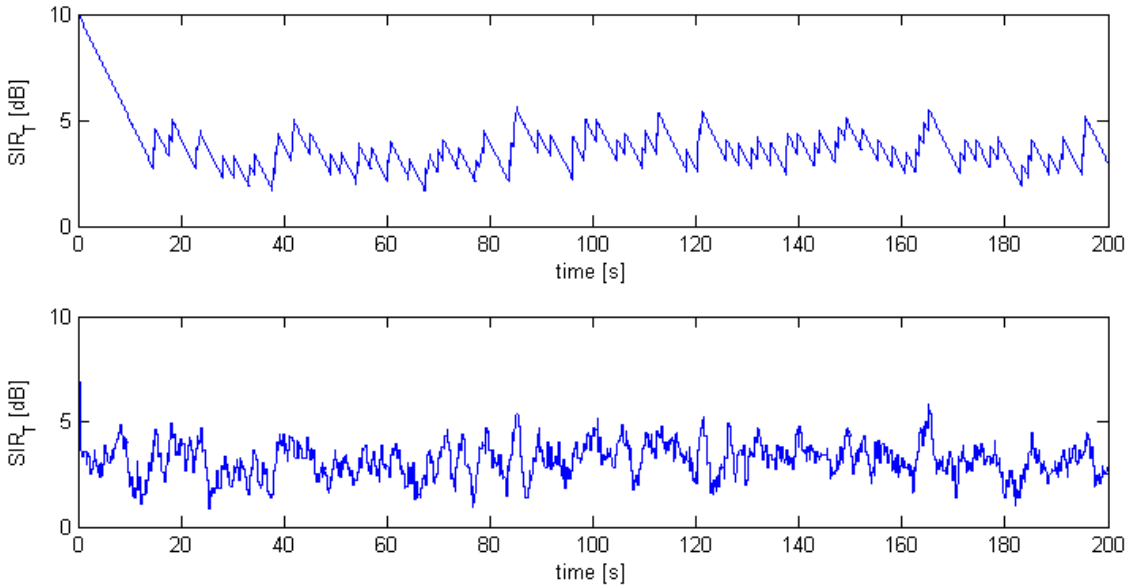

(a) Dynamic scenario, moderate variations.

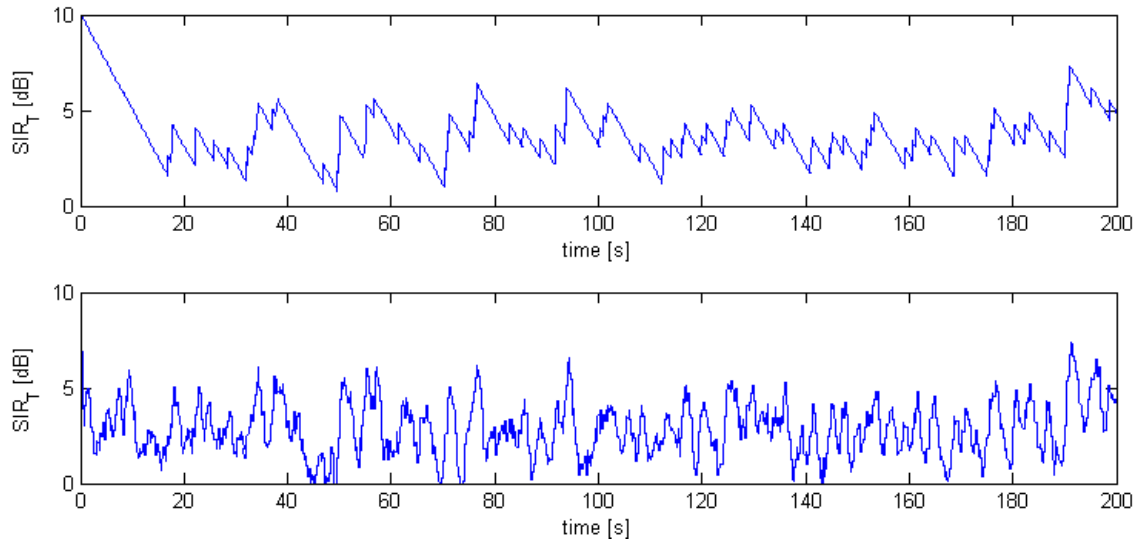

(b) Dynamic scenario, high variations.

Figure 4.7: Simulation of connections with moderate and highly dynamic SIR demands.

SIR demands	Constant		Moderate		Dynamic	
Figure	4.6		4.7(a)		4.7(b)	
Controller	Step	Int	Step	Int	Step	Int
BLER	0.0088	0.009	0.0089	0.0093	0.009	0.0098
mean SIR [dB]	2.67	2.33	3.53	3.15	3.78	2.87

Table 4.1: Example of resulting values for connections with constant, moderate and highly dynamic power demands, "Step" denotes the step algorithm by Sampath, "Int" the method proposed in this work.

the algorithm may be performed to make it better suited for the actual demands. Still there is no visible reason why there should be very fast fluctuations.

4.2.3 Comparison and Conclusions

The overall observations from the simulations are that in a scenario with constant power demands the saving of the proposed algorithm may be at least 0.2 dB of mean power, whereas in dynamic scenarios the benefit of the proposed algorithm is increasing with increasing variations in SIR demands. Maximum savings of 1 dB seem to be feasible, but with an optimized algorithm it could be even more. A summary of the results is given in Table 4.1. It contains the out coming parameters of the simulations shown in Figure 4.6, 4.7(a) and 4.7(b) respectively.

For short durations of a connection the situation looks slighly different. Since the step algorithm needs some tens of seconds to converge, the disired value is likly to not be reached at all. Simulations of connections shorter than half a minute have shown that the achievalbe gain is far above the gain obtained concerning connections with longer durations. As follow up, the commonness of such connections should be further investigated. Note that the QE value could also be used for only setting an adequate initial value for the step algorithm, which is currently in use. This slight modification of the OLPC algorithm would already save a lot of transmit power.

It is interesting to note that neither the step algorithm nor the proposed OLPC algorithm are able to ensure the desired BLER is reached. Both methods lead to a slightly better BLER. In general this is no problem, but it means that there still are further power savings achievable. The reason the step algorithm performs better than required is the slow convergence to the desired BLER. The reason the proposed algorithm performs better than required is due to convexity of the curve shown in Figure 4.5(b) and its linear approximation. Because of the convexity deviations towards better BLER are underestimated, deviations in the other direction are overestimated.

The results are an affirmation of the step algorithm which shows a good performance despite of its simplicity. The advantage of the proposed algorithm on the other hand is abstractly spoken the utilization of an extra parameter. So theoretically, if this parameter bears any information correlated to the value under investigation (i.e. the BLER), there must be a possibility to perform better or at least equal by exploiting this information. Unfortunately the additional gain achieved here was not as big as expected, because of all the practical problems explained above.

Nevertheless the proposed algorithm could be implemented in existing systems by means of a software update in the RNC. It is completely standard compliant requires a very low amount of intervention in the network, is relatively easy to implement in hardware and comes with almost no additional processing demands.

Chapter 5

Conclusions and Outlook

Recent investigations on link level error characteristics revealed constant error patterns in Universal Mobile Telecommunication System (UMTS) connections. The reason was identified to be the Outer Loop Power Control (OLPC) algorithm, which was expected to be Sampath's step algorithm, see [41]. In consequence the question if the OLPC algorithm could be improved was proposed, in order to save transmission power and reduce interference in the UMTS network.

For this work we had the possibility to access a powerful connection tracing tool installed in a live UMTS network. First the analysis of extractable data was performed. This investigation revealed that a lot of information related to the uplink OLPC is transmitted over the Iub-interface, whereas a very small amount of data concerning the downlink OLPC could be extracted. Therefore no further research was done for the uplink case. Concerning High Speed Uplink Packet Access (HSUPA) it turned out that the power control loop indeed deploys comparable instances but the nature of the data transmission is changed radically compared to the conventional transmission case. This in turn was the reason to abandon the research on HSUPA because it would lead to a different problem formulation as in the conventional case and there are few similarities between the two OLPC problems.

The measurements obtained by the tracing tool have been partially verified by means of other measurements of single connections performed at the User Equipment (UE) side. This was done by the aid of dedicated mobile equipment and respective software tools.

Intensive measurements at the Iub-interface showed that Sampath's OLPC algorithm indeed is in use in the respective UMTS network. It uses the Cyclic Redundancy Check (CRC) checksum as input parameter to control the Block Error Ratio (BLER) by variation of the target Signal to Interference Ratio (SIR) value. The distribution of the SIR target value is shown, what gives and idea of the dynamic range of this parameter. Additionally, impairments have been identified and were attributed to the OLPC algorithm.

Furthermore the Quality Estimate (QE) parameter, corresponding to a certain Bit Error Ratio (BER) and transmitted in addition to every Transport Block Set (TBS), was identified to be strongly correlated to the BLER on the radio link. The parameter was exhaustively analyzed and its behavior was interpreted. It is shown that the estimation of the BER in the Base Station (NodeB) is done with the aid of the pilot bits on the Dedicated Physical Control Channel (DPCCH). This lead to a certain amount of Gaussian noise overlaid the actual value. Moreover it turned out that the BLER in relation to the measured QE value is dependent on the coding rate, the coding type, the spreading factor and the gain factor of the actual radio link. The relation between those different parameters was analyzed in detail and a model was built for it. BER curves over SIR target values have been identified. Summarizing, the QE parameter can be used for improvement of the OLPC algorithm.

In consequence the information obtained from the measurements was used to build a model of the Inner Loop Power Control (ILPC) loop as control path for the OLPC. This model is based

on statistical methods, whereby certain simplifications have been made. Two adequate OLPC algorithms have been implemented, i.e. the step algorithm by Sampath and a double integral controller proposed within this work.

Simulations of different scenarios revealed that the proposed algorithm works better than the step algorithm. This is somehow intuitive because of the additional information exploited by the new method, i.e. information carried by the QE parameter. Nevertheless the gain in terms of mean SIR target required by the Serving RNC (SRNC) was identified as moderate. Depending on the dynamics of the radio link, regarding the changes in SIR demands, 0.2 dB to 1 dB transmission power can be saved in the respective UE. These results emphasize the robustness and good performance of Sampath's step algorithm. Still the proposed method is completely standard compliant, easy to implement, needs relatively low intervention in the network and comes with almost no additional processing demands.

During this work many questions arose which could be starting points for further research:

- Investigation on the performance of the power control algorithm of HSUPA would be of interest, because of the migration of packet oriented traffic into this direction.
- Joined analysis of multiuser and multi-cell scenarios could be performed. Within this work more sophisticated models for the ILPC could be build for simulation purposes. Additionally stability studies can be performed by integrating admission control into the model. Simulations may be preformed by means of a system-level simulator.
- The modeling of the dynamic power demands of radio links by a random walk is not very sophisticated. To do better the performance of the ILPC must be determined accurately, what could be done either by means of measurements of single connections or by simulations.
- The commonness of connections with short durations, i.e. below half a minute, should be investigated. For such connections the gain obtained by deployment of the proposed algorithm is much higher than for connections with longer duration.

Appendix A

Curve Fitting

In the following the problem is addressed how a series of measured points can be fit to a function by optimizing the parameters of the function, detailed information can be found in [29]. Therefore first a function has to be chosen and a metric has to be defined in order to evaluate the quality of the fit.

As a possible metric the sum of the distance from the measured points to the curve to be fit could be used. The smallest distance from a point to a line is the perpendicular distance. It is shown in Figure A.1(a).

Anyway it is mathematically simpler to use the vertical distance from a point to a curve as metric. The vertical distance can be calculated by simply taking the difference of the respective values of point and curve along this dimension. This is depicted in Figure A.1(b). Because of mathematical treatment of absolute values is not manageable, a second simplification is done, i.e. the squared distance is taken instead of the distance. By doing so, the expression for the metric is simple and differentiable, what makes its analytical treatment possible. This metric is known as

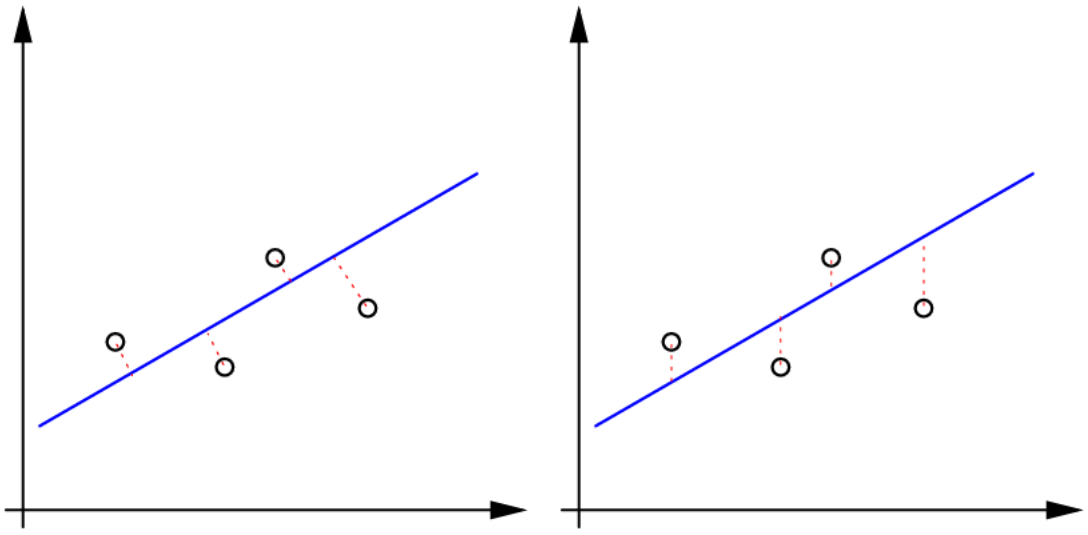

(a) Perpendicular distance from points to curves.

(b) Vertical distance from points to curves.

Figure A.1: Distances from points to curves, applicable as metric.

"Least Squared Error (LSE)" and can be written as

$$E^2 = \sum_i (y_i - f(x_i, \alpha, \beta, ...))^2 \tag{A.1}$$

where "E" denotes the error, "i" the index of the measurement point, "$f()$" the function to be fit to the measurement and "α" and "β" the parameters of the function which have to be optimized.

Now after a metric is introduced, the actual optimization can take place. It is treated in the following sections for different kinds of functions.

A.1 Linear Least Squares

The linear LSE method is also known as "linear regression". This technique is used to estimate the straight line which fits best to a cluster of points. Additionally if the points are not aligned along a straight line, the values of the points may be transformed by a certain function in order to arrange them on a straight line. The minimization problem was solved by Gauss and Legendre independently.

The function which should be fit to the data points writes as

$$f(x_i, \alpha, \beta, ...) = \alpha\, x_i + \beta \tag{A.2}$$

and in consequence the squared error according to Equation A.1 can be written as

$$E^2 = \sum_i (y_i - (\alpha\, x_i + \beta))^2 \tag{A.3}$$

The minimization of the LSE can be calculated analytically by differentiating the expression for the error and setting it to zero.

$$\begin{aligned} \tfrac{\partial E^2}{\partial \alpha} &= -2 \textstyle\sum_i (y_i - (\alpha\, x_i + \beta)) x_i = 0 \\ \tfrac{\partial E^2}{\partial \beta} &= -2 \textstyle\sum_i (y_i - (\alpha\, x_i + \beta)) = 0 \end{aligned} \tag{A.4}$$

This leads to the set of equations

$$\begin{aligned} n\beta + \alpha \textstyle\sum_i x_i &= \textstyle\sum_i y_i \\ \beta \textstyle\sum_i x_i + \alpha \textstyle\sum_i x_i^2 &= \textstyle\sum_i x_i y_i \end{aligned} \tag{A.5}$$

where "n" denotes the number of measured data points. By substitution of

$$s_{xx} = \sum_i x_i^2 \qquad s_{xy} = \sum_i x_i y_i \qquad \overline{x} = \frac{1}{n} \sum_i x_i \tag{A.6}$$

the final results for the optimization problem are

$$\begin{aligned} \alpha &= \tfrac{s_{xy} - n\, \overline{x}\, \overline{y}}{s_{xx} - n\, \overline{x}^2} \\ \beta &= \tfrac{\overline{y}\, s_{xx} - \overline{x}\, s_{xy}}{s_{xx} - n\, \overline{x}^2} \end{aligned} \tag{A.7}$$

A.2 Nonlinear Least Squares - Gauss Fitting

In order to fit measurement points to a Gauss curve, the application of linear LSE estimation is not feasible any more. In this case nonlinear LSE has to be use. It is an iterative method.

The Gaussian curve can be specified by three parameters, the factor "β", the mean "μ" and the variance "σ^2". The function can be written as

$$f(x, \beta, \mu, \sigma^2) \;=\; \frac{\beta}{\sigma\sqrt{2\pi}}\, e^{\frac{(x-\mu)^2}{2\sigma^2}} \tag{A.8}$$

but in the following the nonlinear LSE fitting will be explained in a more general way.

Consider a function

$$y_i \;=\; f(x_i, \lambda_1, ..., \lambda_n) \tag{A.9}$$

where the parameters "λ_j" should be optimized to best fit the measurement points "(x_i, y_i)". First an initial guess of adequate λ_j has to be made, what is arranged in the vector $\underline{\lambda}$. The deviation of the curve to a single measurement point is defined as

$$d\beta_i \;=\; y_i - f(x_i, \underline{\lambda}) \tag{A.10}$$

what can also be written in a vector notation as $d\underline{\beta}$. In consequence the difference $d\underline{\lambda}$ can be calculated which would reduce $d\beta_i$ to zero in a linear way.

$$d\beta_i \;=\; \sum_{j=1}^{n} \frac{\partial f}{\partial \lambda_j}\, d\lambda_j \;\Big|_{x_i, \underline{\lambda}} \tag{A.11}$$

By declaring "A_{ij}" the following

$$A_{i,j} \;=\; \frac{\partial f}{\partial \lambda_j} \;\Big|_{x_i, \underline{\lambda}} \tag{A.12}$$

the matrix "$\mathbf{A}$" can be composed and the relation formulated in Equation A.11 can be rewritten in matrix notation as

$$d\underline{\beta} \;=\; \mathbf{A}\; d\underline{\lambda} \tag{A.13}$$

The deviation $d\underline{\lambda}$ can now be calculated by means of the pseudo-inverse of $\mathbf{A}$ according to

$$d\underline{\lambda} \;=\; (\mathbf{A}^T\mathbf{A})^{-1}\mathbf{A}^T\; d\underline{\beta} \tag{A.14}$$

Applying $d\underline{\lambda}$ to $\underline{\lambda}$ gives a new, better estimate of the parameter set. Now the next iteration may be started. The calculation can be terminated if the LSE term

$$E^2 \;=\; d\underline{\beta}\; d\underline{\beta} \tag{A.15}$$

is considered as small enough for the desired application.

A.3 Generalized Linear Model

The Generalized Linear Model (GLM) is a generalization of the LSE regression. The generalization comprises two points, i.e.

- the linear model may be related to the response variable by means of a link function and
- the magnitude of the variance of the measured values may be depended on the predicted value.

The GLM combines different models into one framework, e.g. the linear regression. This allows for building sophisticated estimators for a manifold of distributions. The main characteristics of the model are the following

- For each set of the parameters of the function to be fit to measured values, the distribution of this values around its mean must be from the exponential family. Normal, Binomial and Poisson distributions for example belong to this family. This fact effects the metric for determination of the error.
- A coefficient vector "$\underline{\lambda}$" defines a linear combination of measured values, $\underline{x}\,\underline{\lambda}$. This is called the "linear predictor".
- A "link function" $g(\cdot)$ is defined in order to transform the measured values according to

$$\mathcal{E}(\underline{y}) \;=\; \underline{\mu} \;=\; g^{-1}(\underline{x}\,\underline{\lambda}) \tag{A.16}$$

  where "$\mathcal{E}(\cdot)$" denotes the expectation. The vector "$\underline{\mu}$" defines the shape of the curve fitted to the measurement.

The optimization of the parameters $\underline{\lambda}$ is done by recursive methods, comparable to the method in the former section. Examples would be the Newton-Raphson method or Fisher's scoring method. More information about the GLM can be found in [38].

For the regression in Chapter 4 a "logistic" function was chosen as link function for transformation of the measurement points. It has the from

$$g(p) \;=\; \mathit{logit}(p) \;=\; \log\left(\frac{p}{1\;-\;p}\right) \tag{A.17}$$

and the respective inverse function is

$$g^{-1}(p) \;=\; \frac{1}{1\;+\;e^{-p}} \tag{A.18}$$

The resulting transformed measurement points $(g(y_i), x_i) \;=\; (y_i', x_i)$ have been fit to a straight line

$$y_i' \;\approx\; \alpha\, x_i \;+\; \beta \tag{A.19}$$

The distribution applied to the model was chosen as binomial.

Appendix B

Connection Setup

In the following an example of a connection setup is shown. The connection corresponds to a call terminated by the user. This example is given in order to show the chronology of different messages. It reveals difficulties of tracing connections due to the manifold of protocols.

The bold vertical lines below the depicted network elements correspond to time lines. Connections between different network elements are symbolized by arrows. The respective caption consists of the name of the protocol which is initiating the connection before the colon and the respective transmitted message after the colon.

The acronyms for the protocol names stand for

- Radio Access Network Application Part (RANAP)
- Radio Resource Control (RRC)
- NodeB Application Part (NBAP)
- Access Link Control Application Part (ALCAP)
- Frame Protocol (FP)
- Mobility Management (MM)
- Call Control (CC)

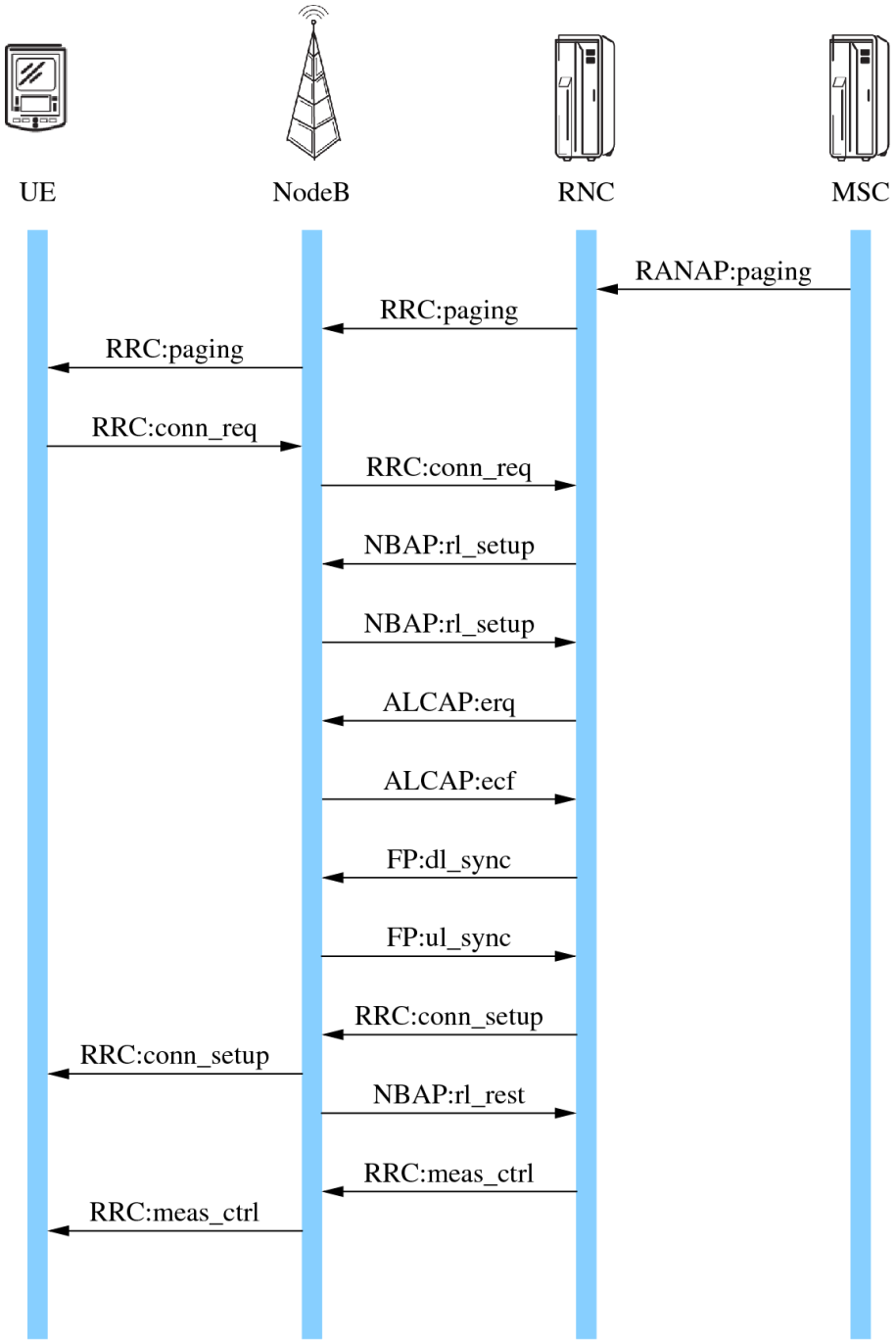
UE
NodeB
RNC
MSC
RANAP:paging
RRC:paging
RRC:paging
RRC:conn_req
RRC:conn_req
NBAP:rl_setup
NBAP:rl_setup
ALCAP:erq
ALCAP:ecf
FP:dl_sync
FP:ul_sync
RRC:conn_setup
RRC:conn_setup
NBAP:rl_rest
RRC:meas_ctrl
RRC:meas_ctrl

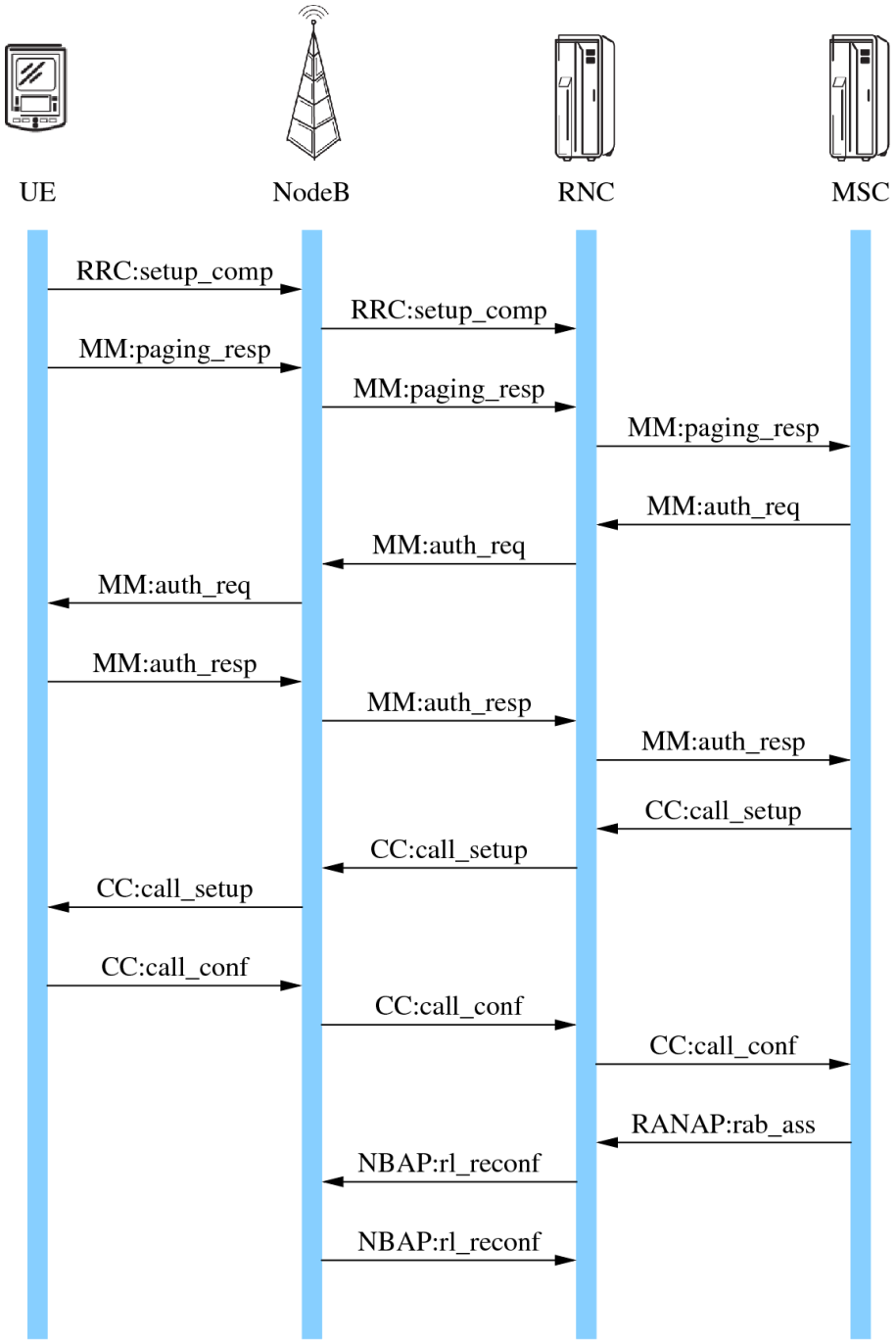
UE
NodeB
RNC
MSC
RRC:setup_comp
RRC:setup_comp
MM:paging_resp
MM:paging_resp
MM:paging_resp
MM:auth_req
MM:auth_req
MM:auth_req
MM:auth_resp
MM:auth_resp
MM:auth_resp
CC:call_setup
CC:call_setup
CC:call_setup
CC:call_conf
CC:call_conf
CC:call_conf
RANAP:rab_ass
NBAP:rl_reconf
NBAP:rl_reconf

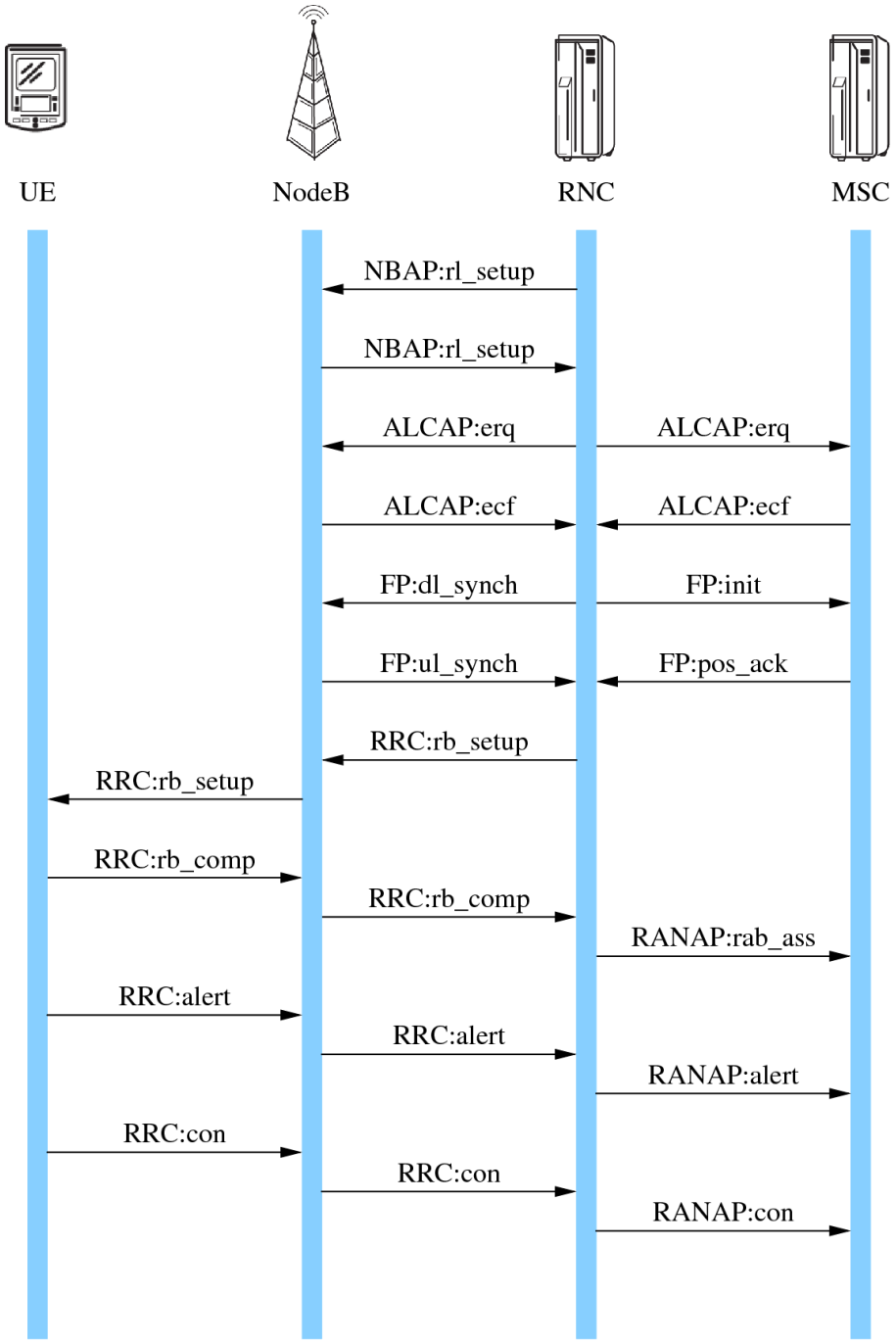
UE
NodeB
RNC
MSC
NBAP:rl_setup
NBAP:rl_setup
ALCAP:erq
ALCAP:erq
ALCAP:ecf
ALCAP:ecf
FP:dl_synch
FP:init
FP:ul_synch
FP:pos_ack
RRC:rb_setup
RRC:rb_setup
RRC:rb_comp
RRC:rb_comp
RANAP:rab_ass
RRC:alert
RRC:alert
RANAP:alert
RRC:con
RRC:con
RANAP:con

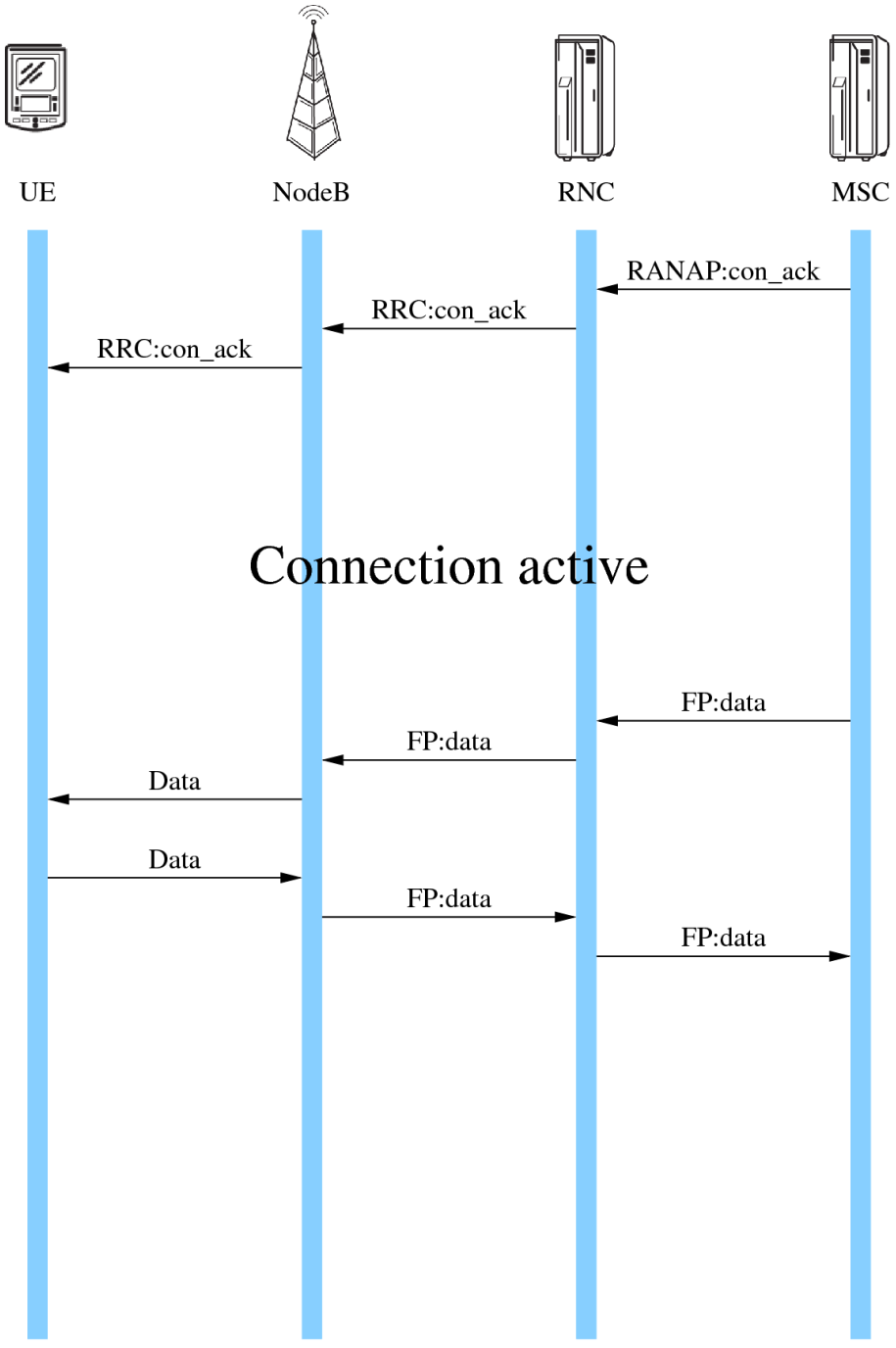

Figure B.1: Connection setup of a user terminated voice call.

Appendix C

Class Diagram of the Data Aquisition Module

In the following the structure of the module used for data extraction at the Iub-interface is explained by the use of a Unified Modeling Language (UML) class diagram. The diagram shows the classes defined in the module and the respective dependencies.

The structure of the classes is divided into three parts

- Class name
- Included variables
- Defined procedures

Dependencies start with a label which identifies the behavior of it and ends with a number, which indicates the number of possible instances, where "*" denotes an arbitrary number.

Note that the figure contains only an overview of the stucture and is not complete, e.g. in the class "TFCS" there are three times as many functions as stated in the figure because the messages look different for UMTS Release 99, Releas 4 and Release 5.

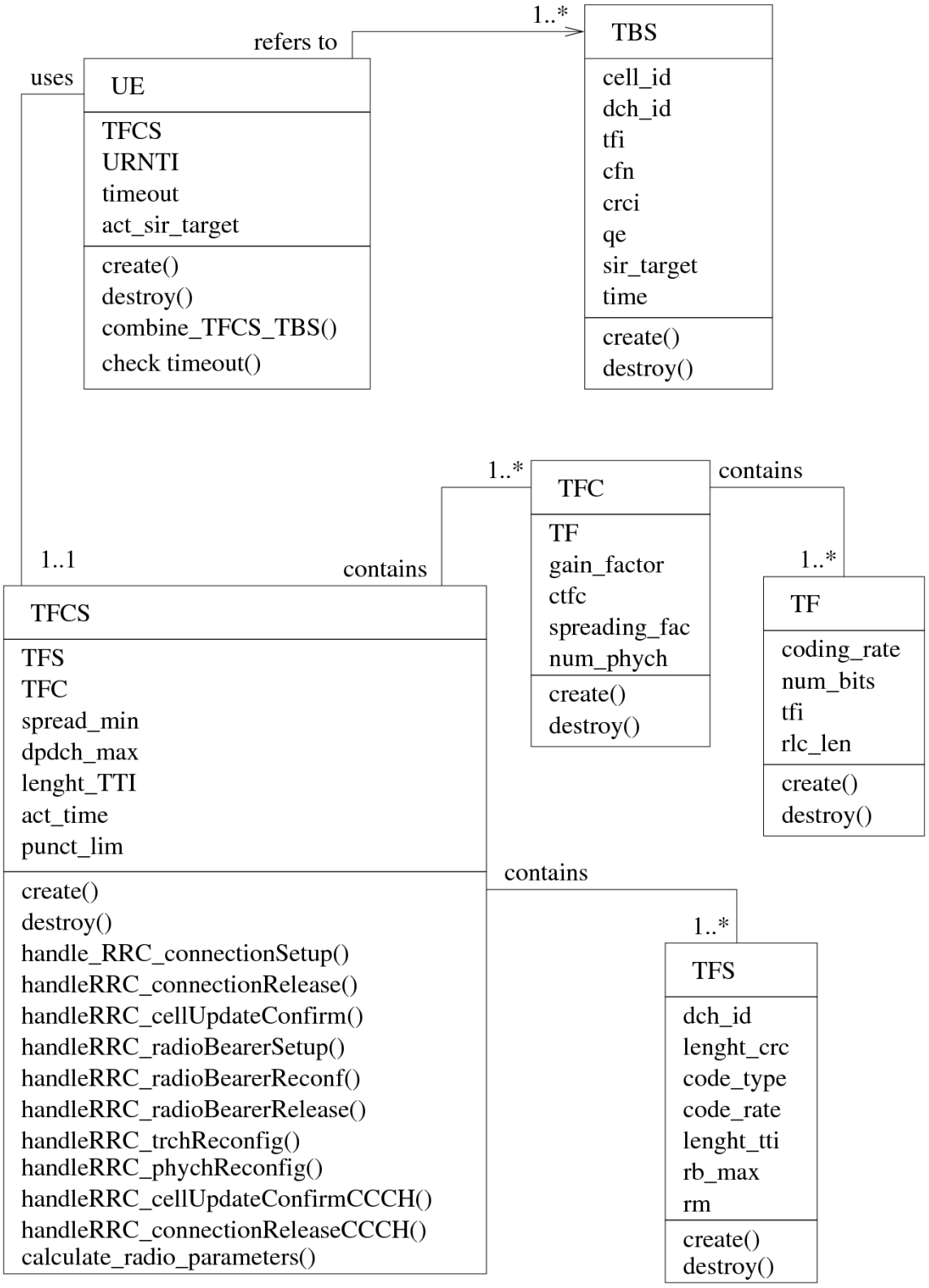

Figure C.1: UML class diagram of the data extraction code for the Iub-interface.

Acronyms

3G	3^{rd} Generation
2G	2^{nd} Generation
3GPP	3^{rd} Generation Partnership Project
4QAM	4-Point Quadrature Amplitude Modulation
ALCAP	Access Link Control Application Part
AMR	Adaptive Multi-Rate
AS	Access Stratum
ATM	Asynchronous Transfer Mode
BCH	Broadcast Channel
BER	Bit Error Ratio
BLER	Block Error Ratio
CC	Call Control
CCTrCH	Common Coded Transport Channel
CDMA	Code Division Multiple Access
CN	Core Network
CRC	Cyclic Redundancy Check
CRCi	CRC-indicator
CRNC	Controlling RNC
CS	Circuit Switched
DAG	Data Acquisition Module
DCH	Dedicated Channel
DECT	Digital Enhanced Cordless Telecommunications
DPCCH	Dedicated Physical Control Channel
DPDCH	Dedicated Physical Data Channel
DRNC	Drift RNC
DSSS	Direct Sequence Spread Spectrum
E-DCH	Enhanced Dedicated Channel
FACH	Forward Access Channel
FBI	Feed-Back Information
FDD	Frequency Division Duplex
FDMA	Frequency Division Multiple Access
FEC	Forward Error Correction
FIR	Finite Impulse Response
FP	Frame Protocol
FSPL	Free Space Path Loss
FTW	Forschungszentrum Telekommunikation Wien
GGSN	Gateway GPRS Support Node
GLM	Generalized Linear Model
GMSC	Gateway MSC
GPRS	General Packet Radio Service
GSM	Global System for Mobile Communications

HARQ	Hybrid Automatic Repeat Request
HF	High Frequency
HSDPA	High Speed Downlink Packet Access
HSPA	High Speed Packet Access
HSUPA	High Speed Uplink Packet Access
HS-DSCH	High Speed Downlink Shared Channel
I	In-phase
ICI	Inter-Cell Interference
ILPC	Inner Loop Power Control
IP	Internet Protocol
ISCP	Interference Signal Code Power
ITU	International Telecommunication Union
LSE	Least Squared Error
MAC	Medium Access Control
ME	Mobile Equipment
MM	Mobility Management
MSC	Mobile-service Switching Center
MRC	Maximum Ratio Combining
NAS	Non-Access Stratum
NBAP	NodeB Application Part
NodeB	Base Station
OFDM	Orthogonal Frequency Division Multiplexing
OLPC	Outer Loop Power Control
OSI	Open System Interconnection
OVSF	Orthogonal Variable Spreading Factor
PCH	Paging Channel
PDU	Packet Data Unit
PN	Pseudo-Noise
PHY	Physical
PLMN	Public Land Mobile Network
PS	Packet Switched
PSTN	Public Switched Telephone Network
Q	Quadrature
QE	Quality Estimate
QoS	Quality of Service
RAB	Radio Access Bearer
RACH	Random Access Channel
RANAP	Radio Access Network Application Part
RAT	Radio Access Technology
RB	Radio Bearer
RF	Radio Frame
RLC	Radio Link Control
RM	Rate Matching
RNC	Radio Network Controller
RNS	Radio Network Sub-system
RRC	Radio Resource Control
RRM	Radio Resource Management
RSCP	Received Signal Code Power
SAP	Service Access Point
SHO	Soft Handover
SGSN	Serving GPRS Support Node
SIR	Signal to Interference Ratio

SMS	Short Message Service
SRNC	Serving RNC
TB	Transport Block
TBS	Transport Block Set
TCP	Transmission Control Protocol
TDD	Time Division Duplex
TDMA	Time Division Multiple Access
TrCH	Transport Channel
TF	Transport Format
TFC	Transport Format Combination
TFCI	Transport Format Indicator
TFCS	Transport Format Combination Set
TFI	Transport Format Indicator
TFS	Transport Format Set
TMA	Traffic Monitoring and Analysis
TTI	Transmission Time Interval
UE	User Equipment
UML	Unified Modeling Language
UMTS	Universal Mobile Telecommunication System
U-RNTI	UTRAN Radio Network Temporary Identifier
USIM	Universal Subscriber Identity Module
UTRAN	UMTS Terrestrial Radio Access Network
VoIP	Voice over IP
WCDMA	Wide-band Code Division Multiple Access

List of Figures

List of Tables

Bibliography

[1] 3GPP. TR 23.907, Technical Specification Group Services and System Aspects, QoS Concept. Technical report, 1999.

[2] 3GPP. TR 25.931, UTRAN functions, examples on signalling procedures. Technical report, 1999.

[3] 3GPP. TR 25.944, Channel coding and multiplexing examples. Technical report, 1999.

[4] 3GPP. TS 23.002, Network Architecture. Technical report, 1999.

[5] 3GPP. TS 25.133, Requirements for support of radio resource management(FDD). Technical report, 1999.

[6] 3GPP. TS 25.201, Physical layer - General description. Technical report, 1999.

[7] 3GPP. TS 25.211, Physical channels and mapping of transport channelsonto physical channels (FDD). Technical report, 1999.

[8] 3GPP. TS 25.212, Multiplexing and channel coding (FDD). Technical report, 1999.

[9] 3GPP. TS 25.213, Spreading and modulation (FDD). Technical report, 1999.

[10] 3GPP. TS 25.214, Physical layer procedures (FDD). Technical report, 1999.

[11] 3GPP. TS 25.301, Radio Interface Protocol Architecture. Technical report, 1999.

[12] 3GPP. TS 25.302, Services provided by the physical layer. Technical report, 1999.

[13] 3GPP. TS 25.321, Medium Access Control (MAC) protocol specification. Technical report, 1999.

[14] 3GPP. TS 25.331, Radio Resource Control (RRC) protocol specification. Technical report, 1999.

[15] 3GPP. TS 25.401, UTRAN overall description. Technical report, 1999.

[16] 3GPP. TS 25.410, UTRAN Iu Interface: general aspects and principles. Technical report, 1999.

[17] 3GPP. TS 25.412, UTRAN Iu interface signalling transport. Technical report, 1999.

[18] 3GPP. TS 25.426, UTRAN Iur and Iub interface data transport & transport signalling for DCH data streams. Technical report, 1999.

[19] 3GPP. TS 25.427, UTRAN Iub/Iur interface user plane protocol for DCH data streams. Technical report, 1999.

[20] 3GPP. TS 25.430, UTRAN Iub interface: general aspects and principles. Technical report, 1999.

[21] 3GPP. TS 25.432, UTRAN Iub interface: signalling transport. Technical report, 1999.

[22] 3GPP. TS 25.433, UTRAN Iub interface Node B Application Part (NBAP) signalling. Technical report, 1999.

[23] 3GPP. TS 25.434, UTRAN Iub Interface Data Transport and Transport Signalling for Common Transport Channel Data Streams. Technical report, 1999.

[24] W. K. M. Ahmed and K. Balachandran. Methods for estimation of the uncoded symbol error rate at the receiver. In *Global Telecommunications Conference, 2002. GLOBECOM '02. IEEE*, volume 2, 2002.

[25] Ascom. TEMS Investigation software suite, weblink: `www.ascom.com/tems`.

[26] M. P. J. Baker and T. J. Mouslsley. Power control in UMTS Release '99. In *3G Mobile Communication Technologies, 2000. First International Conference on (Conf. Publ. No. 471)*, pages 36–40, 2000.

[27] Jeffrey Bannister, Paul Mather, and Sebastian Coope. *Convergence Technologies for 3G NetworksIP, UMTS, EGPRS and ATM*. John Wiley & Sons, LTD, 2004.

[28] Erik Dahlman, Stefan Parkvall, Johan Skold, and Per Beming. *3G Evolution*. Academic Press, July 2007.

[29] Norman R. Draper and Harry Smith. *Applied Regression Analysis*. Wiley-Interscience, April 1998.

[30] K. S. Gilhousen, I. M. Jacobs, R. Padovani, A. J. Viterbi, Jr, and C. E. Iii Wheatley. On the capacity of a cellular CDMA system. *Vehicular Technology, IEEE Transactions on*, 40(2):303–312, 1991.

[31] Alois M. J. Goiser. *Handbuch der Spread-Spectrum Technik*. Springer, 1997.

[32] Gunnar Heine. *UMTS Signalling & Protocol Analysis (UTRAN & UE)*. Inacon, 2003.

[33] Harri Holma and Antti Toskala. *WCDMA for UMTS: Radio Access for Third Generation Mobile Communications*. John Wiley & Sons, Inc., New York, NY, USA, 2000.

[34] Heikki Kaaranen, Are Ahtiainen, Lauri Laitinen, Siamäk Naghian, and Valtteri Niemi. *UMTS NetworksArchitecture, Mobility and Services*. John Wiley & Sons, LTD, 2005.

[35] Wolfgang Karner. *Link Error Analysis and Modeling for Cross-Layer Design in UMTS Mobile Communication Networks*. PhD thesis, TU Wien, 2007.

[36] Chang S. Koo, Sung H. Shin, R. A. Difazio, D. Grieco, and A. Zeira. Outer loop power control using channel-adaptive processing for 3G WCDMA. In *Vehicular Technology Conference, 2003. VTC 2003-Spring. The 57th IEEE Semiannual*, volume 1, 2003.

[37] Jaana Laiho, Achim Wacker, and Tomas Novosad. *Radio Network Planning and Optimisation for UMTS*. John Wiley & Sons, LTD, 2002.

[38] P. Mccullagh and J. A. Nelder. *Generalized Linear Models, Second Edition*. Chapman & Hall/CRC, August 1989.

[39] Fabio Ricciato. Traffic monitoring and analysis for the optimization of a 3g network. *Wireless Communications, IEEE*, 13(6):42–49, Dec 2006.

[40] A. Sampath, P. Sarath Kumar, and J. M. Holtzman. Power control and resource management for a multimedia CDMA wireless system. In *Personal, Indoor and Mobile Radio Communications, 1995. PIMRC'95. 'Wireless: Merging onto the Information Superhighway'., Sixth IEEE International Symposium on*, volume 1, 1995.

[41] A. Sampath, P. Sarath Kumar, and J. M. Holtzman. On setting reverse link target SIR in a CDMA system. In *Vehicular Technology Conference, 1997 IEEE 47th*, volume 2, 1997.

[42] Håkan Silfvernagel. Outer Loop Power Control in a Wideband-CDMA System. Master's thesis, LTU Luleå, 1999.

[43] A. M. Viterbi and A. J. Viterbi. Erlang capacity of a power controlled CDMA system. *Selected Areas in Communications, IEEE Journal on*, 11(6):892–900, 1993.

[44] Bo Wei, Lin Ma, and M. Al Shalash. Outer-Loop Power Control Optimization Analysis and a New Algorithm. In *Vehicular Technology Conference, 2007. VTC-2007 Fall. 2007 IEEE 66th*, pages 1484–1488, 2007.

[45] L. C. Yun and D. G. Messerschmitt. Power control for variable QOS on a CDMA channel. In *Military Communications Conference, 1994. MILCOM '94. Conference Record, 1994 IEEE*, 1994.